

Copyright is owned by the Author of the thesis. Permission is given for a copy to be downloaded by an individual for the purpose of research and private study only. The thesis may not be reproduced elsewhere without the permission of the Author.

Purification and Characterisation  
of a Secreted Glycosidase, from the  
Extreme Xerophile *Wallemia*  
*ichthyophaga*

---

A thesis presented in partial fulfilment of the requirement for the degree in

Master of Science

in

Biochemistry

at Massey University Palmerston North,

New Zealand

Taryn Angela Miller

2014



## Acknowledgments

Firstly, I would like to thank my supervisor Gillian Norris for encouraging me to always strive for my best, for always believing in me, your irreplaceable advice, and for the countless hours spent editing. Your mentoring throughout my masters has helped me develop as a person and a scientist, and I will always be grateful.

I would also like to thank my co-supervisor Mark Patchett for always being available to bounce ideas off, for his invaluable advice, and for editing my thesis.

Thank you to Trever Loo, our lab guru, whose wealth of knowledge and character has helped me with my masters in so many ways. Thank you especially with all the advice and time spent on the chromatography and mass spectrometry experiments.

Also, thank you to Meekyung Ann for never giving up on me. Thank you for all the advice, encouragement, comfort food, and company throughout my journey. I could not have done it without you, and I am a stronger person because of you.

Thank you to my amazing mum and dad. I am so blessed to have such loving and caring parents, and I wouldn't have gotten where I have or be the person that I am if it wasn't for all their encouragement, support, and belief in me.

I would also like to thank the rest of my family as well as all my Auckland and Palmerston North friends for all the encouragement, cups of tea, and for believing in me every step of the way, even when I didn't think I could do it. I would like to specifically thank my brother Gareth, Auntie Anita, Uncle Leon, Auntie Ida, Tracey Cropp, Andrew West, Rhiannon Moloney, Mackenna Dent, Fiona Given, Sarah Richardson, and Mark Thomas.

Special thanks to Natalie Gardner for always being there for me. Thank you for the support, for being a shoulder to cry on, and the many hours of entertainment spent in the decon room and tea room. Your friendship has been a constant source of inspiration.

Finally, thank you to all the other X-lab and IFS/IMBS people who have helped me throughout my thesis, whether it be through giving advice or assisting in an experiment.

Also, thank you to Massey University and LASRA for the opportunity and funding.



## **Abstract**

With recent pressure to reduce the environmental impact of leather production, research has been focused on the development of an alternative depilation method, as the conventional method for depilation contributes up to 60% of the total pollution produced. Contaminated salted ovine pelts stored at LASRA were easily depilated when drum washed, and the resultant leather was of good quality. The pelts were visibly contaminated with microorganisms, and it was thought that these may be secreting enzymes that loosened the wool fibre without damaging key structural skin components. Identification of the enzyme or enzymes was thus of interest.

The microorganism/s responsible for the secretion of the depilation enzyme/s were isolated and identified through sequencing the 16S/18S ribosomal RNA genes. Depilation, using the crude secretome solutions, was then assessed using fresh ovine skin as well as SACPIC, a micro scale staining method used to assess skin structure. Unfortunately, none of the secretomes from either a single or a combination of the microorganisms isolated, had depilation activity.

The secretome of *W.ichthyophaga*, a xerophilic filamentous fungus, which was consistently isolated from the contaminated pelts, was chosen to be characterised using proteomic methods. 1D SDS-PAGE gel/CHIP separation of the proteins in the secretome showed it contained mainly glycosidases, with no lipases, esterases, or proteases identified. Some of the proteins identified had suggested roles in resistance to osmotic pressure, while the remaining proteins were intracellular. Overall, 21 proteins were identified.

A purification procedure involving AEX and SEC was successfully developed for the isolation of one of the glycosidases from the secretome. The resultant purified fractions formed a doublet band when analysed by SDS-PAGE. The reason for this remains unknown, but was shown not to be due to an impurity or heterodimerisation.

The purified glycosidase was identified as belonging to the GH3 family by mass spectrometry. It was found to have a pH optimum of pH 6.0, was optimally active at 10% NaCl, and was itself glycosylated. The glycosidase was able to hydrolyse both  $\alpha$ - and  $\beta$ - linked glycosidic bonds in di- and polysaccharides. Interestingly, both the disaccharide and artificial *p*-nitrophenol forms of galactose were not cleaved by the enzyme.

## Table of Contents

<b>Acknowledgements</b> .....	i
<b>Abstract</b> .....	iii
<b>List of Figures</b> .....	ix
<b>List of Tables</b> .....	xiii
<b>List of Abbreviations</b> .....	xv

### 1.0 Introduction and Aims

#### 1.1 Introduction

1.1.1 Conventional leather process.....	1
1.1.2 Re-evaluating the conventional leather process.....	2
1.1.3 Using enzymes as an alternative method for dewooling.....	2
1.1.4 Skin structure .....	3
1.1.5 Hair follicle.....	4
1.1.6 Factors effecting leather quality.....	6
1.1.7 Contaminated sheep pelts.....	6
1.1.8 <i>Walleimia ichthyophaga</i> .....	7
1.1.9 Fungal secretomes.....	11
1.1.10 Secretome analysis using a proteomic approach.....	14
1.1.11 Mass spectrometry.....	15
1.1.12 Glycosidases.....	16
1.1.13 Glycoside hydrolase family 3.....	17

#### 1.2 Aims

1.2.1 Aims.....	19
1.2.2 Overview of the methodology.....	19

### 2.0 Materials and Methods

<b>2.1 Material</b> .....	<b>21</b>
---------------------------	-----------

## 2.2 Methods

2.2.1 MQ water.....	25
2.2.2 Media.....	25
2.2.3 Isolation by direct transfer.....	25
2.2.4 Isolation by liquid culture.....	25
2.2.5 PCR.....	26
2.2.6 PCR primers.....	27
2.2.7 Agarose gel electrophoresis.....	27
2.2.8 DNA sequencing.....	28
2.2.9 Database searches.....	28
2.2.10 Depilation: fresh skin.....	28
2.2.11 Depilation: Single section depilation method SACPIC visualisation....	28
2.2.12 Secretome preparation for mass spectrometry.....	30
2.2.13 SDS-PAGE.....	30
2.2.14 Coomassie staining of SDS-PAGE gels.....	31
2.2.15 Colloidal Coomassie staining of SDS-PAGE gels.....	32
2.2.16 In-gel tryptic digest.....	32
2.2.17 Mass spectrometry.....	33
2.2.18 Database searches.....	33
2.2.19 Secretome preparation for chromatography.....	34
2.2.20 Chromatograph preparation.....	34
2.2.21 Chromatography fraction standardisation.....	35
2.2.22 Anion exchange chromatography conditions.....	35
2.2.23 Cation exchange chromatography conditions.....	35
2.2.24 Generalised AEX and CEX parameters .....	36
2.2.25 Batch chromatography.....	36
2.2.26 Size exclusion conditions .....	36
2.2.27 SEC standard curve.....	37
2.2.28 Protease activity assay.....	37
2.2.29 Glycosidase activity assay for purification.....	37
2.2.30 Lipase activity assay.....	37
2.2.31 Bradford assay.....	38

2.2.32 Assay conditions for characterisation of glycosidase.....	38
2.2.33 Stability of the glycosidase.....	38
2.2.34 Substrate specificity assays.....	38
2.2.35 PNGase F and Endo H deglycosylation of glycosidase.....	39

### **3.0 Results and Discussion**

#### **3.1 Identification of microorganism from the contaminated salted ovine pelts**

3.1.1 Isolation of microorganisms from the contaminated ovine pelts.....	41
3.1.2 Isolation of microorganisms from the contaminated ovine pelts using agar plates.....	44
3.1.3 Isolation of microorganisms from the contaminated ovine pelts using broths.....	45
3.1.4 Depilation activity.....	47
3.1.5 Addition of dried ground ovine skin to Wilson’s media.....	49
3.1.6 Origin of the depilation activity from <i>W. ichthyophaga</i> .....	49

#### **3.2 Analyse of the protein composition of the secretome of *W.ichthyophaga* using in-gel tryptic digest and EIS-Q-TOF mass spectrometry**

3.2.1 Secretome concentration via precipitation.....	51
3.2.2 Secretome concentration via ultrafiltration.....	52
3.2.3 Addition of dried ground ovine skin.....	54
3.2.4 Protein identification through mass spectrometry.....	54
3.2.5 Molecular weight of secreted proteins using SDS-PAGE.....	60
3.2.6 Mass spectrometry results of the secreted proteins from <i>W.ichthyophaga</i> .....	62

#### **3.3 Purification of a novel glycosidase enzyme from the secretome of *Wallemia ichthyophaga*.**

3.3.1 Anionic and cationic chromatography.....	69
3.3.2 Optimisation of anion exchange chromatography.....	70
3.3.3 Hydrophobic chromatography.....	80
3.3.4 Size exclusion chromatography.....	81

3.3.5 Final purification method using chromatography.....	83
<b>3.4 Characterisation of a secreted glycosidase from <i>W.ichthyophaga</i></b>	
3.4.1 Quaternary structure of the glycosidase.....	97
3.4.2 Deglycosylation of the glycosidase using PNGase F and Endo H.....	98
3.4.3 Mass spectrometry of the final purified glycosidase fraction.....	102
3.4.4 Characterisation of the glycosidase.....	104
3.4.5 Optimum pH.....	105
3.4.6 The effect of NaCl on the activity of the glycosidase.....	107
3.4.7 The effect of metal ions on the activity of the glycosidase.....	108
3.4.8 Stability at 25°C.....	109
3.4.9 Inactivation of the glycosidase.....	110
3.4.10 Mini scale glucose test.....	111
3.4.11 Substrate specificity.....	111
<b>4.0 Conclusion and Future Direction</b>	
<b>4.1 Conclusion.....</b>	<b>115</b>
<b>4.2 Future direction.....</b>	<b>119</b>
<b>5.0 Reference List.....</b>	<b>121</b>

## List of Figures

### 1.0 Introduction and Aims

#### 1.1 Introduction

Figure 1.1.1: Summary of the conventional leather process.....	1
Figure 1.1.2: Diagram of the different layers and structures present in human skin.....	4
Figure 1.1.3: Diagram of the structure of a human hair follicle and pore.....	5
Figure 1.1.4: Phylogenetic tree of <i>Wallemiomycetes</i> in the phylum Basidiomycota.....	7
Figure 1.1.5: Morphological responses of the three <i>Wallemia</i> species to different NaCl concentrations.....	10
Figure 1.1.6: Classical and non-classical secretory mechanisms used by fungi.....	13
Figure 1.1.7: General CAZyme mechanism.....	16

#### 1.2 Aims

Figure 1.2.1: Summary of the methodology used to isolate and identify the enzyme/s responsible from the depilation activity observed from the contaminated pelts.....	19
---	----

### 3.0 Results and Discussion

#### 3.1 Identification of microorganism from the contaminated salted ovine pelts

Figure 3.1.1: Methodology used to isolate the microorganisms from the contaminated salted ovine pelts. Cultures in broths were done in duplicate with a different pelt used for each replicate.....	42
Figure 3.1.2: Examples of the different morphologies of colonies isolated from the contaminated pelts using both agar plates and broths of the three different media.....	43
Figure 3.1.3: SACPIC staining method.....	48

Figure 3.1.4: Fresh skin incubated in the secretome of *W. ichthyophaga* for 72 hours.....48

Figure 3.1.5: An example of a plate that may contain the isolates responsible for the initial depilation detected.....50

### **3.2 Analyse of the protein composition of the secretome of *W.ichthyophaga* using in-gel tryptic digest and EIS-Q-TOF mass spectrometry.**

Figure 3.2.1. 7.5% acrylamide gel of the supernatant and pellet from the TCA-acetone precipitation of the secretome of *W.ichthyophaga*.....52

Figure 3.2.2: SDS-PAGE gel of a secretome from a 2 month old *W.ichthyophaga* culture grown in Wilson’s media made 20% with NaCl, and desalted by ultrafiltration.....53

Figure 3.2.3: *Walleimia ichthyophaga* secretome composition from cultures started from 3 individual colonies.....56

Figure 3.2.4: 7.5% acrylamide gel of the secretome of a *W.ichthyophaga* culture grown from colony.....57

Figure 3.2.5: Methodology used to analyse each band from the SDS-PAGE gel of the whole secretome of *W. ichthyophaga*.....58

Figure 3.2.6: Methodology for the analysis of the proteins present in the whole secretome of *W. ichthyophaga*.....59

Figure 3.2.7: Standard curve of the size marker from the SDS-PAGE of the secretome of *W.ichthyophaga*.....62

Figure 3.2.8 Structural diagram of phytate.....66

### **3.3 Purification of a novel glycosidase enzyme from the secretome of *Walleimia ichthyophaga***

Figure 3.3.1: Trial 1, AEX of the secretome of *Walleimia ichthyophaga* using Q sephadex resin.....72

Figure 3.3.2: Trial 2: AEX of the secretome of *Walleimia ichthyophaga* using Q sephadex resin.....73

Figure 3.3.3: Protein concentration and enzymatic activity in fractions obtained from AEX of the secretome of *Walleimia ichthyophaga*.....75

Figure 3.3.4: Bradford standard curves using 90µL of reagent to 10µL of sample.....	76
Figure 3.3.5: 7.5% acrylamide gel of fractions obtained from AEX, and enzymatic activities.....	77
Figure 3.3.6: 7.5% acrylamide gel of the fractions obtained from the separation of the secretome of <i>Wallemia ichthyophaga</i> using AEX.....	79
Figure 3.3.7: The 3 step gradient elution profile of the secretome of <i>Wallemia ichthyophaga</i> with 10% glycerol using Q sephadex resin.....	80
Figure 3.3.8: The elution profile of fraction F13, fractionated by superdex 200 column.....	81
Figure 3.3.9: 7.5% acrylamide gel of fractions separated by SEC.....	82
Figure 3.3.10: Bradford assays across fractions obtained from AEX.....	83
Figure 3.3.11: The elution profile of the secretome of <i>Wallemia ichthyophaga</i> with 10% glycerol from Q sephadex resin.....	84
Figure 3.3.12: Bradford assays of concentrated fractions obtained from AEX.....	85
Figure 3.3.13: Glycosidase activity across fractions obtained from AEX.....	86
Figure 3.3.14: 7.5% acrylamide gel of fractions obtained from AEX, and specific activity.....	87
Figure 3.3.15: SEC of the fractions C9 and C11 from AEX.....	88
Figure 3.3.16: Bradford assays of fractions obtained from SEC.....	89
Figure 3.3.17: The average protein concentration, measured by Bradford assays, on fractions obtained from SEC.....	90
Figure 3.3.18: Glycosidase activity of fractions obtained from SEC.....	91
Figure 3.3.19: 7.5% SDS-PAGE analysing the concentrated fractions obtained from SEC and specific activity.....	92
<b>3.4 Characterisation of a secreted glycosidase from <i>W.ichthyophaga</i></b>	
Figure 3.4.1: Size exclusion calibration curve using a sephadex 200 column.....	98
Figure 3.4.2: Cleavage sites of endoglycosidases PNGase F and Endo H.....	99
Figure 3.4.3: 7.5% SDS-PAGE of a PNGase digest of the glycosidase from <i>Wallemia ichthyophaga</i> .....	100

Figure 3.4.4: 7.5% SDS-PAGE of a Endo H digest of the glycosidase from <i>Wallemia ichthyophaga</i> .....	101
Figure 3.4.5: Graphical representation of the gene from the glycosidase purified from the secretome of <i>W.ichthyophaga</i> that was identified by mass spectrometry.....	103
Figure 3.4.6: Graphical representation of the possible protein domains present in the glycosidase purified from the secretome of <i>W.ichthyophaga</i> .....	104
Figure 3.4.7: Activity of the glycosidase from <i>Wallemia ichthyophaga</i> at different pH.....	106
Figure 3.4.8: Activity of the glycosidase from <i>Wallemia ichthyophaga</i> using 100mM MES.....	106
Figure 3.4.9: Activity of the glycosidase from <i>Wallemia ichthyophaga</i> over different pH ranges using 100mM citric acid:sodium phosphate.....	107
Figure 3.4.10: Activity of the glycosidase from <i>Wallemia ichthyophaga</i> at different NaCl concentrations in 100mM citric acid: sodium phosphate at pH 6.0.....	108
Figure 3.4.11: Activity of the secreted glycosidase from <i>Wallemia ichthyophaga</i> at different concentrations of EDTA in 100mM citric acid: sodium phosphate.....	109
Figure 3.4.12: The stability of glycosidase from <i>Wallemia ichthyophaga</i> at 25°C.....	110
Figure 3.4.13 Glucose assay kit reaction.....	110
Figure 3.4.14: Standard curve of different glucose concentrations using 1mL reactions from Glucose (GOD) assay kit (Sigma).....	111

## List of Tables

### 2.0 Materials and Methods

#### 2.2 Methods

Table 2.2.1: PCR reaction mixture for rRNA gene amplification.....	26
Table 2.2.2: SDS-PAGE stacking gel components and volumes.....	31
Table 2.2.3: SDS-PAGE separation gel components and volumes.....	31
Table 2.2.4: Reaction mixtures for the PNGase F and Endo H treatment of the purified glycosidase.....	39

### 3.0 Results and Discussion

#### 3.1 Identification of microorganism from the contaminated salted ovine pelts

Table 3.1.1: Summary of the microorganisms isolated from the contaminated salted ovine pelts using agar plates of various media incubated at 25°C.....	44
Table 3.1.2: Summary of the microorganisms isolated from the contaminated salted ovine pelts by culturing in broths of different media incubated at 25°C.....	46

#### 3.2 Analyse of the protein composition of the secretome of *W.ichthyophaga* using in-gel tryptic digest and EIS-Q-TOF mass spectrometry

Table 3.2.1: Molecular weight of each band of the SDS-PAGE of the secretome of <i>W.ichthyophaga</i> using a standard curve.....	61
Table 3.2.2: Proteins identified in the secretome of <i>W.ichthyophaga</i> .....	62

#### 3.3 Purification of a novel glycosidase enzyme from the secretome of *Wallemia ichthyophaga*.

Table 3.3.1: Protein concentrations of unbound fractions from CEX and AEX fractionation.....	70
Table 3.3.2: The gradient profile for anion exchange chromatography; trial one.....	71

Table 3.3.3: The two-step gradient profile run for the anion exchange chromatography; trial two.....	73
Table 3.3.4: The three-step gradient profile run for the anion exchange chromatography.....	78
Table 3.3.5: Glycosidase purification summary.....	93
Table 3.3.6: The overall percentage yield and purification fold for the purification of the glycosidase from <i>W.ichthyophaga</i> .....	94

### **3.4 Characterisation of a secreted glycosidase from *W.ichthyophaga***

Table 3.4.1: Protein identification of bands obtained from SEC and Endo H digestion gels using in-gel tryptic digestion and mass spectrometry.....	102
Table 3.4.2: Domains predicted to be present in the isolated glycosidase protein.....	105
Table 3.4.3: Substrate specificity of the glycosidase secreted from <i>Wallemia ichthyophaga</i> .....	112

## List of Abbreviations

*Listed in alphabetical and then numeral order*

a.a	Amino Acid
AEX	Anion Exchange Chromatography
Abs	Absorbance
APS	Ammonium persulfate
Asn	Asparagine
AU	Absorbance Units
BLAST	Basic Local Alignment Search Tool
BSA	Bovine Serum Albumin
CEX	Cation Exchange Chromatography
cRAP	Common Repository of Adventitious Proteins
CV	Column Volume
DC	Direct Current
DNA	Deoxyribonucleic acid
DPX	Distrene, Plasticiser, Xylene
EDTA	Ethylenediaminetetraacetic acid
Endo H	Endoglycosidase H
EPS	Extracellular Polymeric Substrates
ESI	Electrospray Ionisation
ExpPASy	Expert Protein Analysis System
FAS	Faciclin
Gdp1	Glycerol-3-phosphate Dehydrogenase
GHA	Glycosidase Clan A
GH2	Glycosidase Family 2
GlcNac	N-acetylglucosamine
GMC	Glucose-methanol-choline
GOSs	Galactooligosacchride
HIC	Hydrophobic Chromatography
IEX	Ion Exchange Chromatography
KDa	Kilo Dalton

LASRA	Leather and Shoe Research Association
LB	Luria Broth
M	Molar
MES	2-(N-morpholino)ethanesulfonic acid
MIB	Sodium Malonate, Imidazole, and Boric acid
MS/MS	Tandem Mass Spectrometry
M/Z	Mass to Charge Ratio
PCR	Polymerase Chain Reaction
PNGase F	Peptide -N-Glycosidase F
ProDH	Proline Dehydrogenase
P5CDH	Pyrraline-5-carboxylate Dehydrogenase
Q-TOF	Quadruple Time-of-Flight
RF	Retardation Factor
RNA	Ribonucleic Acid
RPLC	Reverse-Phase Liquid Chromatography
SACPIC	SAfranine Celestin blue Picric acid
SAGE	Serial analysis of gene expression
SDS-PAGE	Sodium Dodecyl Sulfate Poylacrylaminde Gel Electrophoresis
SEC	Size Exclusion Chromatography
SSP	Small Secreted Proteins
TCA	Trichloroacetic acid
TEMED	N,N,N',N'- Tetramethylethylenediamine
TGFB1p	Transforming Growth Factor-Beta-Induced Protein
UniProt	Universal Protein Resource
UV	Ultra Violet
w/v	Weight to Volume
w/w	Weight to Weight
1D	One Dimension
2D	Two Dimensions

## 1.1 Introduction

### 1.1.1 Conventional leather process

Animal skins have been preserved for thousands of years, and used for many purposes such as clothing, weapons, furniture, and shoes. The overall purpose of the conventional leather process is to retain the desirable properties of skin such as flexibility, durability, breathability, and strength, while preventing putrefaction. This is achieved through chemical and enzymatic manipulation of the skin structure resulting in a fixed lubricated open collagen matrix. The conventional leather process can be broken down into four main stages; pre-tanning, tanning, post-tanning, and finishing (Saravanabhavan, Thanikaivelan, Rao, Nair, & Ramasami, 2006). Each of these stages consists of multiple processes as shown in figure 1.1.1. Pre-tanning cleans the hide or skin by removing unwanted proteins, dirt, wool/hair, and fats. This is then followed by tanning, which stabilises the collagen matrix, the main structural component of skin. Finally, the post-tanning and finishing stages add aesthetic value to the leather (Aravindhana *et al.*, 2008).

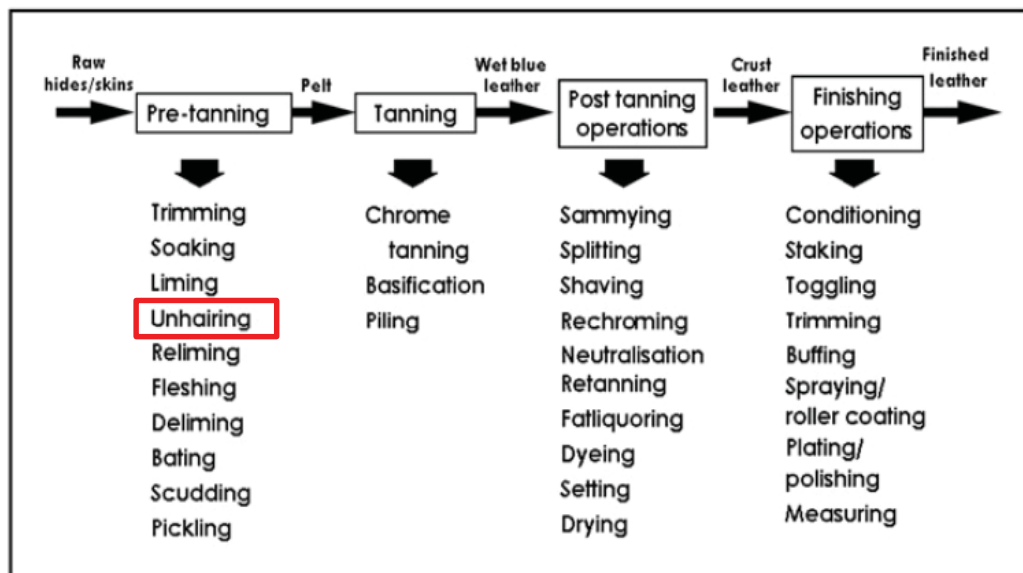


Figure 1.1.1: Summary of the conventional leather process (Aravindhana, Saravanabhavan, Thanikaivelan, Rao, & Nair, 2007). The red box indicates the main focus of this thesis. Reprinted from Journal of Cleaner Production, Vol 15, R. Aravindhana, A chemo-enzymatic pathway leads towards zero discharge tanning, Copyright (2007), with permission from Elsevier.

### **1.1.2 Re-evaluating the conventional leather process**

Recent pressures from both leather consumers and pollution monitoring companies have forced a re-evaluation of the conventional leather process. Some of the main environmental impacts that arise from leather processing are; the use of large quantities of water, harsh chemicals *e.g.* sulfide, and the general inefficiency of the process for example liming, re-liming, and de-liming (Figure 1.1.1) (Nazer, Al-Sa'ed, & Siebel, 2006). A prime concern is the need to eliminate or reduce the use of sulfides and lime. These two chemicals are the main effectors of hair removal, and alone contribute to over 60% of total pollution produced by the industry (Sivasubramanian, Manohar, Rajaram, & Puvanakrishnan, 2008 ). Conventionally lime is used to increase the pH causing the skin to swell. This splits up the fibre bundle sheath and removes the epidermis, along with other unwanted skin components. During liming, the step proceeding depilation, sulfide is added to aid depilation by breaking disulfide bonds present in the bulb of the hair follicle (Thanikaivelan, Rao, Nair, & Ramasami, 2003). After incubation with the lime/sulfide paste, the hair or wool is removed mechanically either by machine or by hand in a process known as scudding (Nazer, *et al.*, 2006).

### **1.1.3 Using enzymes as an alternative method for dewooling**

An alternative method of hair removal currently being investigated, involves the use of enzymes to depilate skin. In India, enzymes that remove hair from goat pelts have been thoroughly investigated, and have resulted in the development of a one-step enzymatic reagent. This reagent, called Biodart, contains a protease for hair removal, and an  $\alpha$ -amylase to open up the fibres for effective penetration (Saravanabhavan, Aravindhan, Thanikaivelan, Rao, & Nair, 2003; Sivasubramanian, Manohar, & Puvanakrishnan, 2008 ; Thanikaivelan *et al.*, 2007). The resultant depilated hides have increased tensile strength, stretch, and grain tightness (Saravanabhavan, *et al.*, 2003; Thanikaivelan, *et al.*, 2007). Furthermore, the removed hair is intact, rather than dissolved, allowing it to be used in other industrial applications. Successful application of this formula to sheep pelts may not be possible due to structural differences that exist between goat and sheep skin.

## Introduction

In general, successful dewooling/unhairing enzymes are alkaline proteases produced by *Bacillus* species (George, Raju, Krishnan, Subramanian, & Jayaraman, 1995; Senthilvelan, Kanagaraj, & Mandal, 2011; Wang *et al.*, 2007), although dewooling enzymes have been isolated from other species such as *Aspergillus oryzae* (Frag & Hassan, 2004). Generally, the enzymes have maximum activity at pH 9.0, and at temperatures that range between 25°C to 50°C. The time required for leather production is also reduced from 66 hours to around 15 hours (Dayanandan, Kanagaraj, Sounderraj, Govindaraju, & Rajkumar, 2003; Frag & Hassan, 2004; Senthilvelan, *et al.*, 2011; Sivasubramanian, Manohar, & Puvanakrishnan, 2008 ; Thanikaivelan, *et al.*, 2007). Overall, the successful use of enzymes in the process of depilating goat pelts has shown that they have the potential to reduce the environmental impact as well as increase the productivity of the leather process. This gives insight, along with supporting evidence, for the discovery and application of a depilating enzyme for sheep pelts.

### **1.1.4 Skin structure**

Skin structure can be divided into two main layers; the external epidermis, and internal dermis (Figure 1.1.2). The epidermis is made up of a keratinised stratified epithelial layer, and provides a physical barrier from the environment (Caspers, Lucassen, Wolthuis, Bruining, & Puppels, 1998). Collagens I and IV make up 60% of the dry weight of the dermal layer, and are responsible for the tensile strength of the skin (Oikarinen, 1994). Elastin, a fibrous protein making up 2%-4% of the dermal volume, is responsible for resilience and suppleness (Ritz-Timme, Laumeier, & Collins, 2003). GAGs (glycosaminoglycans), 0.1-0.3% of the dry weight of skin, are found throughout the skin, and are responsible for skin hydration. Finally, lipids are found throughout the skin structure where they are involved in a variety of functions (Bernstein, Underhill, Hahn, Brown, & Uitto, 1996). After the skin has been processed into leather only the dermal layer remains and is divided into the external grain layer and internal corium layer (R. Edmonds, 2008).

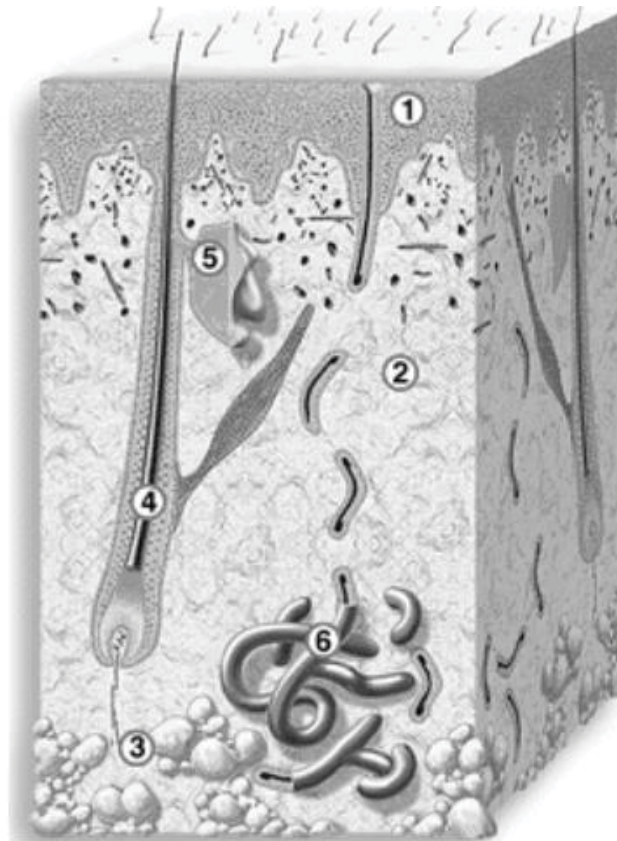


Figure 1.1.2: Diagram of the different layers and structures present in human skin. 1) Epidermis. 2) Dermis. 3) Subcutis. 4) Hair follicle. 5) Sebaceous gland. 6) Sweat Gland (Derler & Gerhardt, 2012). Reprinted from tribology letters, Vol 45, S. Derler, Tribology of Skin: Review and Analysis of Experimental Results for the Friction Coefficient of Human Skin, Copyright (2011), with permission from Elsevier.

### **1.1.5 Hair follicle**

The hair follicle is formed in an epidermal pore embedded in the dermal layer that in turn differentiates to form a hair shaft and sweat gland (Figure 1.1.3). The regulation of post-natal wool growth is controlled by the dermal papilla which is located at the base of the follicle (Oliver & Jahoda, 1988). Upon stimulation of the dermal papilla, wool is formed through the differentiation of the epithelial stem cells, which form a fibre matrix structure at the base of the follicle. For sheep, the follicle contains three thick primary wool fibres and many thinner secondary wool fibres (Lyne, 1961). This is in contrast to goat hair which contains only one primary



### **1.1.6 Factors effecting leather quality**

Testing has shown that the pre-tanning process is a major mediator in the production of high quality leather. Deb Choudhury *et al* (2006) analysed lambskin at various stages of the leather process. He concluded that collagen was the major protein component responsible for the characteristics of the final leather product. This finding was later supported by Edmonds, who concluded that it was the presence of collagen VI in the grain layer, that was specifically linked to the production of high quality leather (R. L. Edmonds *et al.*, 2008). A comparison of the minor protein components was also carried out, and showed that there were more low molecular weight proteins present in high quality leather than low quality leather, suggesting that they also contribute to the final leather quality (Deb Choudhury, *et al.*, 2006). An industrial depilating enzyme therefore needs to avoid targeting both collagen and these low molecular proteins (R. L. Edmonds, *et al.*, 2008). Surprisingly very little is known about the molecular architecture of the final leather product, more specifically the type and arrangement of the biomolecules making up this complex material (Sudha, Thanikaivelan, Aaron, Krishnaraj, & Chandrasekaran, 2009). Research on depilation enzymes can therefore only be assessed through the properties of the final leather product, rather than specifically selecting enzymes to target known key skin components.

### **1.1.7 Contaminated sheep pelts**

In 2011 it was observed that a group of salted sheep pelts, that had been stored for a number of months in an outdoor concrete storeroom at the Leather and Shoe Research Association of New Zealand (LASRA), had developed black spots on both the skin and the wool fibres. When these skins were immersed in water it was found that the wool was easily removed and gave rise to leather of high quality (Ahn, 2012). Importantly, this depilation occurred at ambient temperature. This is advantageous as so far enzymes that have been successfully used to depilate skin at an industrial scale required temperatures above 35°C to work, therefore in New Zealand incubation would need to take place in heated chambers, a requirement that would not be acceptable to the leather industry.

This depilation activity was thought to occur as a direct result of enzymes secreted by the organism/s growing on the skin. Filitcheva found two main organisms on the pelts in her study. The first was *Wallemia ichthyophaga*, which was identified with 98% homology. The second a bacterium, thought to belong to *Acinetobacter calcoaceticus*, but only had 95% homology, and was therefore more likely to be a new species (Filitcheva, Ahn, & Norris, 2011).

### 1.1.8 *Wallemia ichthyophaga*

The fungal kingdom contains the subkingdom Dikarya which is further split into the two phyla Basidiomycota and Ascomycota. The Basidiomycota phylum is then subdivided into three major subphyla: Agaricomycotina, Ustilaginomycotina, and Pucciniomycotina (Hibbett, 2006). Initially, *Wallemia* was thought to be a single species, *Wallemia sebi*, classified under the phylum Basidiomycota (Zalar, de Hoog, Schroers, Frank, & Gunde-Cimerman, 2005). Recent taxonomy studies have reclassified *Wallemia* as a sister subphylum of Agaricomycotina, called Wallemiomycetes (Figure 1.1.4), which contains three species distinguished by both genetic and morphological characteristics: *W. ichthyophaga*, *W. sebi* and *W. muriae* (Zalar, *et al.*, 2005). These isolates have been found in environments with low water activity such as salted/sweet dried foods, as well as hypersaline environments. Interestingly, *Wallemiomycetes* are thought to be the most xerophilic fungi isolated to date (Zajc *et al.*, 2013).

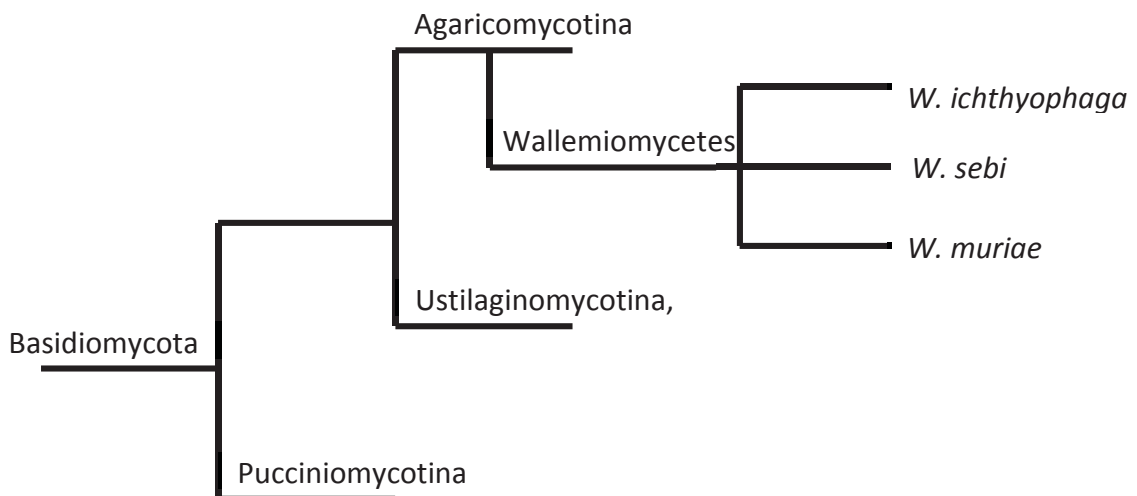


Figure 1.1.4: Phylogenetic tree of *Wallemiomycetes* in the phylum Basidiomycota.

## Introduction

Halotolerant microorganisms have already been utilised in many different industries such as the production of fish and soy sauces, moisturisers and anti-wrinkle creams, polymer production, and food colouring agents (Oren, 2002). Recent studies have looked into the morphological response of the Wallemiomycetes to both high salt (Kuncic, Kogej, Drobne, & Gunde-Cimerman, 2010) and high sugar (Kralj Kunčič, Zajc, Drobne, Pipan Tkalec, & Gunde-Cimerman, 2013) environments. This improved understanding of the adaptations evolved by this extreme halophile could be used to exploit Wallemiomycetes in certain industries, develop or improve established industrial applications involving halophiles, further the fundamental understanding of halophilic microorganisms, and provide supporting evidence towards the existence of three distinct species of Wallemiomycetes.

Firstly all three species were subjected to different NaCl concentrations. Both *W. ichthyophaga* and *W. muriae* required 4% NaCl to grow, while *W. sebi* could grow in the absence of NaCl. Interestingly, *W. ichthyophaga* was the only species that could sustain growth in saturated NaCl (30% NaCl). Overall, although high concentrations of salt impeded the growth rate and final biomass of all three species, *W. ichthyophaga* was less affected than the other two species. The most striking difference observed between *W. ichthyophaga*, when compared to both *W. muriae* and *W. sebi*, was their colony morphology (Figures 1.1.5 A and C). Both *W. muriae* and *W. sebi* formed mycelial pellets, with no differences seen between the morphologies of these two species, while *W. ichthyophaga* formed multicellular clumps made up of individual spherical cells. These two different morphologies, mycelial pellets and multicellular clumps, mirror the different environments populated by each species; *W. muriae* and *W. sebi* are often found in solid salted food, while *W. ichthyophaga* is commonly found in liquid hypersaline environments (Kuncic, *et al.*, 2010).

As the NaCl concentration is increased, the mycelial pellets of *W. muriae* and *W. sebi* become bigger, lighter in colour, and have shorter hyphal tips at their outer edges with increased branching (Figure 1.1.5 A and B). This morphology has been

## Introduction

previously documented in the less salt tolerant fungi *Aspergillus repens*. It is thought that the decreased surface-to-volume ratio reduces the surface area of the fungi in contact with high NaCl concentrations, reducing exposure to osmotic pressure. Conversely, the multicellular clumps formed by *W. ichthyophaga* increase at high NaCl concentrations, although the cell size remains unchanged (Figure 1.1.5 C and D). Again, the effect of this is to reduce exposure to osmotic pressure through reduced surface-to-volume ratio. Although all three species have a bilayer membrane, high concentrations of NaCl cause increased cell wall thickness in *W. ichthyophaga*, while in *W. muriae* and *W. sebi* the cell wall doesn't alter. The increase is predicted to help resist increased osmotic pressure through mechanical protection. Finally extracellular polymeric substances (EPS) are present for all three species, and are suspected to protect the organism against the extreme environment. The levels of EPS in both *W. muriae* and *W. sebi* cell walls remain unaffected by changes in NaCl concentrations, while a decrease in EPS is observed in the cell wall of *W. ichthyophaga*. (Kuncic, *et al.*, 2010). This response by *W.ichthyophaga* is the opposite of what would have been expected, and although there appears to be no explanation for this, EPS production may have been inhibited by high concentrations of NaCl, either directly or indirectly, resulting in the reduced levels of EPS observed.

Similar experiments were done using different concentrations of glucose for all three species. Again the high sugar content decreased both the growth rate and total biomass of all three species, but this time *W. ichthyophaga* was the most affected. The morphological response to high sugar by *W. ichthyophaga* was the same as that observed for NaCl. For both *W. muriae* and *W. sebi* the morphological responses were also the same as that observed for NaCl, apart from the cell wall of *W. sebi* decreasing in thickness while that of *W. muriae* increased (Kralj Kunčič, *et al.*, 2013).

Overall, the three *Wallemia* species have effectively adapted to high osmotic pressure. *W. sebi* and *W. muriae* have adapted to high levels of non-ionic solutes, such as glucose, which inflict turgor-related stress, by decreasing their surface-to-

## Introduction

volume ratio though changes in filament formation, and reduced cellular biosynthesis. Conversely, *W. ichthyophaga* has adapted to high levels of ionic solutes, not only by reducing its cellular surface-to-volume ratio but also by altering its membrane thickness and composition.

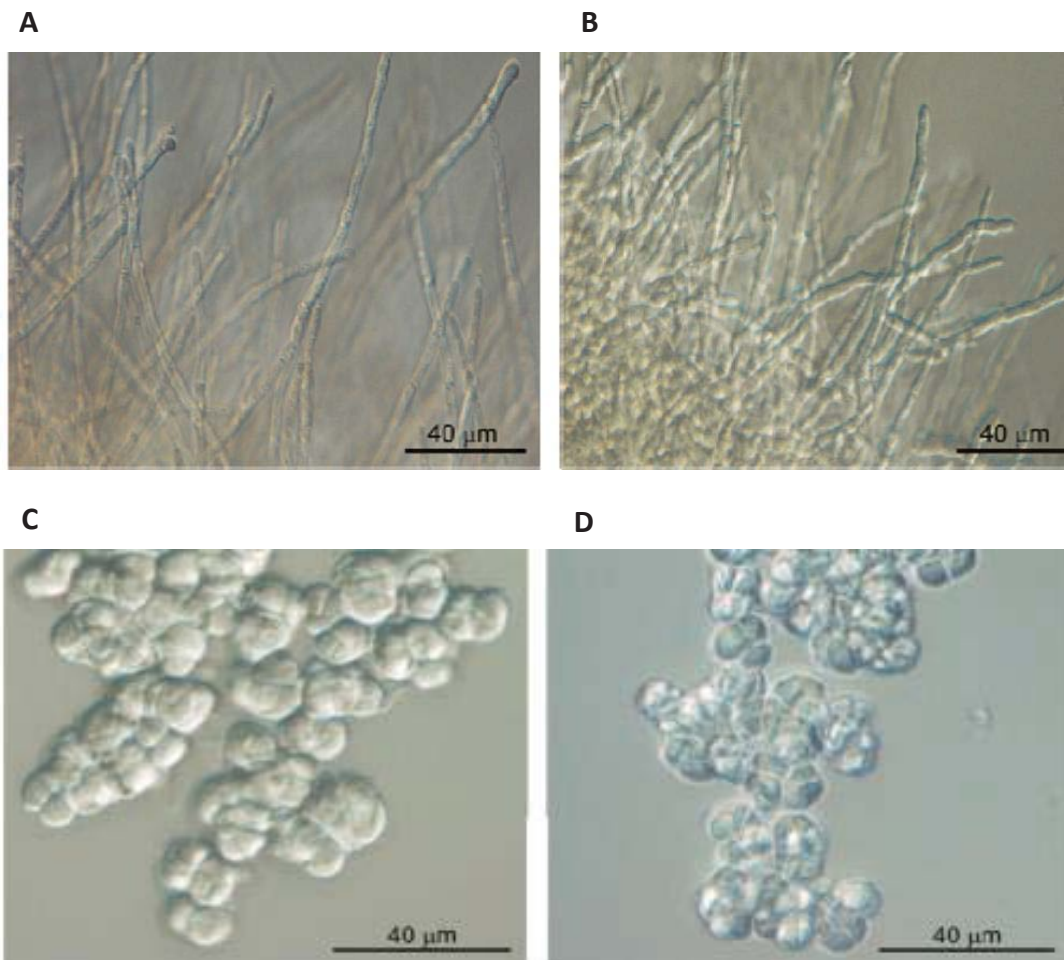


Figure 1.1.5: Morphological responses of the three *Wallemia* species to different NaCl concentrations. A) *W. muriae* or *W. sebi* in 5% NaCl. B) *W. muriae* or *W. sebi* in 20% NaCl. C) *W. ichthyophaga* in 5% NaCl. D) *W. ichthyophaga* in 25% NaCl (Kuncic, *et al.*, 2010). Reprinted from Applied and environmental microbiology, M. Kuncic, Morphological response of the halophilic fungal genus *Wallemia* to high salinity, Copyright (2010), with permission from Elsevier.

Research into the mechanisms *W.ichthyophaga* uses to cope with osmotic stress indicated that glycerol may be used as an osmoprotectant, an inert intracellular molecule used to counter balance osmotic pressure. Glycerol-3-phosphate

dehydrogenase (Gpd1) expression, which regulates the glycerol synthesis pathway, was found to be significantly up-regulated when the organism was grown in NaCl concentrations both below and above the optimal concentration of NaCl (Lenassi *et al.*, 2011). The presence of glycerol is known to decrease the generation of reactive oxidative species produced under stress, and to balance the redox status within the cell. It is also a precursor in the phospholipid biosynthesis pathway, a pathway important to membrane biogenesis (Lenassi, *et al.*, 2011).

Another coping mechanism used by *W. ichthyophaga* in high NaCl environments is the up-regulation of the synthesis of specific cation-transporting ATPases, which regulate H<sup>+</sup>, Na<sup>+</sup>, and Ca<sup>2+</sup> ion concentrations within the cell. There are three types of H<sup>+</sup> pumps present in the plasma membrane of *W.ichthyophaga* that are used to maintain the H<sup>+</sup> gradient. This membrane potential is then used by secondary transporters to regulate other ion concentrations within the cell. The presence of two types of Na<sup>+</sup> transporters the plasma membrane of *W.ichthyophaga*, are important for resistance against Na<sup>+</sup> toxicity. One of these transporters is an antiporter which utilises an electrochemical potential gradient, while the other directly uses ATP. These transporters have complementary roles; at low NaCl concentrations the antiporter is able to resist the Na<sup>+</sup> influx. At higher concentrations, however, the antiporter becomes unstable and the ATPase transporter, a higher throughput pump, is activated. The increase in expression of H<sup>+</sup> and Na<sup>+</sup> cation-transporters, to adapt to high NaCl environments, has also been documented for *S.cerevisiae* (Zajc, *et al.*, 2013).

### **1.1.9 Fungal secretomes**

Research into the secretomes of microorganisms has been of increasing interest over the last 10 years (Brown *et al.*, 2012). Although a wide range of definitions have been used, the secretome is generally defined as the group of extracellular proteins secreted from a cell/tissue/organ/organism at a given time under set conditions. It includes the proteins making up the secretory machinery as well as regulatory proteins involved in regulation of secretion (Tjalsma, Bolhuis, Jongbloed, Bron, & van Dijk, 2000). So far, secretomes from yeast and higher eukaryotes have

## Introduction

been the main focus of research, but interest in other fungal secretomes has recently grown (Bouws, Wattenberg, & Zorn, 2008).

The fungal kingdom consists of microorganisms that usually obtain nutrients from the decomposition of biomass, through extracellular digestion, followed by absorption. These fungi range from saprophytes which decompose organic matter, to pathogens which directly damage their living host. This is achieved, in most part, through the composition of their secretomes, with the diversity in their extracellular hydrolases enabling a wide range of carbon and nitrogen sources to be accessed. Two major enzyme groups present in fungal secretomes are polysaccharide-degrading enzymes for decomposition of biomass, and proteases for penetration into the host cells and/or degradation of proteinaceous material. Other proteins found in fungal secretomes are regulatory proteins, effector proteins, small secreted proteins (SSP) from symbiotic fungi, and symbioses-regulated acidic polypeptides (Girard, Dieryckx, Job, & Job, 2013).

These secreted proteins, in most cases, contain an N-terminal signal sequence, which recruits the proteins to the endoplasmic reticulum. The proteins then fold and are post-translationally modified. Further modification also takes place in the Golgi. Finally the mature protein is secreted, via a transport vesicle, through the cell membrane (Nickel & Rabouille, 2009). Interestingly, studies have found that up to one third of secreted proteins do not contain a signal sequence, these proteins are thought to be secreted through either non-classical or unknown mechanisms (Girard, *et al.*, 2013); interaction with specific proteins *e.g.* with Galectin 1 which in turn interacts with Nce101p (an integrated membrane protein), translocation, vesicles *i.e.* lysosomes/microvesicles/multivesicular bodies, membrane flipping, passive diffusion, or specific transporters (Figure 1.1.6) (Nickel & Rabouille, 2009; Nombela, Gil, & Chaffin, 2006). Post-translational modifications which are commonly found on fungal secreted proteins are glycosylation and disulfide bonds, as both provide thermostability increasing the proteins resistance to the harsh extracellular environment (Girard, *et al.*, 2013).

## Introduction

Fungal secretomes are directly regulated by the resources available as well as the environment. Studies with *Fusarium* have shown that when this fungus is grown on natural cell-wall extract, a complex mixture of protease, lipases, and glycosidases are secreted, but when grown on a simple plant extract media, only a portion of these enzymes are detected. Such strict regulation is advantageous as protein production is a high energy expense to the fungus (Phalip *et al.*, 2005). Regulation of polysaccharide-degrading enzymes is dependent on the type of substrates available, with enzymes secreted in a sequential manner depending on the degree of degradation of the substrate. Conversely, proteases are regulated by environmental pH rather than substrate composition, and work in a synergistic manner, with both exo and endo proteases simultaneously secreted. This means that when the secretome of an individual species is analysed both the culture conditions and age of the culture need to be stated in order to properly define the secretome (Girard, *et al.*, 2013).

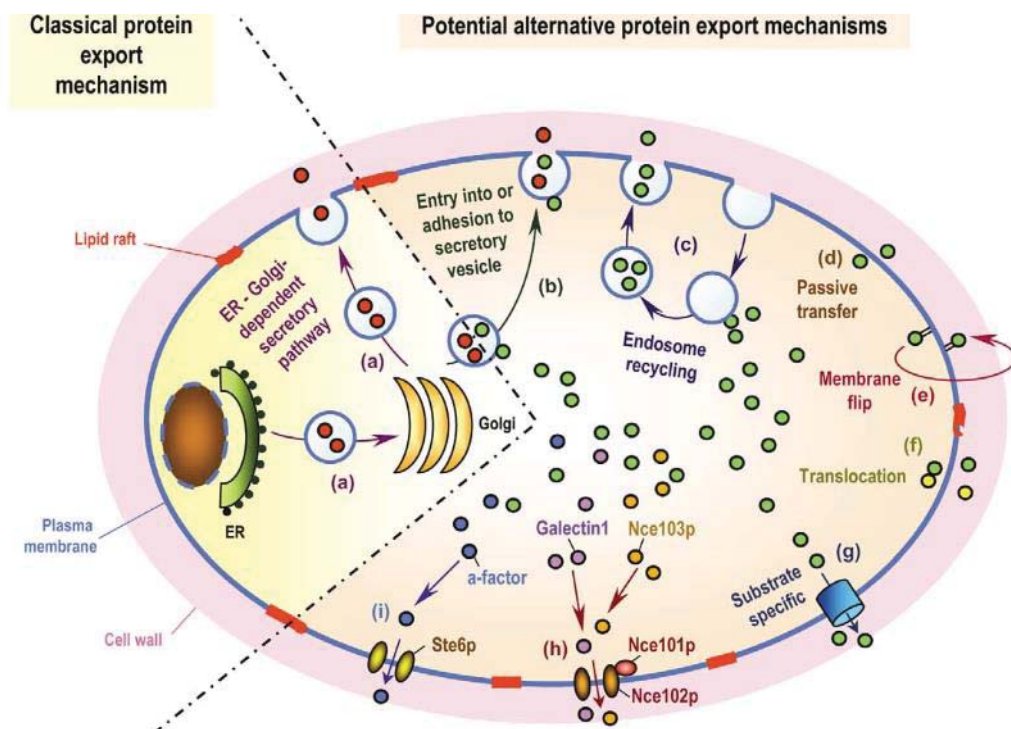


Figure 1.1.6: Classical and non-classical secretory mechanisms used by fungi (Nombela, *et al.*, 2006). Reprinted from Trends in Microbiology, Vol 14, C. Nombela, Non-conventional protein secretion in yeast, Copyright (2006), with permission from Elsevier

## Introduction

Research into the composition and regulation of fungal secretomes has become of increasing interest due to the potential benefits and applications of the secreted biomolecules. White rot fungi, which are capable of degrading xenobiotics and various pollutants, have been utilised in bioremediation, the process of using the metabolic potential of microorganisms to manage industrial waste in an eco-friendly manner (Asgher, Bhatti, Ashraf, & Legge, 2008). Secreted fungal enzymes, especially hydrolyses, are commonly used in human and animal food production, as food additives and/or to aid in the food production process *i.e.* proteases are used during cheese ripening, and xylanases are added to cereals to aid in nutrient uptake (Ghorai *et al.*, 2009). Finally, analysis of secretomes from plant pathogenic and symbiotic fungi, has further developed our understanding of the interactions that exist between the two species, and is used in the agriculture industry for crop management (Ellis, Rafiqi, Gan, Chakrabarti, & Dodds, 2009; Marra *et al.*, 2006).

### **1.1.10 Secretome analysis using a proteomics approach**

Proteomics is the identification and quantification of a subset of proteins expressed by a cell/tissue/organ under specific conditions (Eidhammer, Flikka, Martens, & Mikalsen, 2007) using multidisciplinary technology, and has flourished over the last 5 years. Proteomics has led to the successful analyses of secretomes from a wide range of microorganisms. For example, 80 proteins were identified from the secretome of the parasite *Brugia malayi* (Hewitson *et al.*, 2008), 89 secreted proteins were identified from the filamentous fungi *Botrytis cinerea* (Shah *et al.*, 2009) and 64 abundantly secreted proteins were identified from the bacteria *Bacillus anthracis* (Chitlaru *et al.*, 2007).

Generally, the proteins in a sample are initially fractionated by 1D or 2D gel electrophoresis or nano HPLC, to decrease the number of peptides per sample. This lowers the probability that proteins are incorrectly identified due to the generation of a large number of small peptides. Trypsin digestion of the proteins present in each gel slice/spot or fraction is then carried out and, after extraction of the peptides, further fractionation is common. The mass to charge ratios ( $m/z$ ) of the peptides are then measured in a mass spectrometer. Proteins are identified by

comparing the measured monoisotopic masses and/or sequence of the peptides, which are experimentally generated from each protein, to the theoretical monoisotopic masses and/or sequence of peptides generated by *in silico* digestion of all sequenced proteins in various databases such as SwissProt, NCBI, EMBL and TrEMBL. A perfect or near perfect match is evidence that the peptide in question was generated from a specific protein (Aebersold & Mann, 2003; Walther & Mann, 2010).

### **1.1.11 Mass spectrometry**

Mass spectrometry is a technique used to measure the mass to charge ratio ( $m/z$ ) of a molecule in its gaseous phase. The instrument consists of three parts; ion source, mass analyser, and detector. The ion source is responsible for converting the sample into a charged gaseous state. The ions then pass into the mass analyser which allows only ions within a specific  $m/z$  range, determined by the user, to pass through to the detector. When the ions reach the detector various algorithms are used to calculate the  $m/z$  ratios. Different types of ion source and mass analysers are available, allowing for a wide range of samples to be analysed. Recent advances in mass spectrometry, alongside the development of high-throughput sequencing, has seen rapid growth of proteome and secretome analysis (Yates, Ruse, & Nakorchevsky, 2009).

For processing the data, there are three main mass spectrometry techniques; peptide mass fingerprinting, tandem mass spectrometry (MS/MS ion), and sequence query (Cottrell & London, 1999). Peptide mass fingerprinting identifies proteins through measuring the mass of the peptides alone (Thiede *et al.*, 2005), which can often lead to ambiguous results if the spectrometer has lower mass accuracy. This is overcome by MS/MS, which fragments each peptide peak further allowing for the sequence of that peptide to be obtained. Finally, a sequence query can be used to aid in protein identification by providing additional search parameters such as a predicted sequence and/or physiochemical data (Cottrell & London, 1999).

### 1.1.12 Glycosidases

Carbohydrate-active enzymes (CAZymes) are a group of enzymes which display activity towards glycosidic bonds through either synthesis involving transfer (GT) or transglycosylation (TG) of monosaccharides, or degradation involving hydrolysis (GH) or phosphorylation (GP) of oligosaccharides. Mechanisms for all these reactions can be either retaining, where the anomeric carbon retains the stereochemistry, or inverting, where the anomeric carbon assumes a different stereochemistry e.g. an  $\alpha$  bond is converted to a  $\beta$  bond (Rye & Withers, 2000). The substrate specificity for CAZymes is based on both the linkage (anomer) and stereochemistry (enantiomer) of the substrate. The linkage can be  $\alpha$  or  $\beta$ , and the stereochemistry can be either D- or L.

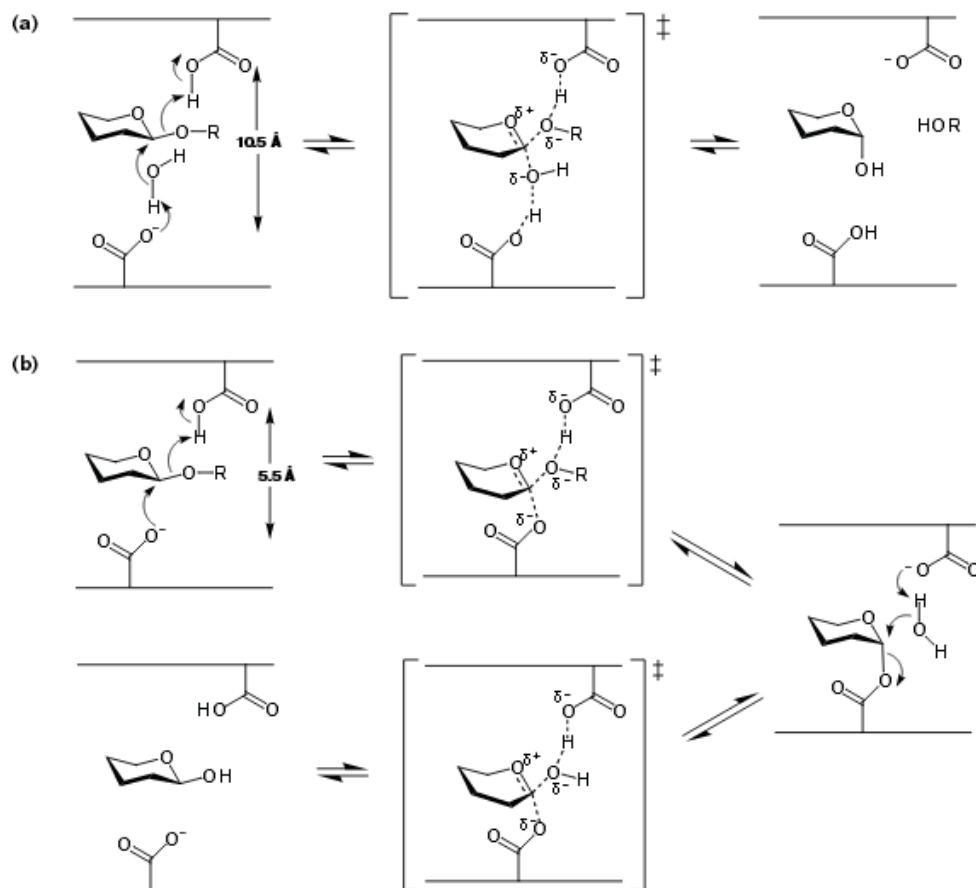


Figure 1.1.7: General CAZyme mechanism involving a) a single displacement nucleophilic attack for inverting enzymes, and b) double displacement nucleophilic attack for retaining enzymes (Rye & Withers, 2000). Reprinted from current Opinion in Chemical Biology, Vol 4, C. Rye, Glycosidase mechanisms, Copyright (2000), with permission from Elsevier.

## Introduction

In 1991 Henrissat and Co developed the online database CAZyme, in which the enzyme types were reorganised into glycosyl hydrolases (GH) or glycosyl transferases (GT), with transglycosidases (TG) being grouped with (GH), and glycosyl phosphatases (GP) belonging to either the GH or GT groups (Henrissat, 1991). Each CAZyme was then grouped into a clan, made up of multiple families, based on its fold and sequence. Enzymes in the same clan share the same three-dimensional catalytic architecture, while enzymes in the same family have sequence similarities. There does not need to be sequence similarities between families in the same clan (Bourne & Henrissat, 2001).

Two models have been proposed for CAZymes: the single or double nucleophilic displacement model, and the oxocarbenium ion intermediate model. Both the single and double nucleophilic displacement models use a pair of acidic amino acids as the catalytic residues and a oxocarbenium ion transition state to catalyse a single displacement (inverting enzymes) or a double displacement (retaining enzyme) (Figure 1.1.7) (Davies, Planas, & Rovira, 2011; Desmet & Soetaert, 2011; Henrissat, Coutinho, & Davies, 2001; Rye & Withers, 2000). Although this model seems to be the more widely accepted mechanism, a review in 2011, argued that the nucleophilic displacement model has many chemical inconsistencies, and that the oxocarbenium ion intermediate model is more plausible. Nevertheless there is still strong support for the nucleophilic displacement model based on the analysis of the mechanism when a range of inhibitors are added (Chiba, 2011).

### **1.1.13 Glycoside hydrolase family 3**

Glycoside hydrolase family 3 (GH3) enzymes, which are yet to be classified within a clan, are widely distributed in bacteria, fungi, and plants. This family consists of glycoside hydrolyases that have a wide range of catalytic functions; such as  $\beta$ -D-glucosidases,  $\alpha$ -L-arabinofuranosidases,  $\beta$ -D-xylopyranosidases, and *N*-acetyl- $\beta$ -D-glucosaminidases. Also the substrate specificities of these glycoside hydrolases can range from broad to narrow or even bifunctional. This extensive variation has led to attempts in classifying these GH3 glycosidases into subfamilies. However a universal

## Introduction

system is yet to be accepted (Harvey, Hrmova, De Gori, Varghese, & Fincher, 2000; J. Lee, Hyun, & Kim, 2011).

There are currently 6 crystal structures available for GH3 enzymes (Cantarel *et al.*, 2009). They are all made up of two domains, N-terminal and C-terminal, with the substrate binding in the domain interface. The N-terminal domain is characterised by a  $(\alpha/\beta)_8$  TIM barrel fold, while the C-terminal domain is a 6 stranded  $\beta$ -barrel made up from 5 parallel and 1 anti-parallel strands with 3  $\alpha$ -helices at either end. There are also three glycosylation sites on the N-terminal domain. Substrate specificity originates from the residues exposed in the domain interface as well as the relative orientation of the two domains (Varghese, Hrmova, & Fincher, 1999)

All GH3 glycosidases have a retaining mechanism, and use the double nucleophilic displacement model of catalysis. An aspartic acid residue has been identified as the catalytic nucleophile and its location is conserved between species, while a glutamine residue has been identified as the acid/base catalyst, with the location variable between species. The general mechanism for double nucleophilic displacement (Figure 1.1.7) involves the formation of a covalent intermediate and two transition states. The first transition state involves the donation of a proton, by a general acid reaction by the glutamine residue, to the glycosidic bond. This triggers the formation of the oxocarbenium ion between the substrate and the nucleophile. Next, the intermediate is formed by the formation of a covalent bond between the substrate and the aspartic acid residue of the glycosidase. A second transition state involves the activation of a water molecule by the glutamine residue, a general base reaction, to form a nucleophile that attacks the covalent bond between the substrate • enzyme intermediate, releasing the product. This restores the charged states of both active site residues (McIntosh *et al.*, 1996; Rye & Withers, 2000).

## 1.2 Aims and methodology

### 1.2.1 Aims

1. Isolate and identify the microorganism/s responsible for the depilation activity.
2. Isolate, identify, and characterise the depilation enzyme/s using proteomics, chromatography, and generalised enzymatic assays.

### 1.2.2 Overview of the methodology

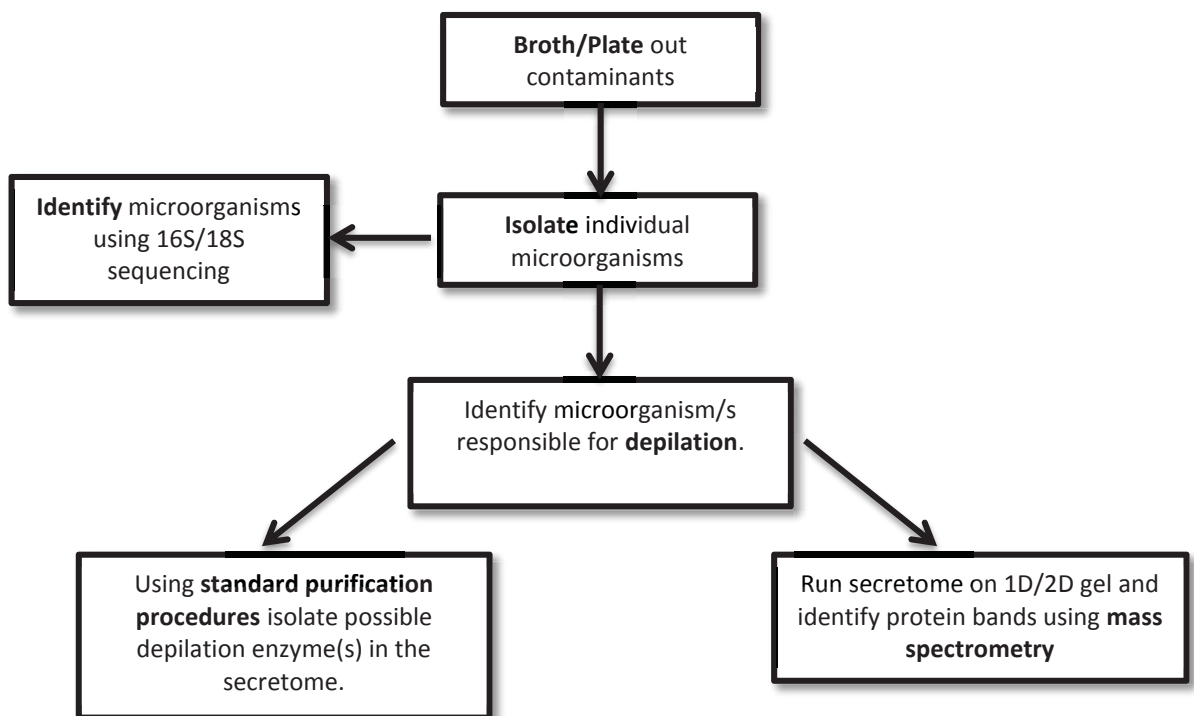


Figure 1.2.2.1: Summary of the methodology used to isolate and identify the enzyme/s responsible from the depilation activity observed from the contaminated pelts.

The methodology used to isolate the secretome of *W.ichthyophaga* is split into three main stages (Figure 1.2.2.1). First the microorganisms contaminating the pelt will be isolated using a range of media and growth conditions. Each isolate will be

## Introduction

identified by their 16S or 18S ribosomal RNA gene sequences. Next the secretome of each isolate, as well as different combinations of isolates, will be tested for depilation activity using raw skin along with a skin specific staining method called SACPIC (R. Edmonds, 2008). Finally any individual isolate or combination that produces industrial quality leather will have their secretomes analysed. This will be achieved using both classical biochemical techniques and proteomics to identify and purify the enzyme/s responsible for the depilation activity. If time allows, the depilation enzyme/s will be cloned and conditions optimised for industrial application.

## 2.0 Materials and Methods

### 2.1 Materials

*Materials are listed alphabetically under the manufacturer. All chemicals were analytical grade unless stated otherwise below.*

Affymatrix

- SDS (ultrapure)

Alright and Wilson

- Picric acid

Apex

- Agarose

BDH Chemical Ltd

- Safranin

Biorad

-2 cm by 18 cm column

Carl Roth GmbH + co

- Haematoxylin

Eppendorf:

- Low binding tubes 1.5 mL

## Materials and Methods

### Fermentas Life Science:

- Unstained Protein Molecular Weight Marker (14 kDa to 116 kDa)

### Fisher Scientific:

- Acetonitrile (Optima \*) 99.9% min
- Methanol  $\geq$  99.8%
- Water (Optima \* LC/MS)

### Fluka

- Celestin blue solution

### GE Healthcare:

- CM Sephadex
- Gel Filtration High Molecular Weight Kit ( 6.5 kDa to 75 kDa)
- Iodoacetamide
- Phenyl-Sepharose
- Source Q 10/80 column
- Superdex™ 200 30/300 column
- Vivaspin 20, 12 pack, 10 kDa MWCO

### LASRA

- Salted Ovine Pelts with Microbial Contamination
- Dried Ground Ovine Skin
- Fresh Ovine Skin

### Life Technologies:

- Platinum® Taq DNA Polymerase and Reagent Kit

## Materials and Methods

- 1Kb Plus DNA Marker

### Merck

- 40% Acrylamide-bis (29.1 :0.9)

### Promega Corporation:

- Wizard<sup>®</sup> Genomic Purification Kit
- Roche Applied Sciences:
- Complete, Mini Protease Inhibitor Cocktail

### Sartorius Stedim Biotech:

- Ministart, Single use Syringe Filter, sterile-EO, non-pyrogenic, hydrophilic. 0.2µm

### Serva

- Servapor<sup>®</sup>, Dialysis Tubing, 16 mm

### Sigma-Aldrich Co:

- APS (99%)
- Azocoll
- Glucose (GO) assay kit
- Endo H from *Streptomyces plicatus*
- Indigo-carmin
- *o*-nitrophenyl-beta-D-glucopyranoside
- *p*-nitrophenyl- butyrate
- TEMED (99%)
- Thesit<sup>®</sup> detergent

## Materials and Methods

- Trypsin from Porcine Pancreas, Proteomic grade, BioReagent, Dimethylated

### Thermo Scientific:

- GeneJET Gel Extraction and DNA Clean up Micro Kit

### Zymo Research:

- DNA Clean and Concentrator-5 kit

### 2.2 Methods

#### 2.2.1 MQ water

Sterile water was obtained from the Barnstead NANOpure® Diamond Life Science (UV/UF) Ultrapure Water System (0.2 µm filter).

#### 2.2.2 Media

Luria Broth (LB) was made according to the manufacturer's instructions but with an additional 20% (w/v) NaCl. Malt medium was made according to the manufacturer's instructions but with an additional 20% (w/v) NaCl. Wilson's medium was as described in the paper "Antifungal activity of *Wallemia ichthyophaga*" by Katherine Wilson (Wilson, Padhye, & Carmichael, 1969) but with 20% (w/v) NaCl. Solid media for agar plates were made with addition of 1% (w/v) agar to the liquid media before sterilisation. Ground dried ovine skin was added to media as required before sterilisation. All media were sterilised by autoclaving at 121°C and 15 psi for 15 minutes.

#### 2.2.3 Isolation by direct transfer

2 cm<sup>2</sup> sections of the contaminated salted skin or wool were placed onto agar plates of each type of medium. Glycerol stocks of the previously isolated *W. ichthyophaga* were also streaked onto agar plates of each type of medium. All plates were wrapped in Parafilm and incubated at 25°C for 1.5 months. Colonies were chosen based on their morphology, and sub-cultured through single colony streaking using the appropriate agar plate, until pure colonies were obtained. Pictures of the colonies, on the agar plates, were taken using a Nikon DSL camera.

#### 2.2.4 Isolation by liquid culture

2 cm<sup>2</sup> sections of the contaminated salted pelts were added to flasks each containing 50 mL of a selected medium. A loop full of glycerol stock of the previously isolated *W. ichthyophaga* was also added to 50 mL of each type of medium. Duplicates of all broths were incubated at 25°C for 1.5 months, without shaking, in duplicate. 100 µL of each culture was then spread on agar plates of the

## Materials and Methods

corresponding medium, and sealed with Parafilm. After 1 month of incubation at 25°C, each type of microorganism, identified by colony morphology, was selected and sub-cultured through single colony streaking using the respective agar plate, until pure cultures were obtained.

### 2.2.5 PCR

Isolated microorganisms from the contaminated salted ovine pelts were identified by sequencing the 16S ribosomal RNA gene for bacterial species, or the 18S ribosomal RNA gene for fungal species. Genes were amplified using 25 µL PCR reaction mixture as described in table 2.2.1;

Table 2.2.1: PCR reaction mixture for rRNA gene amplification

Reagent	Volume (µL)
10X Platinum® Taq Buffer	2.5
Water	18.9
50 mM MgSO <sub>4</sub>	1
50 ng/µL DNA Template	1
10 mM dNTP mix ( 10 mM each dNTP)	0.5
10 mM each Primer	0.5
5 U/µL Platinum® Taq Polymerase	0.1

Genomic DNA was extracted from single colonies of the isolated microorganisms using a Wizard Genomic DNA Purification Kit (Promega Corporated) and used as the PCR template. PCR was performed on a BioMetra T-Gradient Theromcyler according to the following programme;

## Materials and Methods

Denaturation at 94°C	1 minute	1X
Denaturation at 94°C	1 minute	} 30X
Annealing at 50°C	1 minute	
Amplification at 72°C	1 minute	
Amplification of 72°C	10 minute	1X

All PCR products were purified using a DNA clean and concentrator-5 kit (Zymo Research). All DNA concentrations from the genomic DNA extractions and in PCR reactions were measured using a NanoDrop™ 1000 Spectrophotometer (Thermo Scientific), according to the manufacturer's instructions.

### **2.2.6 PCR primers**

The oligonucleotide primers used to identify the isolated microorganisms were a kind gift from J.Filitcheva (Filitcheva, *et al.*, 2011). Their sequences are shown below:

16S rRNA gene primers:

- Forward 5'-AGAGTTTGATCCTGGCTCAG-3'
- Reverse 5'-GGTTACCTGTTAGGACTT-3'
- 1500 bp expected PCR product size.

The 18S rRNA gene primers:

- Forward 5'-TTAGCATGGAATAATGGAATA-3'
- Reverse 5'-TCTGGACCTGGTGAGTTTCC-3'
- 400 bp expected PCR product size.

### **2.2.7 Agarose gel electrophoresis**

4 µL of a PCR mix was added to 1 µL of loading dye before being run on 30 mL 1% agarose gel in 1X TAE buffer at 90 V for 40 minutes. The gel was then stained in 0.1 mg/mL ethidium bromide solution for 20 minutes, washed in water for 2 minutes, and then visualised on a Molecular Imager® Gel Doc™ XR + System with Image Lab™ Software. A 1 Kb Plus DNA marker was run alongside the samples.

### **2.2.8 DNA sequencing**

DNA sequencing reactions contained; 3.2 pmol of either the forward or reverse PCR primer, 2 ng of PCR product per 100 bp of the product size, therefore for 16S PCR product 8 ng was used and for 18S PCR product 30 mg was used, and then made up to 15  $\mu$ L with sterile MQ. Each reaction was sequenced using a capillary ABI3730 Genetic Analyzer (Applied Biosystems Inc) by Massey Genome Services.

### **2.2.9 Database searches**

Ambiguities in the sequencing results were resolved manually by inspection of the chromatograph. The sequence, in FASTA format, was used as the query sequence in BLASTn megablast searches of the non-redundant nucleotide collection (nr/nt) NCBI database.

### **2.2.10 Depilation activity: fresh skin**

50 mL broths of Wilson's media (20% NaCl) containing either individual or a combination of the isolated microorganisms were grown for 1.5 months at 25°C. 10 cm<sup>2</sup> sections of fresh sheep skin were then added, and the depilation checked daily by manually pulling on the wool fibres. The experiment was run until the control, containing only growth medium and skin, depilated due to the natural flora present on the unsterilized fresh skin.

### **2.2.11 Depilation-Single section depilation method with SACPIC visualisation**

0.5 cm<sup>2</sup> sections of frozen ovine skin were cut 20  $\mu$ m in thickness with a microtome (Leica), and dried on a glass slide overnight. 20  $\mu$ L of concentrated enzyme/secretome was incubated on the prepared skin at 25°C for 16 hours. The following slide staining procedure was then carried out at room temperature:

## Materials and Methods

MQ water	Wash
Celestin blue solution	5 mins
MQ water	Wash
1 g/L Haematoxylin	Wash
MQ water	Wash
Scott's "tap water"	2 mins
MQ water	Wash
Safranine	5 mins
70% ethanol	Wash
Absolute ethanol	Wash
Picric acid in ethanol	2 mins
70% ethanol	Wash
Absolute ethanol	Wash
Picro-indigo-carmin	2 mins
MQ water	Wash

### Celestin blue:

10 g iron alum was dissolved in 200 mL MQ water and mixed overnight. 0.1 g Celestin blue powder was then added, heated slowly until boiling in a flask, then boiled for 3 mins and cooled. The resulting solution was filtered, and 6.8 mL of glycerol was added.

### Scott's "tap water":

2 g/L sodium bicarbonate

20 g/L magnesium sulfate

### Safranine solution:

Add the following ingredients and mix for 1 hour

2 g safranine

49 mL absolute ethanol

49 mL MQ water

## Materials and Methods

Picric acid in ethanol:

- 0.5 mL picric acid (Saturated aqueous solution)
- 50 mL absolute ethanol

Picric acid-indigo-carmin

- 0.125 g indigo carmine powder
- 50 mL picric acid (Saturated aqueous solution)

Picric acid is stored as a solution under oil as this acid becomes explosive when exposed to air. For preparation of Picric acid in ethanol and Picric acid-indigo-carmin, all surfaces and equipment are thoroughly washed with excess water to prevent the picric acid solution drying out and to dilute the acid.

The skin sections were preserved by washing three times with 70% ethanol and then three times absolute ethanol, before being fixed in xylene and DPX. The skin sections were then visualised using a light microscope (R. Edmonds, 2008).

### **2.2.12 Secretome preparation for mass spectrometry**

20 mL of culture was filtered through glass wool to remove large cellular debris. The flow-through was then filtered through a 0.2 µm filter (Startorius Stedim Biotech), and concentrated 10-fold using a 10 kDa cut-off ultrafiltration device (Vivaspin- GE). The retentate was desalted by diluting with 19 mL of MQ water and reconcentrating 20-fold. This dilution-reconcentration step was performed three times in total.

### **2.2.13 SDS-PAGE**

Differing percentages of acrylamide were used to separate the proteins present in the secretome of *Wallemia ichthyophaga*. Gels were cast and run using the discontinuous buffer method (Table 2.2.2 and Table 2.2.3) in a Mini Protean III system (BioRad). Both the stacking and separating gels were degassed for 15 minutes before the ammonium persulfate and TEMED were added. All gels were

## Materials and Methods

run at 150 V until the dye front reached the bottom of the gel. An unstained protein marker (Fermentas Life Science) was used to calibrate the gel.

Table 2.2.2: SDS-PAGE stacking gel components and volumes

	7.5% gel	10% gel	15% gel
MQ Water (mL)	5.3	4.65	3.6
1.5 M Tris-HCl pH 8.8 (mL)	2.5	2.5	2.5
10% (w/v) SDS (mL)	0.1	0.1	0.1
Acrylamide/Bis (40%) ratio 19/1 (mL)	1.85	2.5	3.75
10% Ammonium persulfate (w/v) (mL)	0.1	0.1	0.1
TEMED (mL)	0.01	0.01	0.01

Table 2.2.3: SDS-PAGE separation gel components and volumes

	(mL)
MQ Water	6.4
1.5 M Tris-HCl pH 6.8	2.5
10% (w/v) SDS	0.1
Acrylamide/Bis (40%) ratio 19/1	1
10% Ammonium persulfate (w/v)	0.1
TEMED	0.01

For all samples 5x SDS loading dye was added in a 2:8 ratio ie 4  $\mu$ L of dye for 16  $\mu$ L of sample, and boiled for 3 minutes in a boiling bath.

### **2.2.14 Coomassie staining of SDS-PAGE gels**

Polyacrylamide gels were stained for 20 minutes, with agitation, in a solution containing 50% (v/v) methanol and 10% (v/v) acetic acid in water with 1 g/L Coomassie Brilliant Blue R-250. The gels were then washed with Milli-Q water

before being destained with a 50% (v/v) methanol and 10% (v/v) acetic acid in water.

### **2.2.15 Colloidal Coomassie staining of SDS-PAGE gels**

For increased sensitivity and/or identification of the protein bands by mass spectrometry some polyacrylamide gels were stained with agitation, for a minimum of 24 hours, in colloidal Coomassie solution (25 g/L ammonium sulfate, 3 ml/L of 85% phosphoric acid, 5 mL/L of 5% Coomassie Blue G-250, in water).

### **2.2.16 In-gel tryptic digest**

Bands were excised with a clean scalpel blade and sliced into pieces on a clean glass plate before being transferred to a 1.5 mL Eppendorf tube. The gel slices were then destained and dehydrated as follows:

200  $\mu$ L of 100 mM  $(\text{NH}_4)\text{HCO}_3$ / 50% methanol for 5 minutes until colourless

200  $\mu$ L of 25 mM  $(\text{NH}_4)\text{HCO}_3$ / 50% acetonitrile for 2 minutes

100% acetonitrile for 30 secs

(all supernatants discarded after each step)

The samples were then dried using a SpeedVac DNA 110 Concentrator (Savant). The gel slices were reduced and alkylated as follows: samples were rehydrated in 50  $\mu$ L fresh 25 mM DTT (dithiothreitol) in 25 mM  $(\text{NH}_4)\text{HCO}_3$  for 1 hour at 56°C. The excess liquid was aspirated off, and 50  $\mu$ L of 55 mM iodoacetamide in 25 mM  $(\text{NH}_4)\text{HCO}_3$  was added to the gel slices and incubated at room temperature in the dark for 20 minutes. The sample was then washed with 500  $\mu$ L of MQ water. The gel slices were then dehydrated with 200  $\mu$ L of 25 mM  $(\text{NH}_4)\text{HCO}_3$ / 50% acetonitrile for 2 minutes, and the liquid aspirated off. Finally 200  $\mu$ L of 100% acetonitrile was added for 30 secs and the liquid aspirated off. The samples were dried using a SpeedVac DNA 110 Concentrator (Savant). The proteins in the gel slices were then digested in-gel by the addition of 50  $\mu$ L of trypsin in 25 mM  $(\text{NH}_4)\text{HCO}_3$ , containing 200 ng of trypsin. Following an overnight incubation at 35°C, the peptides were extracted as follows: the trypsin solution was carefully removed from each tube and transferred

to a new Eppendorf tube using a pipette. Buffer A (5% formic acid in water) was added to the digested gel slices, and the sample was sonicated (Elmasonic S 15H, Total Lab System Ltd) for 5 minutes. The tubes were briefly centrifuged, 2 min at 14100 X g before each solution was removed and pooled with the trypsin solution. Buffer B (5% formic acid in 50:50 water:acetonitrile) was then added to the digested gel slices, sonicated for 5 minutes, and then centrifuged as before. The solution was removed and pooled with the trypsin solution/buffer A solution, and the pooled fractions (trypsin solution, buffer A, and buffer B) were then concentrated to 20  $\mu$ L using the SpeedVac. Before mass spectrometry, the samples were centrifuged at 13,000 rpm for 20 minutes to remove any insoluble particles.

### **2.2.17 Mass spectrometry**

An 8  $\mu$ L sample was autoinjected into an Agilent 1200 nano-flow LC system with a Chip Cube interface and loaded into a 43 mm C18 ProteinID(II) HPLC-Chip (Agilent Technologies, Germany). The initial mobile phase was comprised of 0.1% (v/v) formic acid in water at a flow rate of 0.3 mL/min and each sample was eluted with a linear gradient, changing to 0.1% (v/v) formic acid in 45% acetonitrile, 55% water over 30 minutes. The LC eluant was subjected to electrospray ionization (ESI) at a capillary voltage of 1,875 V in the mass spectrometer (Agilent 6520 Q-TOF, Agilent Technologies, Hanover, Germany). Sample analyses were performed in positive ion mode and the data were converted to centroid mode for storage. MS scans (100-1700  $m/z$ ) were obtained with fragmentor and skimmer voltages at 175 and 65 V, respectively. The five most abundant ions were subjected to MS/MS fragmentation at a collision energy slope of 3.8 V/100 Da with an offset of +2.5 V.

### **2.2.18 Database searches**

Total ion chromatograms (TIC) obtained were examined, and ions extracted and exported in mzData format for searches using Agilent MassHunter Workstation Qualitative Analysis software version B.03.01 (Agilent Technologies, Santa Clara, CA, USA). Searches were performed on the local Labkey server (Nelson *et al.*, 2011) using the following parameters: Non-redundant database restricted genus *Wallemiomycetes* with the addition of cRAP (Mascot), carbamidomethyl cysteines

## Materials and Methods

as fixed modification, and peptide charge of +2 and +3. Each band was analysed using search criteria that specified the enzyme used to hydrolyse the protein was either trypsin (trypsin specific cleavage at both ends) or semi-trypsin (trypsin specific cleavage at only one end of the peptide). Search results were filtered as follows; equal to or greater than 2 unique peptides, and peptide score equal to or greater than 0.9. Two methods of analyses were done: First, all excised bands (1-20) and digestion types (trypsin and semi-trypsin), per secretome (A1, B1, B2, C1, and C2), were pooled into one sample, i.e. for secretome A1: A1-1 semi-trypsin, A1-1 trypsin, A1-2 semi-trypsin, A1-2 trypsin etc. Proteins identified in all pooled secretomes were selected. Second, only semi-trypsin was used as the enzyme, with each band in each secretome compared, i.e. for band 1: A1- semi-trypsin, B1- semi-trypsin, B2- semi-trypsin, C1- semi-trypsin, and C2- semi-trypsin.

### ***2.2.19 Secretome preparation for chromatography***

50 mL of culture was first filtered through glass wool to removed large cellular debris. The flow-through was filtered through a 0.2 µm filter (Sartorius Stedim Biotech) and dialysed at 4°C for 24 hours against 1 L of the appropriate chromatography buffer. The dialysis buffer was replaced after 12 hours. The sample was then diluted to 200 mL with buffer and re-filtered through a 0.2 µm filter.

### ***2.2.20 Chromatography preparation***

If the resin was in dried form it was hydrated and equilibrated in the appropriate buffer following the manufacturer's instructions (GE Healthcare). For resin pre-swollen and stored in ethanol, the beads where washed with water and equilibrated in the appropriate buffer until the flow-through had the same conductivity and pH as the buffer. The equilibrated resin was then packed into a column and connected to the AKTA Explorer FPLC (GE Healthcare). Pre-packed columns were connected to the AKTA Explorer, then equilibrated with the appropriate buffer.

### **2.2.21 Chromatography fraction standardisation**

The protein concentrations of all fractions showing absorbances at 280 nm were measured using the Bradford assay. Some fractions were diluted to ensure the  $A_{595\text{nm}}$  reading fell within the range of the protein standard curve (0 mg to 0.1 mg at 595 nm) where the absorbance (abs) and protein concentration (mg/mL) are proportional. This measurement was then used to calculate the volume of solution required to achieve a final protein concentration of 1 mg/mL. Fractions were concentrated using 10 kDa cut off ultrafiltration devices (Vivaspin- GE). The final protein concentration was then re-measured, and again fractions were diluted to ensure the measured concentrations fell within the range of the standard curve.

e.g Fraction C11 from AEX

Original fraction absorbance	0.105 Abs at 595 nm
Sample was concentrated 10 fold to obtain a reading of 1.0 Abs at 595nm	
Theoretical concentrated absorbance	1.05 Abs at 595 nm
Actual concentrated absorbance	0.8 Abs at 595 nm
Actual concentration factor	7.6-fold

### **2.2.22 Anion exchange chromatography conditions**

A Source Q (GE Healthcare 10/80 or 2 cm by 18 cm- Biorad) column was connected to the AKTA explorer (GE Healthcare), equilibrated in 10 mM HEPES pH 7.0 (conductivity of 200  $\mu\text{S}/\text{cm}$ ) that had been filtered through a 0.2  $\mu\text{m}$  filter (Sartorius Stedim Biotech). The previously prepared sample (section 2.2.19) was loaded directly onto the column *via* the sample pump P-950.

### **2.2.23 Cation exchange chromatography conditions**

A CM Sephadex (2 cm by 18 cm -Biorad) column was connected to the AKTA explorer, equilibrated with 10 mM sodium phosphate pH 7.0 (conductivity of 1.276 mS/cm), that had been filtered through a 0.2  $\mu\text{m}$  filter (Sartorius Stedim Biotech).

The previously prepared sample (section 2.2.19) was loaded directly onto the column *via* the sample pump P-950

### **2.2.24 Generalised AEX and CEX conditions**

The following parameters were kept constant:

8 CV equilibration step with buffer A

5 CV initial wash step with buffer A

1 CV final wash step with 100% buffer B

One column volume= 40 mL.

Buffer A= the appropriate buffer for the resin.

Buffer B= buffer A made 2 M in NaCl

The proteins were eluted with differing gradients of the buffer B as described in the results and discussion section 3.3.

### **2.2.25 Batch chromatography**

2 heaped teaspoons of pre-equilibrated resin was added to a flask containing 100 mL of prepared secretome. Both secretome and resin were pre-equilibrated in the appropriate buffer. The flask was incubated at 4°C overnight with stirring. After this time the resin was packed into a column (2 cm by 18 cm- Biorad), and connected to the AKTA Explorer (GE Healthcare), where it was washed with 8 CV of equilibration buffer. Bound proteins were eluted with the gradient between 0% and 100% buffer B over 10-15 CV as discussed in section 3.3. Again the sample was loaded directly onto the column *via* the sample pump P-950

### **2.2.26 Size exclusion conditions**

A Superdex 200 (GE Healthcare 10/300) column was connected to the AKTA explorer (GE Healthcare), and equilibrated in 10 mM sodium phosphate pH 7.0, that had been filtered through a 0.2 µm filter (Sartorius Stedim Biotech). 150 µL of sample was injected using a 200 µL loop.

### **2.2.27 SEC standard curve**

The gel filtration high molecular weight kit (GE Healthcare) was used to produce a standard curve for the Superdex 200 column. Chromatography was carried out under the same conditions used for the SEC step in the purification of the glycosidase.

### **2.2.28 Protease activity assay**

Azocoll (Sigma-Aldrich Co) a chromogenic substrate which when hydrolysed releases a collagen-linked azo dye, resulting in a red pigmentation with an absorbance maximum at 520 nm, was used to test for protease activity. 10  $\mu$ L of enzyme was incubated with 90  $\mu$ L of 5 mg/mL solution of Azocoll in 100 mM potassium phosphate buffer pH 7.0 at 37°C for 15 minutes. The reaction was stopped by centrifuging the reaction mixture at 14100 times gravity for 10 minutes to pellet the uncleaved Azocoll substrate. The absorbance of the supernatant at 520 nm was then measured using a spectrophotometer.

### **2.2.29 Glycosidase activity assay for purification**

Enzyme catalysed hydrolysis of *o*-nitrophenyl- $\beta$ ,D-glucopyranoside (Sigma-Aldrich) releases an *o*-nitrophenol group, which is in a pH-dependent equilibrium. The intensity of this colour can be measured at 420 nm. 10  $\mu$ L of enzyme was incubated with 90  $\mu$ L of 1.25 mM *o*-nitrophenyl- $\beta$ ,D-glucopyranoside in 100 mM sodium acetate pH 7.0 at 25°C for 15 minutes. The reaction was stopped by the addition of 100  $\mu$ L 1 M sodium carbonate. The alkaline conditions convert almost all the nitrophenol product to the yellow nitrophenoxide anion, increasing the sensitivity of the assay. The absorbance of the reaction product at 420 nm was then measured using a spectrophotometer.

### **2.2.30 Lipase activity assay**

Upon cleavage of the ester bond *p*-nitrophenyl butyrate (cloudy white solution) (Sigma-Aldrich) releases the *p*-nitrophenyl group resulting in a clear yellow solution, which absorbs at 420 nm. 10  $\mu$ L of enzyme was added to 100  $\mu$ L of 98% *p*-

nitrophenyl butyrate in 100 mM potassium phosphate buffer pH 7.0, resulting in an instant colour change and a transparent solution.

### **2.2.31 Bradford assay**

Bradford protein assays (Kruger, 2009) were carried out in 96-well microtiter plates. Each reaction contained 90  $\mu\text{L}$  Bradford reagent with 10  $\mu\text{L}$  of sample and the absorbance was read at 595 nm.

### **2.2.32 Assay conditions for characterisation of glycosidase**

All assay of the purified glycosidase followed the protocol: 10  $\mu\text{L}$  of 0.1 mg/mL protein solution was added to 90  $\mu\text{L}$  of *o*-nitrophenyl- $\beta$ ,D-glucopyranoside in the appropriate buffer with or without added EDTA/NaCl. The reaction mixture was incubated at room temperature for 5 minutes, then 100  $\mu\text{L}$  of sodium carbonate was added to stop the reaction. The absorbance was then measured at 420 nm.

### **2.2.33 Stability of the glycosidase**

Six tubes (1.5mL Eppendorf) containing 10  $\mu\text{L}$  of 0.1 mg/mL glycosidase and 80  $\mu\text{L}$  of 100 mM citric acid:phosphate buffer (100 mM citric acid mixed with 100 mM phosphate buffer at a ratio to give a final pH 6.0) at pH 6.0, were incubated at 25°C for 0, 1, 2, 4, 6 or 24 hours. Then 10  $\mu\text{L}$  of 1.25 mM *o*-nitrophenyl- $\beta$ ,D-glucopyranoside in 100 mM citric acid:phosphate buffer was added, and the reaction mixture incubated for 5 minutes at 25°C. 100  $\mu\text{L}$  of 1 M sodium carbonate was added to stop the reaction, and the absorbance was read at 420 nm.

### **2.2.34 Substrate specificity assays**

10  $\mu\text{L}$  of 0.1 mg/mL glycosidase was added to 90  $\mu\text{L}$  of 40 mM disaccharide in 100 mM citric acid:phosphate buffer pH 6.0. The reaction was incubated for 4 hours at 25°C, then heated at 70°C for 5 minutes. Any glucose formed during the incubation was assayed using the Glucose (GO) assay kit (Sigma-Aldrich): an additional 100  $\mu\text{L}$  of 100 mM citric acid:phosphate buffer pH 6.0 was added to the reaction mixture to make the final volume up to 200  $\mu\text{L}$ . 400  $\mu\text{L}$  of assay reagent was then added and the reaction mixture was incubated at 37°C for 30 minutes. 400  $\mu\text{L}$  of 12 M  $\text{H}_2\text{SO}_4$

was added to stop the reaction and develop colour. The absorbance was read at 520nm.

### **2.2.35 PNGase F and Endo H deglycosylation of glycosidase**

The purified glycosidase from *W.ichthyophaga* was buffer-exchanged into 50 mM sodium phosphate pH 7.0 (for PNGase F) or 50 mM sodium citrate pH 5.5 (for Endo H), by ultrafiltration (Vivaspin MWt cut off 10 kDa). The reactions described in table 2.2.4 were each done in a 10  $\mu$ L volume:

Table 2.2.4: Reaction mixtures for the PNGase F and Endo H treatment of the purified glycosidase.

	Glycosidase (1 mg/mL)	0.1% SDS	40 mM DTT	1 mg/mL PNGase F or Endo H	Respective Buffer
Control	7 $\mu$ L	-	-	-	3 $\mu$ L
Native	7 $\mu$ L	-	-	1 $\mu$ L	2 $\mu$ L
Denatured	7 $\mu$ L	1 $\mu$ L	1 $\mu$ L	1 $\mu$ L	-
PNGase Native control	-	-	-	1 $\mu$ L	9 $\mu$ L
PNGase denatured control	-	1 $\mu$ L	1 $\mu$ L	1 $\mu$ L	7 $\mu$ L

To denature the glycosidase, SDS, and DTT were added to the appropriate tubes and, the mixture boiled for 10 minutes. The PNGase F (kindly gifted from T Loo) or Endo H (Sigma-Aldrich) solutions were then added and mixed and the sample incubated for 4 hours at 30°C. The reactions were analysed by 12.5% SDS-PAGE using the method described in 2.2.13.

## Materials and Methods

### **3.1 Identification of microorganisms from the contaminated salted ovine pelts**

#### ***3.1.1 Isolation of microorganisms from the contaminated ovine pelts***

The contaminated salted ovine pelts, once depilated, were processed through to leather following the conventional method. The resultant leather was of industrial quality, and had increased tensile strength when compared to leather depilated by the conventional sulfide/lime method. These results indicated that one or more of the contaminating microorganisms secreted one enzyme or a cocktail of enzymes that loosened the wool fibre allowing it to be removed cleanly from the skin. Importantly, there was little damage to the surrounding skin structure resulting in an undamaged leather product. These results are possibly due to the substrate specificity of the enzyme/s. The use of a specific enzyme product for depilation as an alternative method to chemical depilation is an aim that has long been desired in the industry. The first step in isolating this putative depilation enzyme/s is to identify the microorganism/s responsible for its production.

LB and Malt were chosen as both are non-selective media, and therefore reduce the chance of any favouritism towards a particular species or type of microorganism during the isolation process. Previous research by J.Filitcheva isolated *Wallemia ichthyophaga*, a xerophilic filamentous fungus, from the contaminated salted ovine pelts, and glycerol stocks of this possible depilation candidate were kindly donated (Filitcheva, *et al.*, 2011). A media used by Katherine Wilson, shown to enhance the growth of *W. ichthyophaga*, was therefore also chosen for the isolation process. This media will be referred to as Wilson's media. All media contained 20% NaCl as the contaminated pelts were stored as raw salted skins, achieved by applying excess salt granules directly onto the skin surface. It was therefore assumed that the target microorganism would have high salt tolerance in order to grow under these conditions. Two isolation methods involving either 1% agar plates or broths of each type of media mentioned above were investigated (Figure 3.1.1). All cultures were incubated at ambient temperature (25°C).

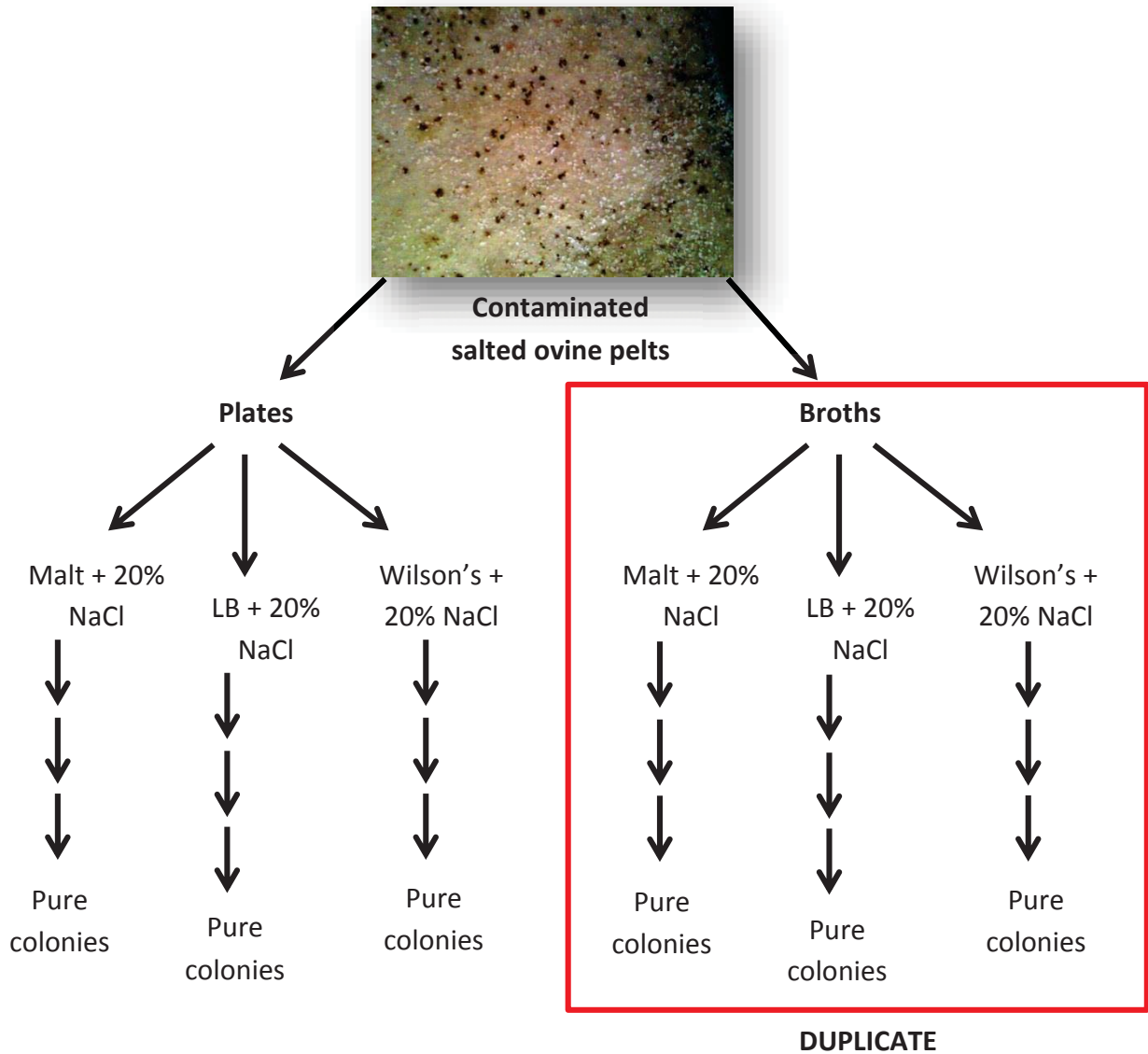


Figure 3.1.1: Methodology used to isolate the microorganisms from the contaminated salted ovine pelts. Cultures in broths were done in duplicate with a different pelt used for each replicate.

Colonies of different morphologies, obtained from the contaminated pelts after 1.5 months of incubation using either agar plates or broths, were re-plated on their respective media until pure cultures of each colony type were obtained (Figures 3.1.1 and 3.1.2). Glycerol stocks containing the *W. ichthyophaga* were also re-cultured under the same conditions. Each organism was then identified through sequencing either the 16S ribosomal RNA gene for bacteria, or the 18S ribosomal RNA gene for fungi.

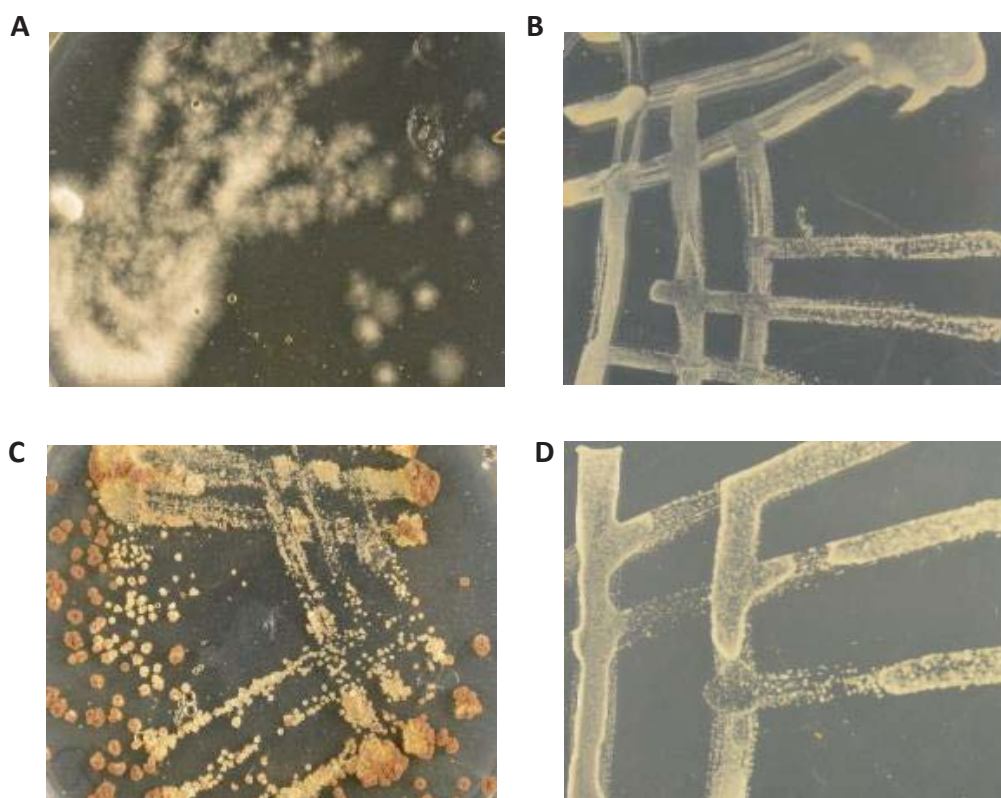


Figure 3.1.2: Examples of the different morphologies of colonies isolated from the contaminated pelts using both agar plates and broths of the three different media. A) *Phialosimplex* species. B) *Chromohalobacter*. C) *Wallemia ichthyophaga*. D) *Debaryomyces hansenii*.

Interestingly all genomic DNA templates extracted from the isolated microorganisms resulted in a PCR product when amplified with the 16S ribosomal RNA conserved primers. This PCR product originated from the Gram positive bacterium *Bacillus megaterium*, and was found even in DNA templates from the 'pure' isolate samples where the 18S ribosomal RNA gene was amplified, suggesting that all cultures were contaminated with this bacterium. Interestingly, multiple Gram stains of cells from each colony did not detect the presence of any Gram positive spore formers. This was not unexpected as apart from a few moderately halophilic *Bacillus* species such as *Bacillus halophilus* which can tolerate up to 15% NaCl, the *Bacillus* genus does not tolerate salt (Arahal & Ventosa, 2002).

## Results and Discussion

Furthermore, *Bacillus* species have been shown to be a common laboratory contaminant (Altayar & Sutherland, 2006; Drobniowski, 1994; Flint, Palmer, Bloemen, Brooks, & Crawford, 2001; Knisely, 1966). The resultant 16S rRNA PCR product is therefore most likely due to environmental contamination. When both the genomic DNA extractions and PCR reaction preparations were repeated in a class 1 fume hood, *Bacillus megaterium* 16S rRNA PCR products were not synthesised, consistent with the 'environmental contaminant' hypothesis.

### **3.1.2 Isolation of microorganisms from contaminated ovine pelts using agar plates**

Microorganisms from contaminated pelts, when directly transferred onto agar plates, resulted in the isolation of the budding yeast *Debaryomyces hansenii* on Wilson's media. No growth was observed on either the Malt or LB agar plates. Unexpectedly, *W. ichthyophaga*, previously isolated from the same pelts by J.Filitcheva, was not re-isolated from the pelts in this experiment. However, the organism was re-cultured on LB from glycerol stocks (Table 3.1.1).

Table 3.1.1: Summary of the microorganisms isolated from the contaminated salted ovine pelts using agar plates of various media incubated at 25°C.

Media	Microorganism source	Microorganism identification	Sequence similarity
Wilson's + 20% NaCl	Skin	<i>Debaryomyces hansenii</i>	100
Wilson's + 20% NaCl	Wool	<i>Debaryomyces hansenii</i>	100
LB + 20% NaCl	Glycerol stocks	<i>Walleimia ichthyophaga</i>	99

*Debaryomyces hansenii* is an osmotolerant yeast that has been isolated from environments with low water activity such as sea salt, wine, meat, and cheese (Gunde-Cimerman, Ramos, & Plemenitaš, 2009). In the laboratory, *D. hansenii* is

known to grow in media containing up to 4 M or 23% NaCl (w/v). This highly heterogeneous species is divided into two varieties; *D. hansenii* var. *fabryi* and *D. hansenii* var. *hansenii*. The two variants are commonly distinguished by their differing optimum growth temperatures, their ability to ferment different carbon sources, and their differing lipase and protease activities. *D. hansenii* is involved in the commercial production of surface-ripened cheeses. It deacidifies the culture medium by using lactic acid as a carbon source, promoting the growth of less acid-tolerant coryneform bacteria which are involved in the cheese ripening process. In addition, the proteolytic and lipolytic enzymes produced by *D. hansenii* directly aid in the ripening process. The culture supernatant of *D. hansenii* was therefore further investigated for depilation activity (Breuer & Harms, 2006).

### **3.1.3 Isolation of microorganisms from contaminated ovine pelts using broths**

Incubation of sections of the contaminated ovine pelt in broths of each medium resulted in the isolation of different microorganisms when compared to when agar plates were used. Overall, Wilson's media supported growth of filamentous fungi, while LB supported growth of bacterial species. Wilson's medium successfully re-isolated *Wallemia ichthyophaga*, along with two other filamentous fungal species from the genus *Phialosimplex*, while LB medium isolated two Gram negative rod-shaped bacteria, *Chromohalobacter marismortui* and *Chromohalobacter canadensis* (Table 3.1.2). Again no growth was observed on Malt media.

As discussed in the introduction, *W. ichthyophaga* is a xerophilic filamentous fungi from the phylum *Basidiomycetes*. This particular species is thought to be the most halophilic fungus discovered to date, requiring 9% NaCl to grow and tolerating saturated NaCl concentrations (Kuncic, *et al.*, 2010; Zajc, *et al.*, 2013). The salted skin conditions are therefore a fitting environment for the isolation of *W. ichthyophaga*, making this fungus a plausible candidate for the source of the depilation activity.

## Results and Discussion

Table 3.1.2: Summary of the microorganisms isolated from the contaminated salted ovine pelts by culturing in broths of different media incubated at 25°C.

Media	Microorganism source	Microorganism identification	Sequence similarity (%)
Wilson's + 20% NaCl	Skin with wool	<i>A Phialosimplex</i> species	100
Wilson's + 20% NaCl	Skin with wool	<i>Wallemia ichthyophaga</i>	99
Wilson's + 20% NaCl	Skin with wool	<i>A Phialosimplex</i> species	98
LB + 20% NaCl	Skin with wool	<i>Chromohalobacter marismortui</i>	97
LB + 20% NaCl	Skin with wool	<i>Chromohalobacter canadensis</i>	97

The genus *Phialosimplex* was first discovered in 2010, and was classified as belonging to the Trichocomaceae family, which is part of the phylum Ascomycetes (Sigler *et al.*, 2010). There are currently two species in this genus; *P. caninus* and *P. chlamydosporus*. Both species have been isolated from immunocompromised canines with systemic mycosis making research into this genus medically important (Sigler, Hanselman, Ruotsalo, Kar Tsui, & Richardson, 2013). Unexpectedly, a species from the *Phialosimplex* genus was isolated from a marine environment in 2012, and was shown to require NaCl for growth, tolerating at least 25% (w/v) NaCl (Ravindran *et al.*, 2012). The isolation of this halophilic fungus from the contaminated skins is therefore possible, but due to the pathogenic nature of this microorganism the secretome was not investigated.

Finally, *Chromohalobacter* is a moderately halophilic Gram-negative genus which contains bacteria that can grow in NaCl concentrations between 3% and 15%. This genus contains four species, and is classified under the family Halomonadaceae which is part of the Proteobacteria phylum (Sánchez-Porro, Tokunaga, Tokunaga, & Ventosa, 2007). The microorganisms isolated have only a 97% sequence homology to these four species, suggesting they are a new species from this genus (Stackebrandt & Goebel, 1994). Most research into the *Chromohalobacter* genus has been on its taxonomy, but several proteases and lipases from the different species in this genus have been purified and characterised (Kumar, Karan, Kapoor, Singh, & Khare, 2012; Prakash, Vidyasagar, Madhukumar, Muralikrishna, & Sreeramulu, 2009; Vidyasagar, Prakash, Jayalakshmi, & Sreeramulu, 2007). As *Chromohalobacter* is a relatively poorly characterised genus, it was unexpected that a species from this genus was isolated using media containing 20% NaCl. Nevertheless, its secretome was investigated for depilation activity.

### **3.1.4 Depilation activity**

10 cm<sup>2</sup> pieces of fresh sheep skin were incubated in the secretomes of each organism, isolated and identified from the salted ovine pelts as previously discussed, and depilation was monitored daily. If depilation was observed, the condition of the skin was examined using the SACPIC staining method (Figure 3.1.3.)

When all isolates, excluding the *Phialosimplex* species, were tested individually for depilation activity using fresh skin, only the secretome of *W. ichthyophaga* removed wool (Figure 3.1.4). Depilation was achieved in 72 hours, and as seen in the inset of figure 3.1.4, the epidermal layer was removed and the skin was undamaged. Due to the natural skin flora and general decomposition processes, the control incubations (skin in the respective medium) did depilate but only after six days of incubation. Methods of sterilising the skin samples such as ethanol, UV, and autoclaving, were investigated but either the skin was not sterilised or the skin was badly damaged

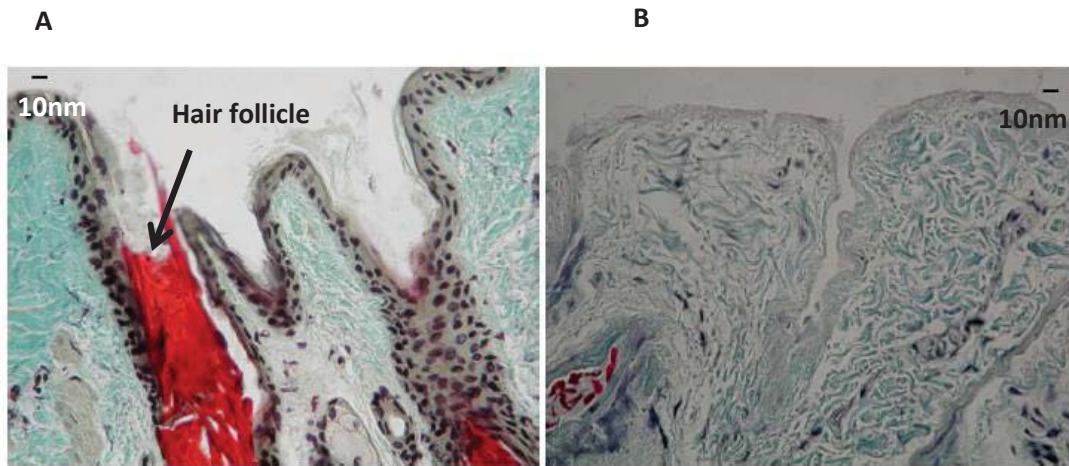


Figure 3.1.3: SACPIC staining method. A) an example of non-depilated skin. B) an example of depilated skin (R. Edmonds, 2008). Reprinted from Journal of Agricultural and Food Chemistry, R. Edmonds, Using proteomics, immunohistology, and atomic force microscopy to characterize surface damage to lambskins observed after enzymatic dewooling, Copyright (2008), with permission from Elsevier.

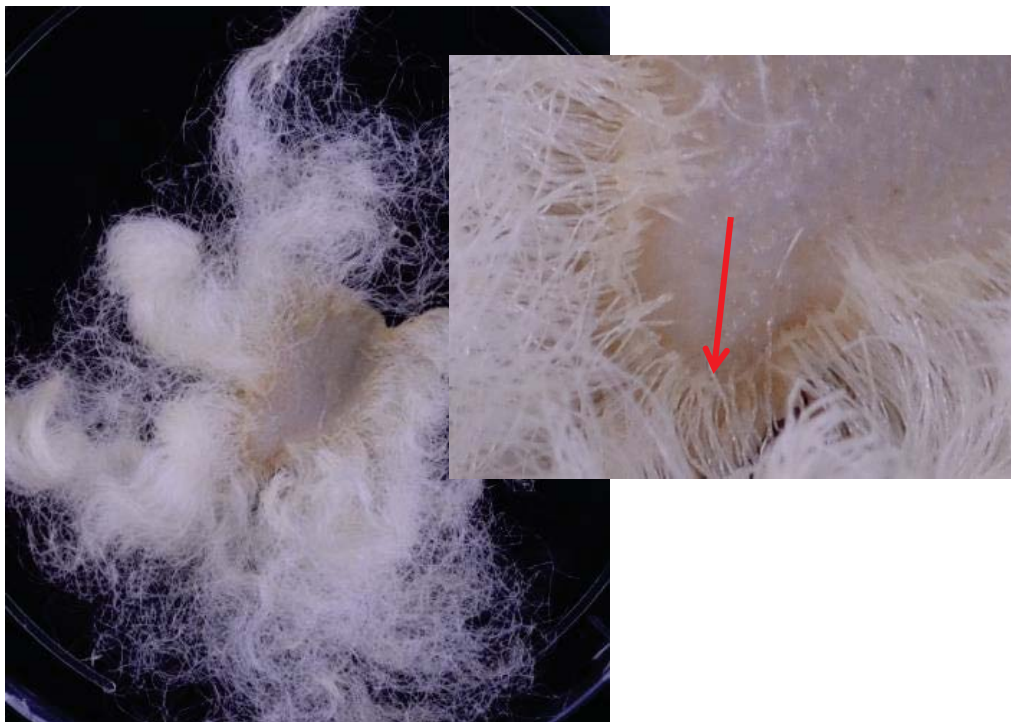


Figure 3.1.4: Fresh skin incubated in the secretome of *W. ichthyophaga* for 72 hours. The inset is a close-up of the depilated skin and shows the removal of the epidermal layer (red arrow).

The secretome of *W. ichthyophaga* was then concentrated using ultrafiltration, and then used to dewool a section of skin that was subsequently analysed using SACPIC (Section 2.2.11) (Figure 3.1.3). This time depilation was not observed. Further experiments using secretomes from different *W. ichthyophaga* cultures, attained from both sub-cultured colonies and colonies isolated during different experiments, also had no depilation activity *i.e.* the depilation observed in the initial experiments could not be replicated. Possible explanations for this phenomenon are: i) that a depilation specific *W.ichthyophaga* strain was isolated but lost during culturing, ii) the depilation enzyme was down-regulated upon removal of the substrate, and iii) the culture was not pure and a secondary contaminant, removed during sub-culturing, was the true source of the depilation activity.

### **3.1.5 Addition of dried ground ovine skin to Wilson's media**

To test the possibility that the depilation enzyme had been down-regulated in the absence of skin derived substrate/s, dried ground ovine skin was added to the media used to culture *W. ichthyophaga*. It was thought that this might stimulate protease production by providing missing substrate/s present in ovine skin. The addition of skin, however, had no effect on the depilation activity of the secretome, indicating that the loss of depilation activity is less likely to be due to the down-regulation of enzymes.

### **3.1.6 Origin of the depilation activity from *W. ichthyophaga***

Tracing the sub-cultured agar plates back to the original culture responsible for the depilation activity first observed, resulted in the identification of two possible agar plates. Upon further inspection, both plates contained a white mucoid growth coexisting with the *W. ichthyophaga* cells (Figure 3.1.5). This was identified as *D. hansenii*, a previously isolated contaminant. Unfortunately, when both pure and mixed cultures of *D. hansenii* and *W. ichthyophaga* were grown, and the resultant culture supernatants were incubated with fresh skin pieces, no depilation activity was observed. The other microorganisms previously isolated were also co-cultured with *W. ichthyophaga*, and tested with fresh skin, but once again no depilation occurred.

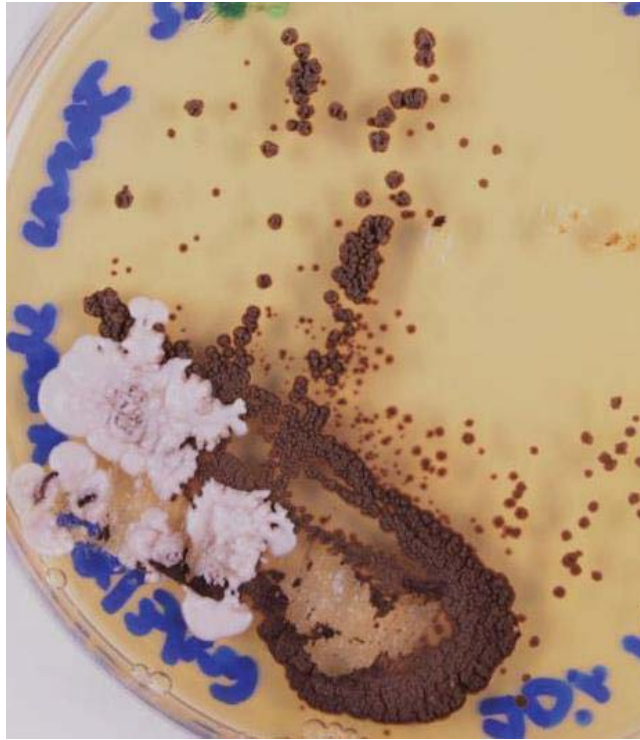


Figure 3.1.5: An example of a plate that may contain the isolates responsible for the initial depilation detected.

Finally, the whole original contaminated salted pelt was directly incubated in Wilson's media at 25°C for 2 months. The culture supernatant was then tested with fresh skin, but even this mixed culture failed to depilate. This would suggest that either the culture conditions did not support the growth of the microorganism/s responsible for the depilation activity or it was the environmental conditions that the pelts were kept in, rather than the microorganism themselves, that were responsible for the depilation.

### **3.2 Analysis of the protein composition of the secretome of *W.ichthyophaga* using in-gel tryptic digest and EIS-Q-TOF mass spectrometry.**

Due to *Wallemia ichthyophaga* being consistently isolated from the contaminated ovine pelts and the extreme salt tolerance of this fungus, the secretome was further investigated. Proteomic techniques are frequently used as a tool to analyse the protein composition of secretomes. The method used in this study involved an initial separation of the proteins in the secretome by 1D SDS-PAGE. Before SDS-PAGE analysis, the samples were de-salted and concentrated. Precipitation and ultrafiltration were investigated as possible methods. Once well-defined bands were obtained, they were then excised from the gel and identified using in-gel tryptic digestion followed by MS/MS.

#### **3.2.1 Secretome concentration via precipitation**

First precipitation, often used to clean up a pellet before it is digested with trypsin for proteomic analysis, was chosen as a method of desalting and concentrating the secretome of *W.ichthyophaga*. Ethanol and acetone, weak precipitating reagents, both normally remove excess salts upon precipitation of the proteins, but when either was added to the secretome, NaCl precipitated along with the protein. Ethanol and acetone were thus deemed to be unsuitable to clean up the secretome. TCA-acetone, a stronger precipitating reagent, was then tested, and when mixed with the secretome, precipitated the protein content but not the NaCl. The pellet was then resolubilised in a minimum volume 10  $\mu$ L of 10% SDS, along with 2  $\mu$ L loading dye, before being analysed by SDS-PAGE. Most of the bands were sharp, showing no smearing, apart from in the high molecular weight region where the bands were more diffuse.

Overall, the protein composition appeared to be simple enough to analyse using 1D SDS-PAGE rather than 2D SDS-PAGE. The secretome contained proteins and/or protein subunits between the molecular weights of 20 kDa and 100 kDa, with the majority of proteins having molecular weights over 50 kDa. Not all proteins were

## Results and Discussion

resolubilised as indicated by the three bands in lane 1, even in 10% SDS (Figure 3.2.1).

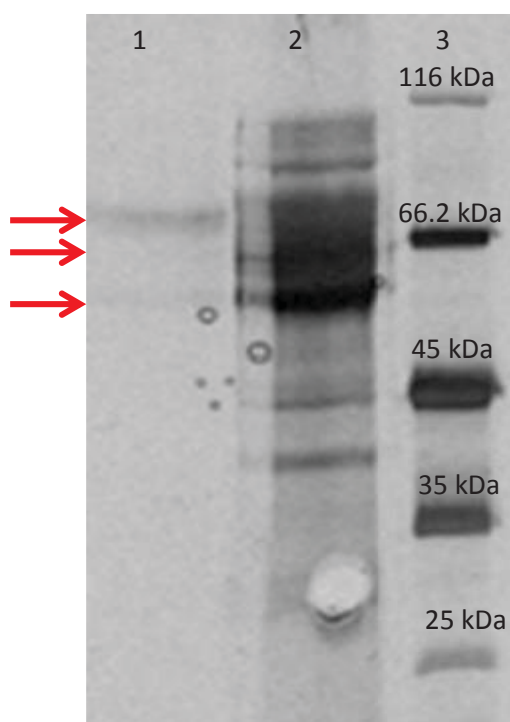


Figure 3.2.1. 7.5% acrylamide gel of the supernatant (Lane 1) and pellet (Lane 2) from the TCA-acetone precipitation of the secretome of *W.ichthyophaga*, silver stained. Lane 3 contains the standard marker. Arrows indicate unsolubilised proteins.

### **3.2.2 Secretome concentration via ultrafiltration**

An alternative method for concentrating and desalting secretomes is to use ultrafiltration. The advantage of this method is that the proteins remain in their native fold therefore maintaining enzymatic activity. Unfortunately, proteins can bind to the filter or to the plastic of the ultrafiltration device. An ultrafiltration device with a 10 kDa MWt cut off was used. This cut off value was chosen as the TCA-acetone precipitation gel (Figure 3.2.1.) showed that the most abundant secreted proteins were all above 10 kDa.

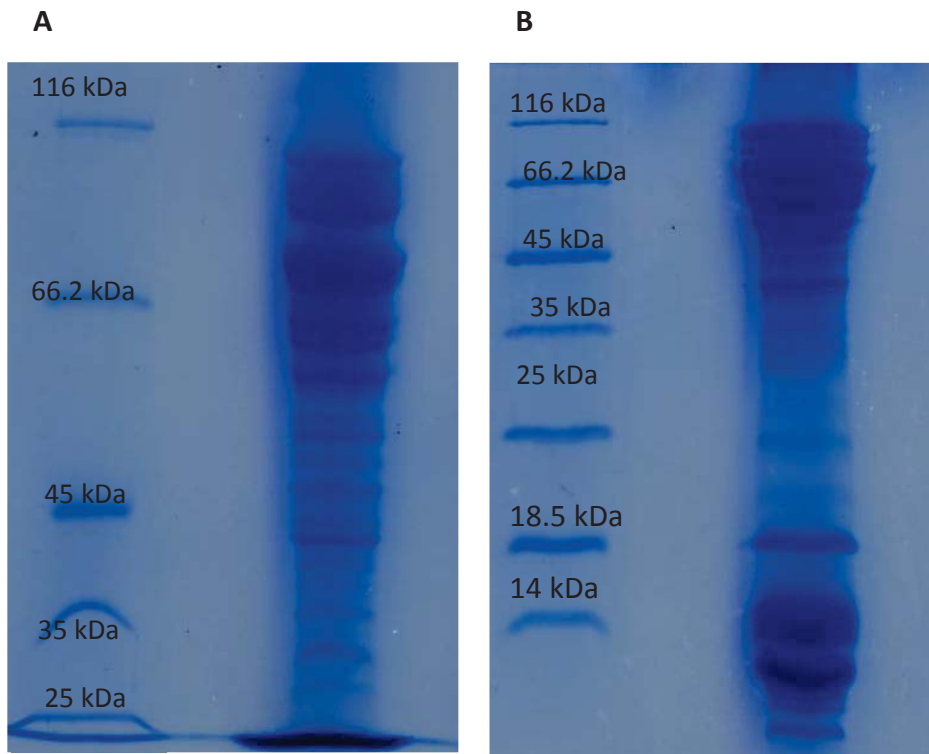


Figure 3.2.2: SDS-PAGE gel of a secretome from a 2 month old *W.ichthyophaga* culture grown in Wilson's media made 20% with NaCl, and desalted by ultrafiltration. The gel is stained in Colloidal Coomassie. A) 7.5% Acrylamide gel: Lane 1: marker, and Lane 2: secretome. B) 15% Acrylamide gel: Lane 1: marker, and Lane 2: secretome.

Ultrafiltration successfully desalted and concentrated the secretome as shown in figure 3.2.2, where SDS-PAGE analysis shows a series of well resolved bands. The 7.5% gel was used to resolve the high molecular weight region (lefthand gel in Figure 3.2.2), while the lower molecular weight proteins were resolved on a 15% gel (righthand gel in Figure 3.2.2) The similarities in the band patterns between figure 3.2.1 and 3.2.2 suggest that, loss of protein through binding to the ultrafiltration device was minimal. The 15% gel resolved proteins with molecular weights below 20 kDa that were not seen on the 7.5% gels. Bands with molecular weights lower than 10 kDa could possibly represent i) subunits of proteins of greater molecular weight or ii) aggregates of proteins with molecular weights lower than 10 kDa, that

have now been separated by SDS. These experiments showed that the best method for desalting and concentrating the secretome of *W.ichthyophaga* is ultrafiltration. It can also be concluded that colloidal Coomassie was sufficiently sensitive to detect the proteins. This is important as proteins stained with colloidal Coomassie (G-250) can be successfully destained and identified by mass spectrometry, in contrast to the more conventional Coomassie stain, that is difficult to remove from the protein bands, and has a potential to interfere with the analyses of the proteins by mass spectrometry.

### **3.2.3 Addition of dried ground ovine skin**

As *W.ichthyophaga* was isolated from ovine pelts, it was important to investigate if the presence of extra protein in the media would induce the production of proteases in the secretome, as it is known that fungi readily adapt to their environments by modulating the battery of extracellular enzymes that they produce (Girard, *et al.*, 2013).

Again ultrafiltration was used to desalt and concentrate the secretome, but the addition of skin caused the membrane to clog. The resultant concentrate had a gelatinous consistency, and both ultracentrifugation and solvent precipitation failed to produce a protein pellet. The change in consistency was most likely due to dissolved collagen from the ground skin forming a gel that could not easily be removed. This notion was supported by SDS-PAGE which showed only a smear rather than well resolved bands. Undoubtedly proteases were involved in the breakdown of collagen, but unfortunately without the presence of skin, the proteases were not secreted.

### **3.2.4 Protein identification through mass spectrometry**

To reduce the complexity of proteomic analysis, proteins are commonly pre-fractionated, either by SDS-PAGE or by 2D chromatography, before being analysed by mass spectrometry. A complex proteome is usually fractionated before analysis to increase the number of proteins identified. Trypsinolysis of a very complex sample can lead to misinterpretation due to overlapping peaks, peak broadening,

## Results and Discussion

and multiple charged states of larger peptides. Also, as some peptides produced from a protein by trypsin may not be unique to that protein, misidentification is possible. Thus fractionating before trypsinolysis simplifies the spectra, and prevents misinterpretation. Using 1D PAGE to pre-fractionate however presents its own series of problems. This is because a protein may be seen in the gel as an intact protein, and also as a fragment of lower molecular weight as a result of proteolysis occurring *in situ*, or during isolation. For this reason, all fractions, in other words all the peptides identified from all the bands on the gel, were combined. Accuracy using the proteomics approach is therefore achieved by establishing a balance between enough peptides being present for a reliable identification, and reduction in the protein complexity of the secretome to reduce misidentification.

Both biological and technical replicates were performed on the secretome of *W.ichthyophaga*. The biological replicates involved three genetically distinct colonies/secretomes being analysed, while the technical replicates involved each band from these secretomes being analysed twice by mass spectrometry. Figure 3.2.3 shows that, under the same growth conditions, colonies of *W.ichthyophaga* will secrete similar proteins. This was expected as protein regulation is dictated by both resource availability and environmental conditions such as temperature and pH (Girard, *et al.*, 2013), which were consistent for all three colonies. The bands that were excised and labelled per colony are shown in figure 3.2.4.

## Results and Discussion

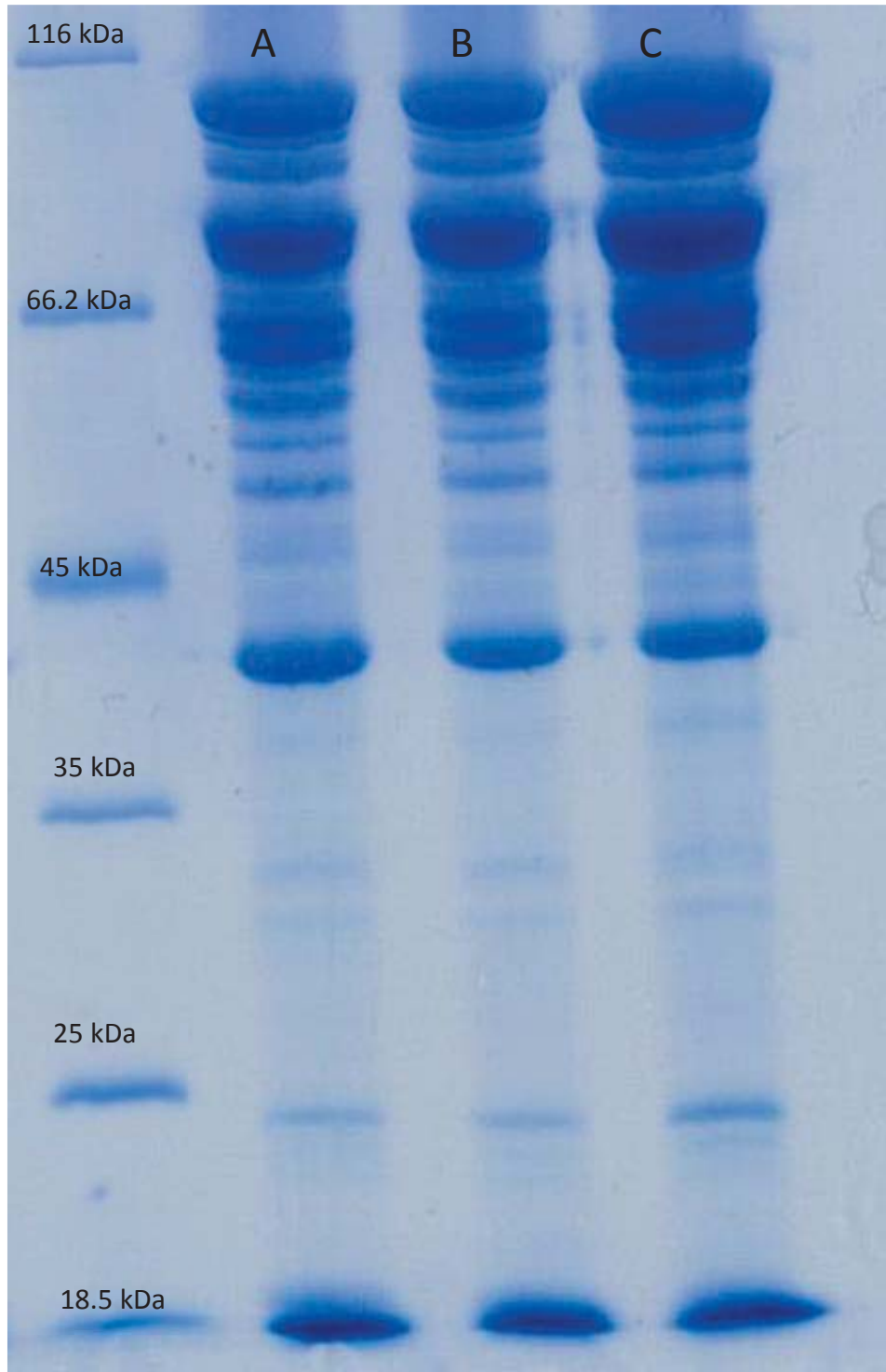


Figure 3.2.3: *Wallemia ichthyophaga* secretome composition from cultures started from 3 individual colonies (Lanes A, B, and C) analysed by 7.5% SDS-PAGE and stained with colloidal Coomassie.

## Results and Discussion

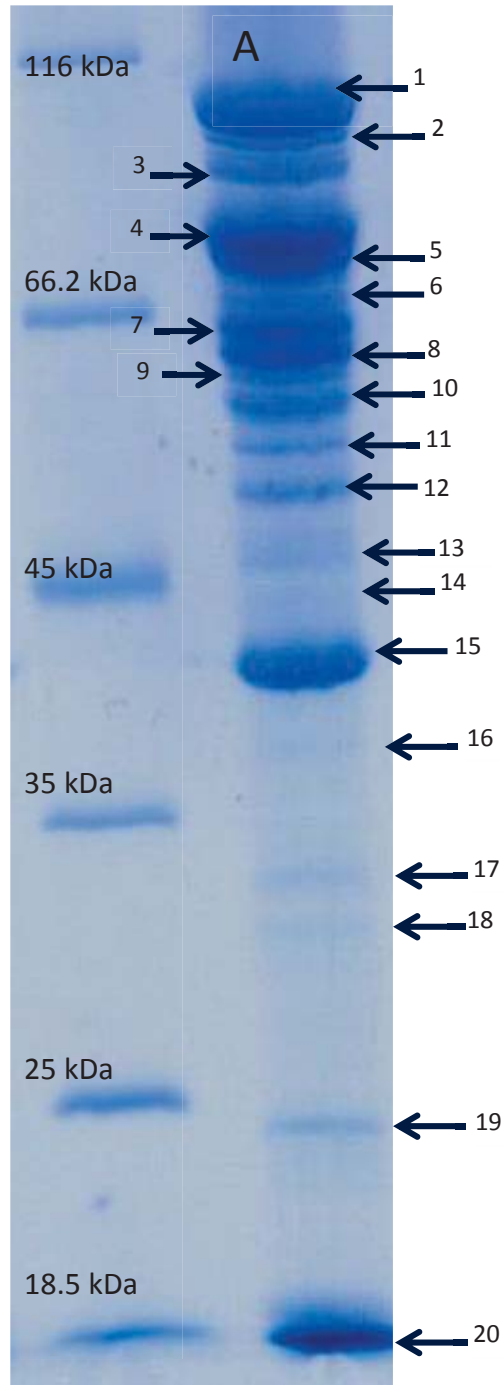


Figure 3.2.4: 7.5% acrylamide gel of the secretome of a *W.ichthyophaga* culture grown from colony A. Bands analysed by mass spectrometry are indicated by arrows.

## Results and Discussion

The resultant peptide mass and peptide sequence lists for each band were searched against the *Wallmeiomycetes* database which contains the genome sequences of *W.sebi* and *W.ichthyophaga*. The cRAP database, from Mascot, was also added to the *Wallmeiomycetes* database. This database contains commonly encountered contaminants that result from the isolation and digestion processes such as peptides from human keratin and trypsin fragments (autolysis). Including it allows peptides matching these proteins to be excluded. The databases were searched using the X!tandem search engine via Labkey, the Massey University local server.

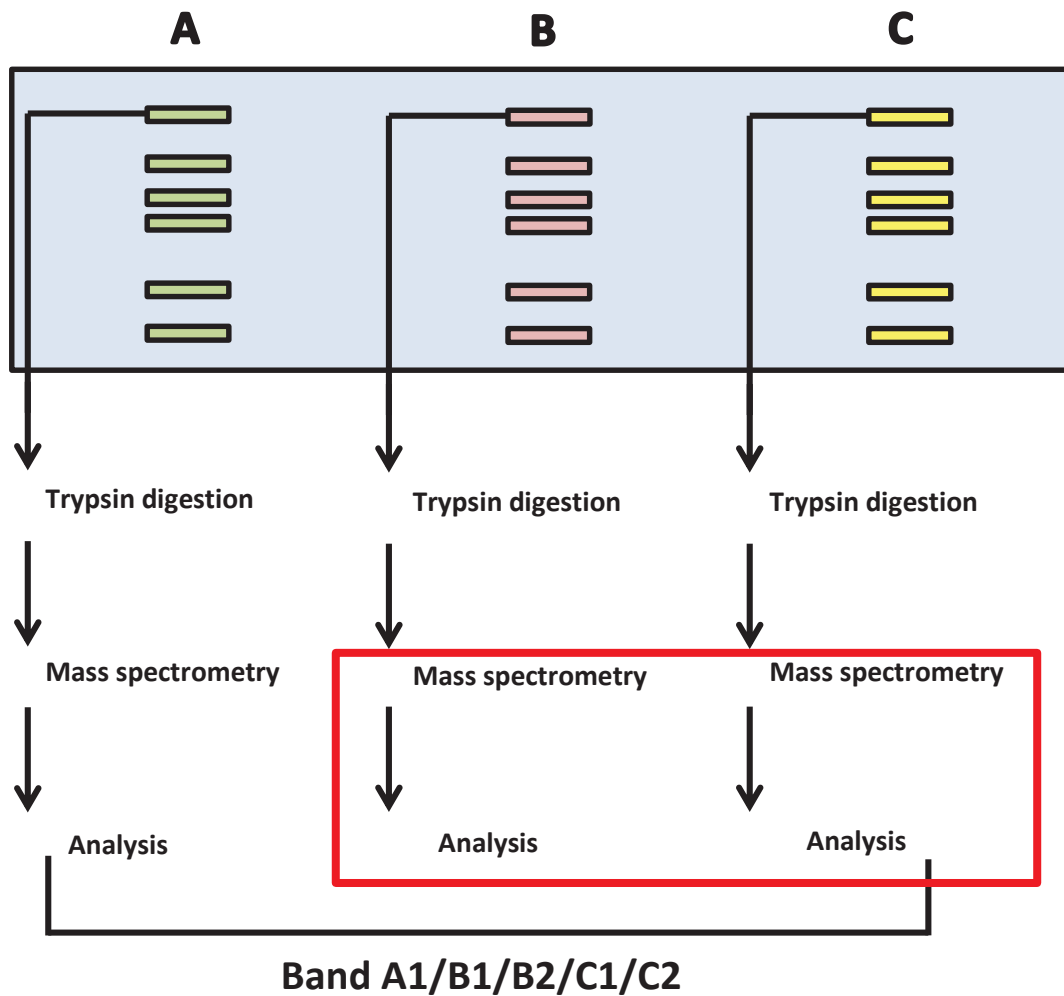


Figure 3.2.5: Methodology used to analyse each band from the SDS-PAGE gel of the whole secretome of *W. ichthyophaga*, using in-gel tryptic digestion and mass spectrometry of cell colonies A, B, and C. The red box represents the steps repeated per duplicate.

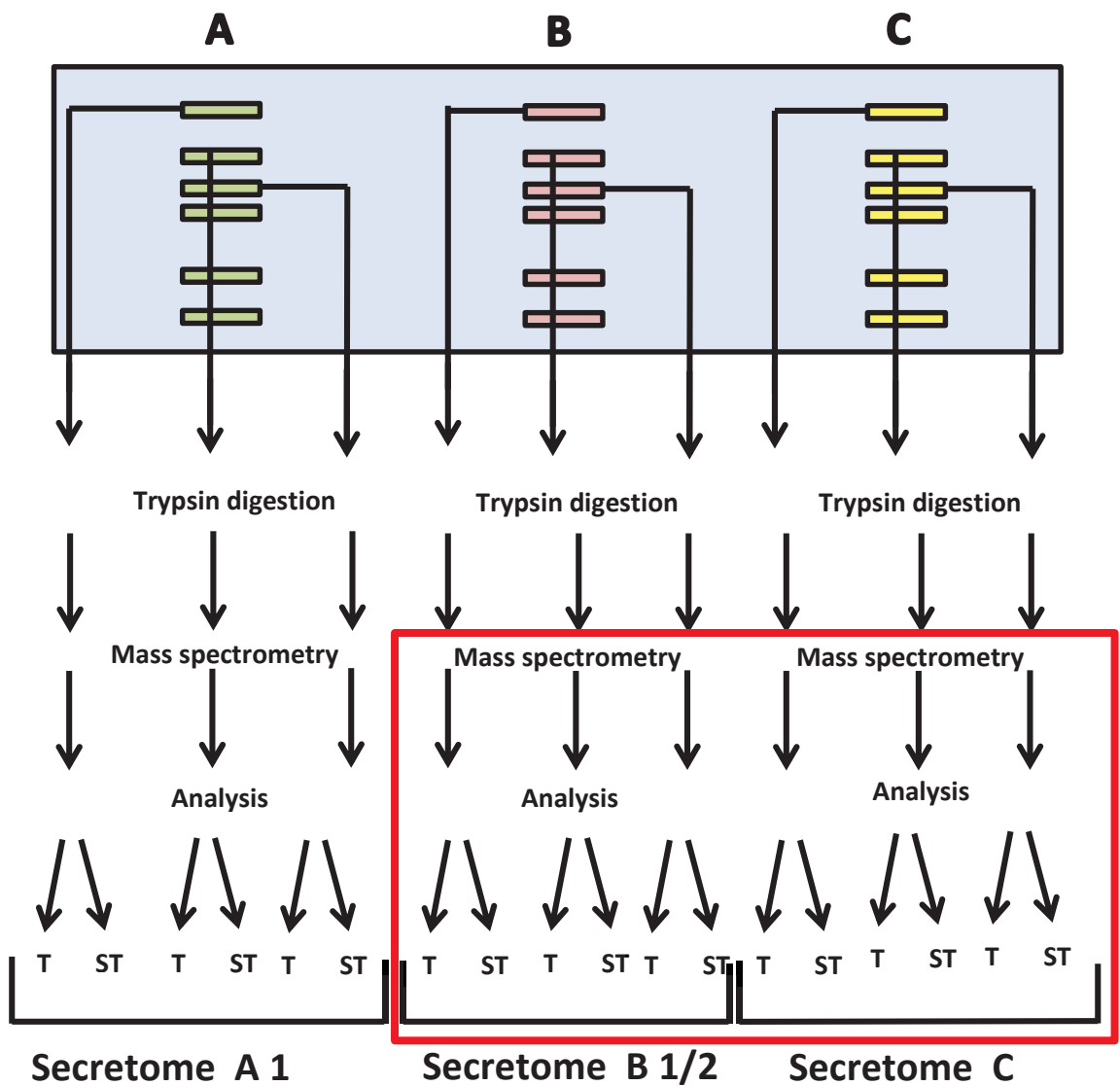


Figure 3.2.6: Methodology for the analysis of the proteins present in the whole secretome of *W. ichthyophaga*, using in-gel tryptic digestion and mass spectrometry of cell colonies A, B, and C. The red box represents the steps repeated per duplicate. T= Trypsin digestion. ST= Semi-trypsin digestion.

Overall, five different samples were analysed; secretome A (A1), secretome B technical replicate 1 (B1), secretome B technical replicate 2 (B2), secretome C technical replicate 1 (C1), and secretome C technical replicate 2 (B2). Two methods of analyses were used: first the whole secretome of each sample was analysed

(Figure 3.2.6), then each band across all samples was analysed (Figure 3.2.5). For the whole secretome, each band in each lane was excised, digested with trypsin, and subjected to nano HPLC followed by mass spectrometry analysis. The data produced from each band in each lane was analysed using Mascot specifying first trypsin then semi-trypsin as the protease used. For identification, the *Wallemiomycete* + cRAP database was used, and the masses and sequences found in each band within a lane, for both trypsin and semi-trypsin digestion, were combined for the search (Figure 3.2.6). Only proteins identified in all five samples were accepted as being present in the secretome (Table 3.2.2).

Individual analysis of the bands used slightly different search criteria in which only semi-trypsin was defined as the protease. The masses and sequences from each band for all five samples were then combined, and compared to the *Wallemiomycete* + cRAP database for identification. This was repeated for all 20 bands (Figure 3.2.5). Proteins present in at least 3/5 of the samples were accepted as being present in the secretome. The proteins identified are listed in table 3.2.2. All proteins identified from the whole secretome analyses method were identified in the individual band analysis method, but the proteins in italics (Table 3.2.2) were only identified in the individual band analysis *i.e.* identified in 3/5 or 4/5 samples.

### **3.2.5 Molecular weight of secreted proteins using SDS-PAGE**

Molecular weight markers on a denaturing gel can be used to create a standard curve relating the RF value of protein bands to the log of their molecular weight. The RF value is the ratio between the distance travelled by the dye front in centimetres (cm) and the distance travelled by the protein band in centimetres. The molecular weight of the protein bands (Table 3.2.1) in the corresponding lanes of each secretome sample, can then be estimated from this standard curve (Figure 3.2.7). This provides another check on the proteins identified in each band by mass spectrometry.

## Results and Discussion

Table 3.2.1: Molecular weight of each band of the SDS-PAGE of the secretome of *W. ichthyophaga* using a standard curve.

<b>Band number</b>	<b>Molecular weight (KDa)</b>
1	91.3
2	87.5
3	83.8
4	77.9
5	74.6
6	71.5
7	68.4
8	65.5
9	63.7
10	61.9
11	58.4
12	54.3
13	51.3
14	49.8
15	43.1
16	38.4
17	32.3
18	29.6
19	22.8
20	17.6

## Results and Discussion

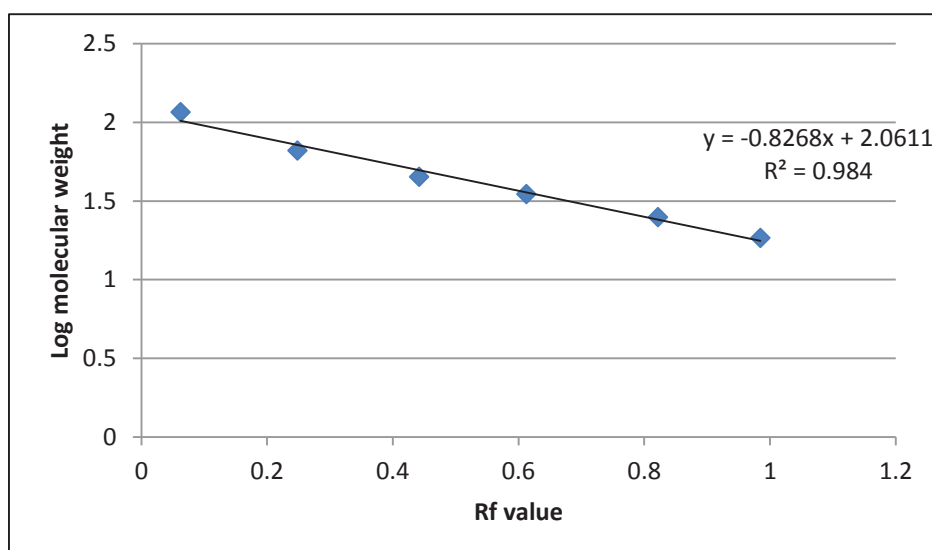


Figure 3.2.7: Standard curve of the size marker from the SDS-PAGE of the secretome of *W.ichthyophaga*.

### 3.2.6 Mass spectrometry results of the secreted proteins from *W.ichthyophaga*

Table 3.2.2: Proteins identified in the secretome of *W.ichthyophaga*

Band number	Band MWt (kDa)	Mass spectrometry (MWt in kDa)	Protein identified by mass spectrometry	Protein accession number
1	91.3	86.2	Putative $\beta$ -glycosidase L	EOQ98916.1
2	87.5	86.2	Putative $\beta$ -glycosidase L	EOQ98916.1
		87	<i>putative beta-glucosidase G</i>	EOR02940.1
3	83.8	86.2	Putative $\beta$ -glycosidase L	EOQ98916.1
		93.2	Choline dehydrogenase	EOQ99109.1
		107.5	$\alpha$ -glycosidase	EOR01404.1
4	77.9	86.2	Putative $\beta$ -glycosidase L	EOQ98916.1
		107.5	$\alpha$ -glycosidase	EOR01404.1
5	74.6	86.2	Putative $\beta$ -glycosidase L	EOQ98916.1

## Results and Discussion

		62	3-phytase A	EOQ99308.1
		107.5	$\alpha$ -glycosidase	EOR01404.1
<b>6</b>	71.5	86.2	Putative $\beta$ -glycosidase L	EOQ98916.1
		107.5	$\alpha$ -glycosidase	EOR01404.1
<b>7</b>	68.4	107.5	$\alpha$ -glycosidase	EOR01404.1
<b>8</b>	65.5	58.8	Putative invertase	EOQ98970.1
		107.5	$\alpha$ -glycosidase	EOR01404.1
<b>9</b>	63.7	58.8	Putative invertase	EOQ98970.1
		107.5	$\alpha$ -glycosidase	EOR01404.1
<b>10</b>	61.9	59.7	Delta-1-pyrroline-5-carboxylate dehydrogenase	EOR03614.1
<b>11</b>	58.4	57.7	Hypothetical protein	EOQ99297.1
<b>12</b>	54.3	57.7	Hypothetical protein	EOQ99297.1
		47.1	$\alpha$ -glycosidase	EOR01404.1
<b>13</b>	51.3	51	Hypothetical protein	EOQ98965.1
<b>14</b>	49.8	92.2	tRNA (adenine(58)-N(1))-methyltransferase non-catalytic subunit TRM6	EOQ99196.1
		46	Glucan 1,3-beta-glucosidase	EOQ99558.1
<b>15</b>	43.1	92.2	tRNA (adenine(58)-N(1))-methyltransferase non-catalytic subunit TRM6	EOQ99196.1
		46	Glucan 1,3-beta-glucosidase	EOQ99558.1
		39.7	3-isopropylmalate dehydrogenase	EOR00095.1
		183.8	<i>Chitin synthase 1</i>	EOR04866.1
<b>16</b>	38.4	92.2	tRNA (adenine(58)-N(1))-methyltransferase non-catalytic subunit TRM6	EOQ99196.1
		36.2	Transaldolase	EOQ99355.1

## Results and Discussion

<b>17</b>	32.3	35	Glutathione S-transferase omega-like 2	EOQ98849.1
<b>18</b>	29.6	28	<i>putative proteasome subunit alpha type-5</i>	EOQ98832.1
		56.9	Bleomycin hydrolase	EOR01765.1
		49.8	<i>Transforming growth factor- beta-induced protein ig-h3</i>	EOR01805.1
<b>19</b>	22.8		No proteins identified	
<b>20</b>	17.6	16.5	Glia maturation factor beta	EOQ99163.1
		26.1	Glucosamine 6-phosphate N- acetyltransferase 1	EOR04057.1
		17.8	<i>Lactoylglutathione lyase</i>	EOR00764.1

Note: protein names in *italics* are found in 3 or 4 of the samples but not all 5.

# band MWt (kDa) values obtained from the SDS-PAGE gel of the secretome (Figure 3.2.4)

From this work, the secretome of *W.ichthyophaga* seems to be mainly dominated by carbohydrate hydrolases. Glycosidases identified with high confidence were a putative  $\beta$ -glycosidase L, a putative  $\beta$ -glycosidase G, an invertase, and a glucan 1-3- $\beta$ -glucosidase, along with one  $\alpha$ -glucosidase. Interestingly, no proteases were identified in the secretome, apart from bleomycin hydrolase which is an intracellular protease, and highly specific to bleomycin (Joshua-Tor, Xu, Johnston, & Rees, 1995). It would therefore not hydrolase the Azocol substrate used to assess protease activity. This lack of protease activity was unexpected as the epidermal skin layer alone contains at least 60% collagen, as well as elastin and other numerous glycoproteins. One would therefore expect at least some protease activity given the type of environment that *W.ichthyophaga* was isolated from. This finding was supported by the general protease assay performed, using the whole secretome, which did not show any activity. There were also no lipases or esterases identified, even though these were detected using general assays. It is most likely that these proteins were lost or degraded during separation and/or processing.

## Results and Discussion

Choline dehydrogenase was also identified in the secretome of *W.ichthyophaga*. This was unexpected as this intracellular membrane bound enzyme is found in eukaryotes and bacteria but not in fungi (Roeßler & Müller, 2001). Choline dehydrogenase has been grouped into the super family glucose-methanol-choline (GMC) oxidoreductase, through sequence alignment alone, even though the presence of a flavin-binding domain, characteristic of this family, has not yet been confirmed. Choline dehydrogenase is involved in the catalysis of choline to glycine-betaine via a betaine-aldehyde intermediate (Gadda & McAllister-Wilkins, 2003). Glycine-betaine is an osmoprotectant, and is used by salt tolerant organisms as a compensatory mechanism for the osmotic stress encountered through intracellular accumulation, and has been used to engineer salt tolerant plants. (Lilius, Holmberg, & Bülow, 1996).

There have been no choline dehydrogenase genes or proteins identified in fungi. However, cellobiose dehydrogenase, another member of the GMC oxidoreductase family, has been extensively studied in fungi. This secreted enzyme is used to degrade cellulose, a  $\beta(1-4)$  linked glucose polysaccharide produced by green plants, algae, and oomycetes (Zámocký, Hallberg, Ludwig, Divne, & Haltrich, 2004) as a carbon source. The presence of a choline dehydrogenase in *W.ichthyophaga*, while unlikely, could explain the high salt tolerance of this fungus, and may have retained this enzyme from distant ancestors during evolution due to environmental pressures. Alternatively, this protein may have been misidentified as choline dehydrogenase rather than cellobiose dehydrogenase, as both proteins are in the same superfamily. However, this alternative scenario is unlikely due to the very strict parameters used for data analysis, and that the peptides identified as belonging to choline dehydrogenase were scattered throughout the sequence, rather than a section of the protein *i.e.* a shared flavin-binding domain.

A phytase was also identified in the secretome of *W.ichthyophaga*. Phytate (myo-inositol hexakisphosphate) is the main form of organic phosphate storage in plants, and contributes to 20-50% of the total soil phosphate reservoir (Sajidan *et al.*, 2004). Both fungi and bacteria obtain this stored phosphate through the secretion

## Results and Discussion

of phytases (Lassen *et al.*, 2001). Phytases are grouped into histidine acid phosphatases, plant purple acid phosphatases, and *Bacillus* beta-propeller phytases (Sajidan, *et al.*, 2004), as well as being classified by the specific position of the phosphate ester bond that they hydrolyse. The phytase (3-phytases A) identified in the secretome of *W.ichthyophaga* is a member of the histidine acid phosphatase family, and cleaves the phosphate group at position 3 (Figure 3.2.8) (Berka, Rey, Brown, Byun, & Klotz, 1998). It is possible that this enzyme is present in the secretome of *W.ichthyophaga* as a mechanism for obtaining phosphate from the environment. Although unlikely, it is possible that this enzyme is responsible for the lipase/esterase activity detected in the secretome using the general substrate *p*-nitrophenyl-butyrate, which has a particularly labile ester bond. The high salt tolerant or possible xerophilic phytase may be of interest to the livestock industry as a way to minimise the phosphate levels present in monogastric animals' manure through addition of the enzyme to feed (Lassen, *et al.*, 2001).

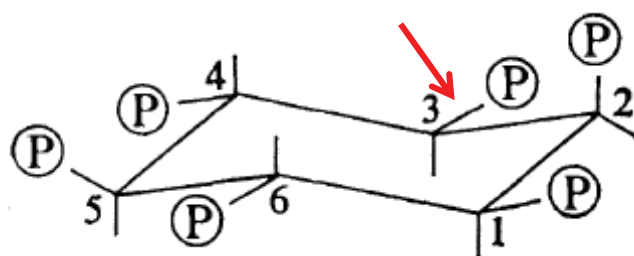


Figure 3.2.8: Structural diagram of phytate, the substrate cleaved by phytases. P=phosphate groups with corresponding numbers (Johnson & Tate, 1969). The phytase identified in the secretome of *W.ichthyophaga* cleaves at position 3, as indicated by the red arrow. Reprinted from Canadian Journal of Chemistry, Vol 47, L. Johnson, Structure of "phytic acids", Copyright (1969), with permission from Elsevier.

As previously mentioned, an invertase ( $\beta$ -D-fructofuranoside-fructohydrolases) was identified in the secretome. This family of glycosylated enzymes hydrolyses the  $\beta$ (1-

2) linkage in sucrose to release glucose and fructose. Invertases have been mainly studied in yeast, along with some fungi, and have been classified as belonging to the GH32 family of glycosidases due to the presence of a N-terminal  $\beta$ -propeller domain and a C-terminal  $\beta$ -sandwich domain (Aranda *et al.*, 2006) (Kadowaki, de Cassia Garcia, da Conceicao Silva, & Aoki, 2013). Invertases are commonly used in the food industry, for example in the production of jams and candies, to prevent crystallisation of the sugars preventing 'grittiness', or in the conversion of fondant to liquid for the production of liquid filled chocolates (Dial & Moore, 1997; Saulo, 2002). It is therefore not surprising that an invertase is present in the secretome of *W.ichthyophaga*, as it would enable the organism to utilise sucrose as a carbon source. This enzyme is known to be glycosylated which would explain the difference between the observed molecular weight from the SDS-PAGE data, and the molecular weight of the protein that was identified from mass spectrometry of the band.

Interestingly,  $\Delta$  1-pyrroline-5-carboxylate dehydrogenase (P5CDH), an enzyme that belongs to the aldehyde dehydrogenase super-family (Sophos & Vasiliou, 2003) which catalyses the second step in the degradation of proline, was identified in the secretome. In this pathway proline is first converted to  $\Delta$  1-pyrroline-5-carboxylate by proline dehydrogenase (ProDH), and then converted to glutamate by P5CDH (Elthon & Stewart, 1981). Both ProDH and P5CDH are mitochondrial enzymes, and control the levels of internal proline. High levels of internal proline have been associated with drought tolerance in plants, while high levels of external proline have been shown to induce apoptosis (Deuschle *et al.*, 2001). It would seem counterintuitive that P5CDH is present in *W.ichthyophaga*, but the accumulation of glutamate, the end product from P5CDH, is associated with resistance to osmotic stress. This mechanism to protect against osmotic pressure through an osmoprotectant has been observed in *W.ichthyophaga* before through glycerol accumulation. Glutamate could therefore be an additional or alternative osmoprotectant used by this fungus, regulated by environmental conditions (Hua, Lichens, Guirao, & Tsai, 1986).

## Results and Discussion

The transforming growth factor-beta-induced protein (TGFB1p) has only so far been identified in invertebrates, and on this basis it is very unlikely to be present in the secretome of *W.ichthyophaga*. However, the fasciclin (FAS) domain, that is present in four copies for TGFB1p, is found in other membrane bound and extracellular proteins, and furthermore, has been identified in fungi (Andersen *et al.*, 2004; Paulsrud & Lindblad, 2002). Thus any protein containing the FAS domain may mistakenly be identified by mass spectrometry as TGFB1p. This would explain the large molecular weight difference observed between the SDS-PAGE data, which gave a molecular weight of 29.6 kDa, and mass spectrometry data, which gave a molecular weight of 49.8 kDa. This is because the FAS domain alone, from the FAS domain containing protein, could provide enough peptides to misidentify it as TGFB1p. This is supported by the peptides from the sample matching only a section of the protein identified by mass spectrometry, rather than across the whole sequence, which is most likely a shared FAS domain.

A large portion of the proteins identified in the secretome of *W.ichthyophaga* were fungal intracellular proteins: isopropylmalate dehydrogenase, a fragment of chitin synthase, *transaldolase*, tRNA methyltransferase subunit, putative proteasome subunit, glutathione S-transferase omega-like 2, bleomycin hydrolase, Lactoylglutathione lyase, and glucosamine 6-phosphate N-acetyltransferase 1. A possible explanation is that these proteins are released into the secretome, upon cellular lysis, and because they are present at high cellular concentrations, are detected by mass spectrometry. Only glia maturation factor beta which is predominantly found in astrocytes (Lim, Zaheer, Yorek, Darby, & Oberley, 2000), has been possibly misidentified.

### **3.3 Purification of a novel glycosidase enzyme from the secretome of *Wallemia ichthyophaga*.**

#### **3.3.1 Anionic and cationic chromatography**

The first step in ionic exchange chromatography (IEX) was to determine whether anionic or cationic resin (solid phase) would bind the protein of interest; CM sephadex (GE Healthcare, cation exchange) and Q sephadex (GE Healthcare, anion exchange) were chosen. To find the binding conditions, pH 7.0 was initially used to determine whether the pI of the protein was acidic or basic. In most cases the buffering ions need to be the same charge as the functional groups of the IEX resin to prevent the ions partaking in the ion exchange process, therefore two different buffer systems were chosen, one for each type of resin. For cation exchange chromatography (CEX) 10mM sodium phosphate pH 7.0 was used, while for anion exchange chromatography (AEX) 10mM HEPES pH 7.0 was used. The use of HEPES, a zwitterion, does contradict this common practice, but this rule does not apply in all cases (Scopes, 1994). The conductivities of these buffers were 1.276 mS/cm and 200  $\mu$ S/cm respectively.

Before the secretome was incubated with the solid phase both the conductivity and pH were adjusted to match the IEX conditions. The secretome used was from a broth of *Wallemia ichthyophaga* cultured in Wilson's media made 20% NaCl with the addition of 1% (w/v) dried ground ovine skin (refer to section 3.1.5), that had been incubated at 25°C for 2 months without shaking. The broth was first filtered through glass wool to remove large cellular debris. The pH of the resultant media was pH 5.5 which was adjusted to pH 7 using 0.1 M sodium hydroxide. The resultant conductivity was 197.9 mS/cm, as measured on a conductivity meter E-14 (Horiba), and was 1000 fold greater than the lowest conductivity of the two buffers selected for IEX, and was adjusted accordingly.

200 mL of appropriately equilibrated secretome was then split evenly between 40 mL of each solid phase, Q sephadex resin for anionic and CM sephadex resin for cationic, and incubated overnight with rotation at 4°C. The protein content the

unbound fraction *i.e.* the buffer solution was measured using the Bradford assay. (Table 3.3.1)

Table 3.3.1: Protein concentrations of unbound fractions from CEX and AEX fractionation

Fraction	Bradford assay (absorbance at 595nm)
Secretome	0.174
Q unbound fraction	0.022
CM unbound	0.120

Only 30% of the protein present in the secretome of *Wallemia ichthyophaga* at pH 7.0 bound to the CM resin (Figure 3.3.1B), in contrast to the 89% that bound to the Q resin (Figure 3.3.1A). Anion exchange chromatography was therefore chosen as the first step to fractionate the secretome of *W.ichthyophaga*.

### 3.3.2 Optimisation of anion exchange chromatography

Addition of 1% (w/v) dried ovine skin to the media, in an attempt to induce the secretion of potential depilating enzymes by *W.ichthyophaga*, failed to enhanced depilation activity of the secretome. Furthermore, the addition of dried skin increased the complexity of the protein content to such an extent that the secretome could no longer be separated on SDS-PAGE. Skin was thus omitted from the media for all future experiments.

Next a pre-packed Q sephadex column (GE Healthcare 10/80) using the two-step gradient profile shown in table 3.3.2, was used to test whether the bound protein could be eluted. The culture used was grown under the same conditions as before but with dried skin omitted.

## Results and Discussion

Table 3.3.2: The gradient profile for anion exchange chromatography; trial one.

Time (minutes)	Step	Column volumes (1CV=40 mL)	% Buffer B
0	Equilibrate	5	0
200	Wash	2	0
280	Elute	10	30
680	Elute	5	100
880	Wash	1	100
920	Equilibrate	1	0

The resultant elution profile (Figure 3.3.1) shows that protein is eluted in a single broad peak between 20% and 40% buffer b (10 mM HEPES pH 7.0 with 2 M NaCl). The large differences in absorbance readings from AEX throughout this chapter are most likely due to differences in the total amount of protein present in the original culture analysed. All cultures were 50 mL, but ranging from 1.5 months to 2 months of incubation. Also different amounts of the initial *W.ichthyophaga* cells were used to start each culture.

The elution profile was changed to a linear gradient between 10% and 40% buffer b over 5 column volumes (CV), followed by a linear gradient from 40% to 100% over another 5 CV (Table 3.3.3), using the same conditions as before, in attempt to achieve better protein separation.

Figure 3.3.2 shows that using these conditions the secretome is separated into several peaks that are not well resolved. Peak fractions were analysed by SDS-PAGE then assayed for protease, lipase, and glycosidase activity. These general assays were used to determine which peak/s contained active enzymes. A single activity was then chosen and the corresponding general assay used to develop a protocol for a selected enzyme.

## Results and Discussion

As the peak profile was obtained by monitoring the elution at 280 nm, which can have a contribution from other cellular molecules such as DNA, fractions were assayed using the Bradford method. These standard curves were constructed with BSA concentrations ranging from 0.02-0.1 mg/mL and 0.1-1.0 mg/mL (Figure 3.3.4). A micro format assay was used where 90  $\mu$ L of reagent was added to 10  $\mu$ L of the sample in a 96 well plate. A linear relationship between protein concentrations of 0.02 mg/mL to 0.1 mg/mL at an absorbance of 595 nm was obtained, while for the higher concentrations a polynomial curve was fitted. All samples were assayed with the appropriate dilutions to ensure the absorbances fell within one of the standard curves.

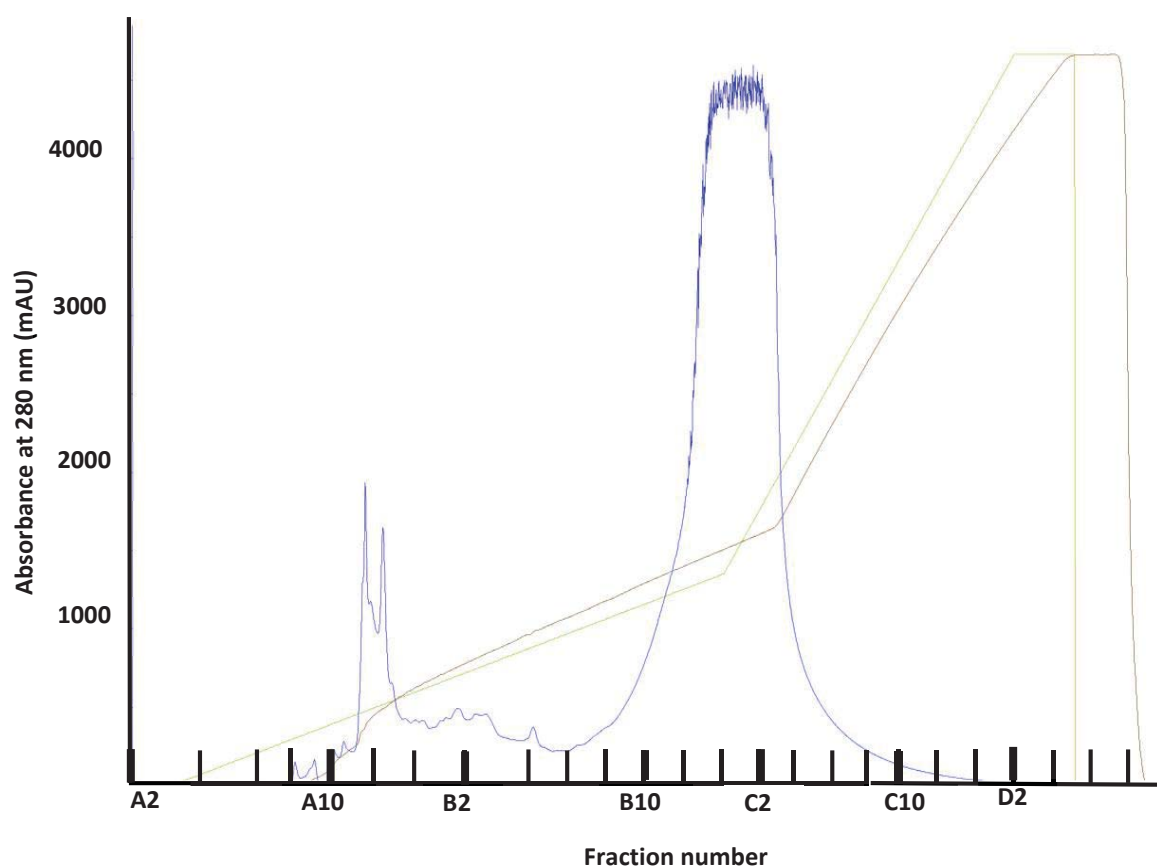


Figure 3.3.1: Trial 1, AEX of the secretome of *Wallemia ichthyophaga* using Q sephedex resin; buffer A (10 mM HEPES pH7.0) and buffer B (10 mM HEPES pH7.0 with 2 M NaCl). Blue line: absorbance at 280 nm with corresponding y axis. Brown line: Conductivity. Green line: Concentration in % buffer B. X axis: each partition represents 2 fractions.

## Results and Discussion

Table 3.3.3: The two-step gradient profile run for the anion exchange chromatography; trial two.

Time (minutes)	Step	Column volumes (1CV=40)	% Buffer B
0	Equilibrate	5	0
200	Wash	3	0
320	Elute	5	10-40
520	Elute	5	100
720	Wash	1	100
760	Equilibrate	1	0

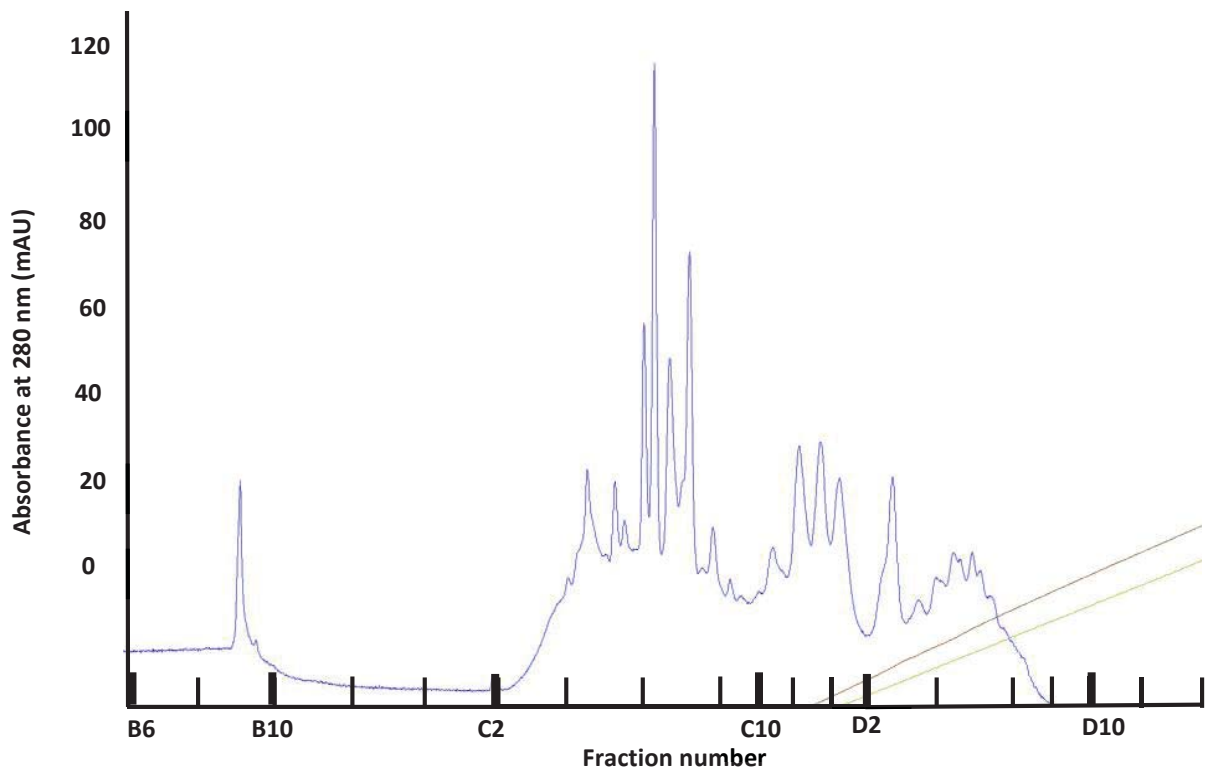


Figure 3.3.2: Trial 2: AEX of the secretome of *Wallemia ichthyophaga* using Q sephadex resin; buffer A (10 mM HEPES pH7.0) and buffer B (10mM HEPES pH7.0 with 2 M NaCl). Blue line: absorbance at 280 nm. Brown line: Conductivity. Green line: Concentration of % buffer B. X axis: Each partition represents 2 fractions.

## Results and Discussion

When the two methods for estimating protein concentration were compared, the A280 (Figure 3.3.2) and Bradford (Figure 3.3.3) elution profiles were very different. This difference in protein concentrations suggests that the early fractions contain no protein and are most likely DNA (confirmed by SDS-PAGE), while the later fractions predominantly contain protein. Fractions containing protein (Figure 3.3.3) were then concentrated to 1 mg/mL by ultrafiltration (Vivaspin- 10 Kb cut off), before being analysed by SDS-PAGE and tested for lipase, glycosidase, and protease activities.

Interestingly, no protease activity could be detected in any of the fractions using the Azocol assay, suggesting that *W.ichthyophaga* does not secrete free proteases. This is supported by the results obtained from the proteomic analysis of the secretome separated by SDS-PAGE, which did not identify any secreted proteases (Section 3.2.6). It is thus not surprising that the secretome failed to depilate the sheep skin as most depilation mixtures contain proteases (Section 1.3).

It is possible that the assay was not sensitive enough or that the substrate used was not suitable for any proteases present preventing their detection. An alternative possibility is that the proteases were in the small fraction that did not bind or that not all the bound protein was eluted off. The latter is unlikely as the column was washed with 100% 2 M NaCl. Both lipase and glycosidase activities were measured in the fractions C5 to D6 (Figure 3.3.3). Lipase activity was found in multiple fractions, while glycosidase activity was found in a single fraction that did not overlap with the lipase. The active fractions were then analysed using SDS-PAGE as shown in figure 3.3.5.

## Results and Discussion

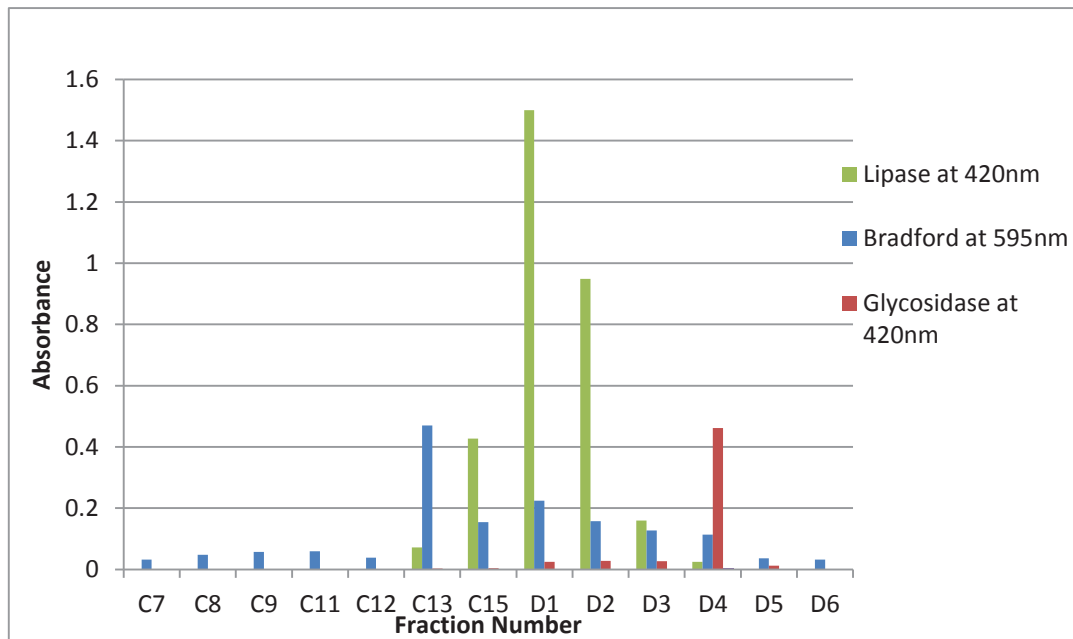
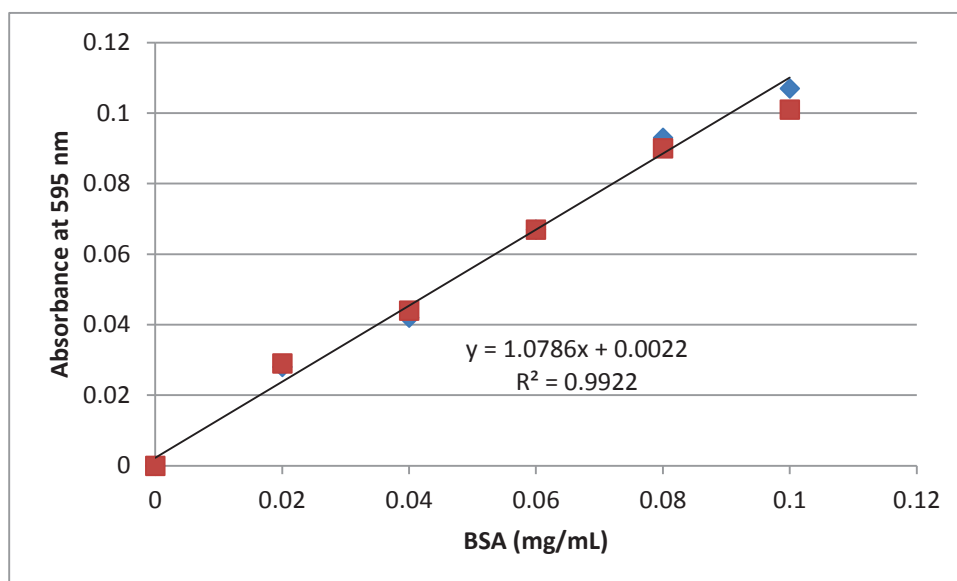


Figure 3.3.3: Protein concentration and enzymatic activity in fractions obtained from AEX of the secretome of *Walleimia ichthyophaga*. All activity assays were carried out using fractions concentrated to a protein concentration of 1 mg/mL. Absorbance readings were then taken as follows; Bradford at 595 nm, Glycosidase at 420 nm, Lipase at 420 nm, and Protease at 520 nm.

Figure 3.3.5 shows individual bands for each fraction. As the protein concentrations of each fraction had been standardised for both the SDS-PAGE and activity assays, the activities could be tentatively linked to particular band/s. The lipase activity is spread over multiple fractions, in which the dominant bands have molecular masses ranging from 60 KDa to 80 KDa. Any one of these could be responsible for the activity (Table 3.2.1). It is possible that multiple lipases may be secreted by *W.ichthyophaga*, a result that was not supported by the proteomic analysis of the secretome (section 3.2.5) where no known lipases were identified. As glycosidase activity was only present in one fraction, fraction D4, there is a high probability that the band with a molecular mass of approximately 90 KDa is the glycosidase (Table 3.2.1), and because the activity appears to be concentrated in a single peak this fraction was subjected to further purification.

## Results and Discussion

A



B

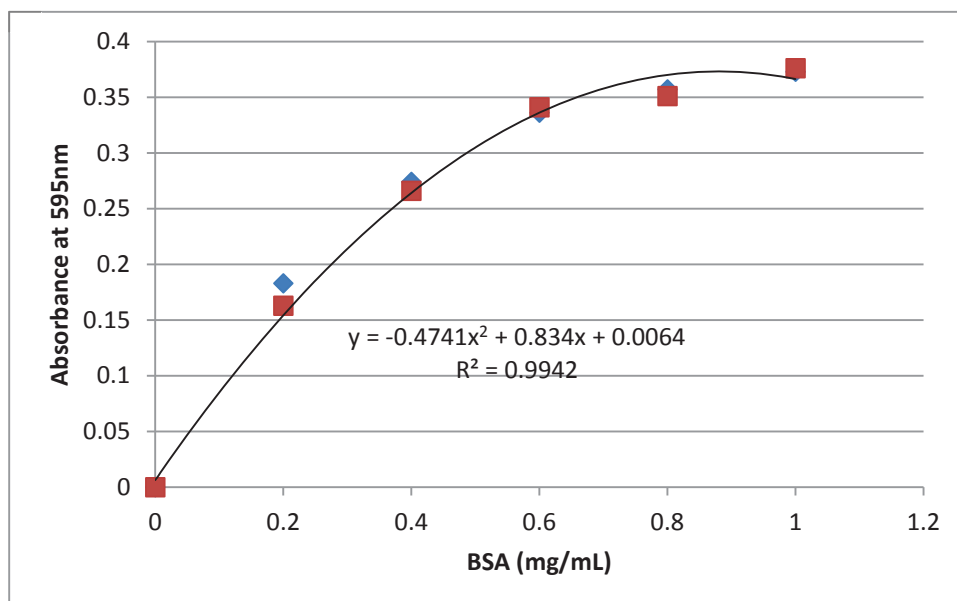


Figure 3.3.4: Bradford standard curves using 90  $\mu$ L of reagent to 10  $\mu$ L of sample. A) Standard curve covering BSA concentrations of 0 mg/mL to 1 mg/mL. B) The linear section of the standard curve covers BSA concentrations of 0 mg/mL to 0.1 mg/mL. The red and blue lines represent duplicate assays.

## Results and Discussion

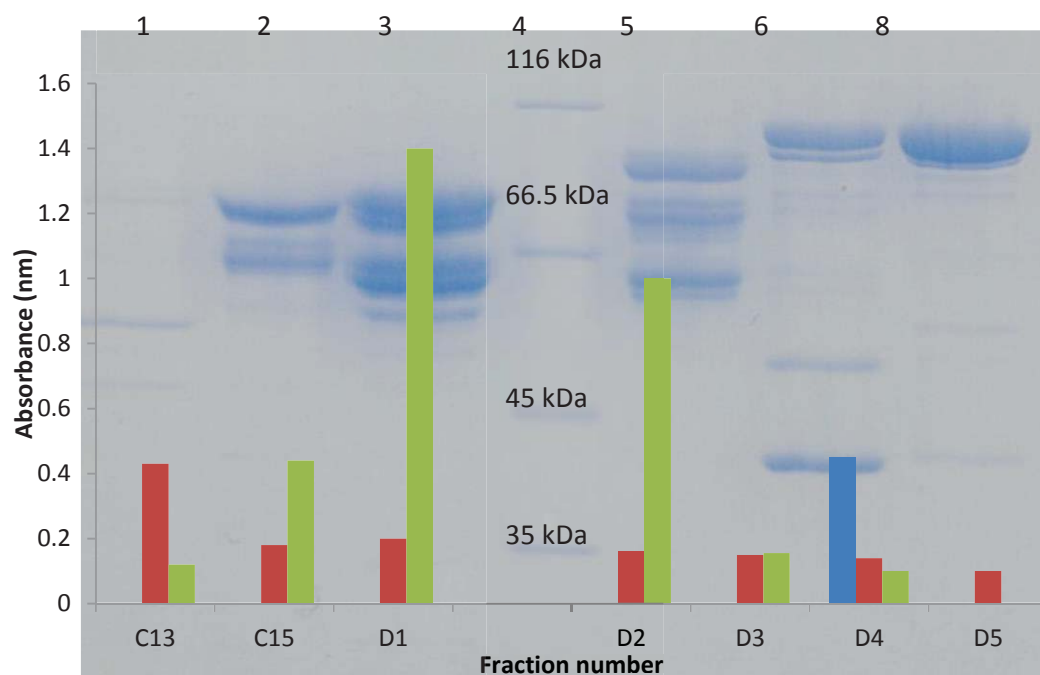


Figure 3.3.5: 7.5% acrylamide gel of fractions obtained from AEX, stained with colloidal Coomassie (G-250). The elution pattern is overlaid with a graph of the respective enzymatic activities and protein concentrations present in each fraction: Red: Protein concentration using the Bradford assay. Green: Lipase activity. Blue: Glycosidase activity. Purple: Protease activity. Lane 1: fraction C13, Lane 2: fraction C15, Lane 3: fraction D1, Lane 4: standard marker, Lane 5: fraction D2, Lane 6: fraction D3, Lane 7: fraction D4, Lane 8: fraction D5.

One problem, evident early in the purification process, was that glycosidase activity was lost after 3 days storage at 4°C. A common substance used to stabilise proteins and maintain activity is glycerol which protects both the tertiary and secondary structures of the enzyme, preventing heat-induced unfolding and aggregation (Meng *et al.*, 2004). The conversion of reactants to products, by an enzyme, involves an intermediate state or activation complex of the bound enzyme and substrate. The addition of glycerol, raises the free energy of this activation complex, shifting the equilibrium that exists between the native state and denatured state, towards the native state by stabilising the active enzyme (Meng *et al.*, 2004);

## Results and Discussion

Without glycerol:

E (native) → ES complex (intermediate) → **E (denatured)**

With glycerol:

**E (native)** ← ES complex (intermediate) → E (denatured)

Anion exchange chromatography was repeated using the same conditions as before except for the addition of glycerol to both the sample and the buffers to 10%. This did not affect the elution profile, nor did it adversely affect the glycosidase assay. It did however markedly improve the stability of the enzyme. Fractions with glycosidase activity were stored at 4°C and the activity was monitored over 6 weeks. Over one week the activity decreased by only 11%, and was detectable for up to 1 month. When the active fraction was flash frozen in liquid nitrogen and stored at -80°C for a month, 30% of activity was lost.

The protocol for AEX was further modified, to improve the separation, by adding an additional wash at 15% buffer B (Table 3.3.4) to allow time for proteins with a lower retention time to fully dissociate from the column, before the target glycosidase was eluted.

Table 3.3.4: The three-step gradient profile run for the anion exchange chromatography.

Time (minutes)	Step	Column volumes (1CV=40)	% Buffer B
0	Equilibrate	5	0
200	Wash	3	0
320	Elute	5	10-15
360	Elute	1	15
560	Elute	5	15-30
600	Wash	1	100
640	Equilibrate	1	0

## Results and Discussion

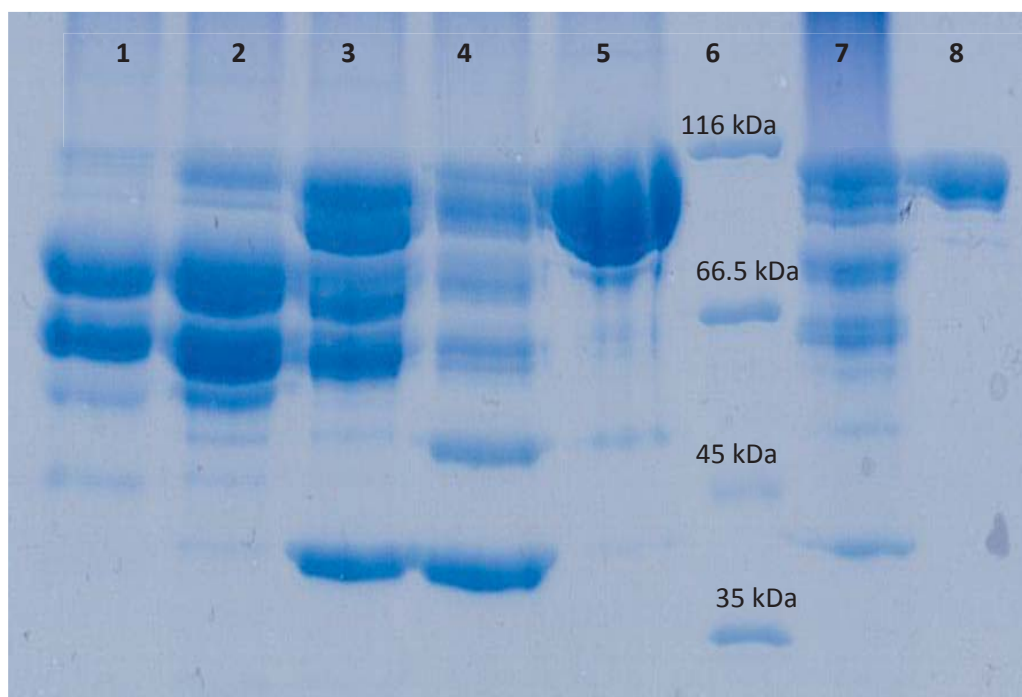


Figure 3.3.6: 7.5% acrylamide gel of the fractions obtained from the separation of the secretome of *Wallemia ichthyophaga* using AEX, stained with colloidal Coomassie G-250. Lane 1: fraction E2, Lane 2: fraction E5, Lane 3: fraction E10, Lane 4: fraction E13, Lane 5: fraction F13, Lane 6: standard marker, Lane 7: fraction G2, Lane 8: fraction G3.

The resultant elution profile (Figures 3.3.6 and 3.3.7) shows that the glycosidase was successfully separated from other secreted proteins into a single fraction (F13). The ratio of 260 nm/280 nm Abs was used as an indication of the possible DNA content in each fraction. SDS-PAGE analysis confirmed that the major protein present in this fraction was a single protein with a molecular mass of 90 KDa. The next step was to further purify the glycosidase by exploiting other properties such as molecular weight (size exclusion chromatography-SEC) or hydrophobicity (hydrophobic interaction chromatography-HIC).

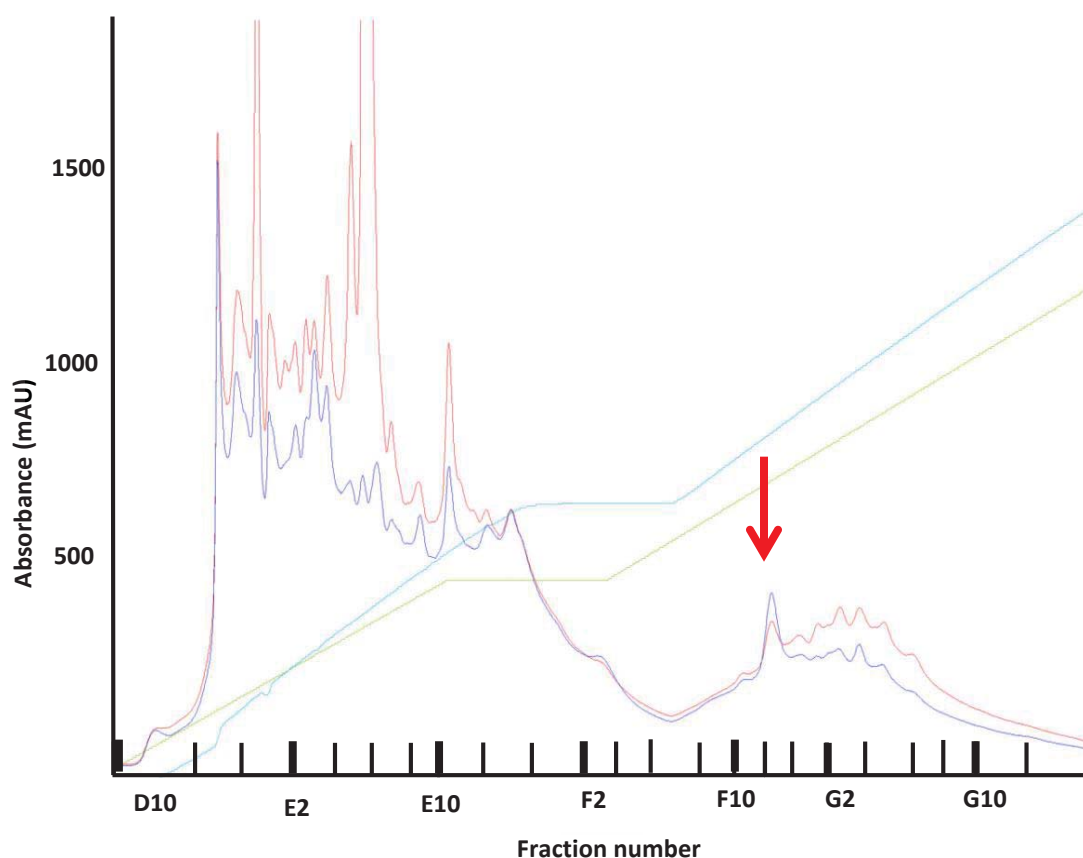


Figure 3.3.7: The 3 step gradient elution profile of the secretome of *Wallemia ichthyophaga* with 10% glycerol using Q sephadex resin; buffer A (10 mM HEPES pH7.0 and 10% glycerol) and buffer B (10mM HEPES pH7.0 with 2 M NaCl and 10% glycerol). The active peak is indicated by the red arrow. Dark Blue line: absorbance at 260 nM. Red line: absorbance at 280 nm. Green line: Conductivity. Light Blue line: concentration of % buffer B. X axis: each partition represents 2 fractions.

### 3.3.3 Hydrophobic chromatography

The fraction containing glycosidase activity was then subjected to HIC column. Again, the first step was to find conditions conducive to binding the protein of interest to the column. NaCl, a more chaotropic salt than  $(\text{NH}_4)_2\text{SO}_4$ , was initially trialled as it was used to elute the proteins during AEX, and is known to give improved separation in HIC (Queiroz, Tomaz, & Cabral, 2001). Trials with 1 mL of sample showed that under these conditions, the protein did not bind to the resin. All of the proteins present in the band were found in the supernatant/flow through, and as expected, the supernatant tested positive for glycosidase activity. Changing

the salt to a more lyotropic  $(\text{NH}_4)_2\text{SO}_4$  also failed to induce binding, therefore HIC was not used.

### 3.3.4 Size exclusion chromatography

An alternative method for purifying proteins is (SEC). This is commonly used as a polishing step in the purification process. As the active fraction was relatively pure, SEC was feasible.

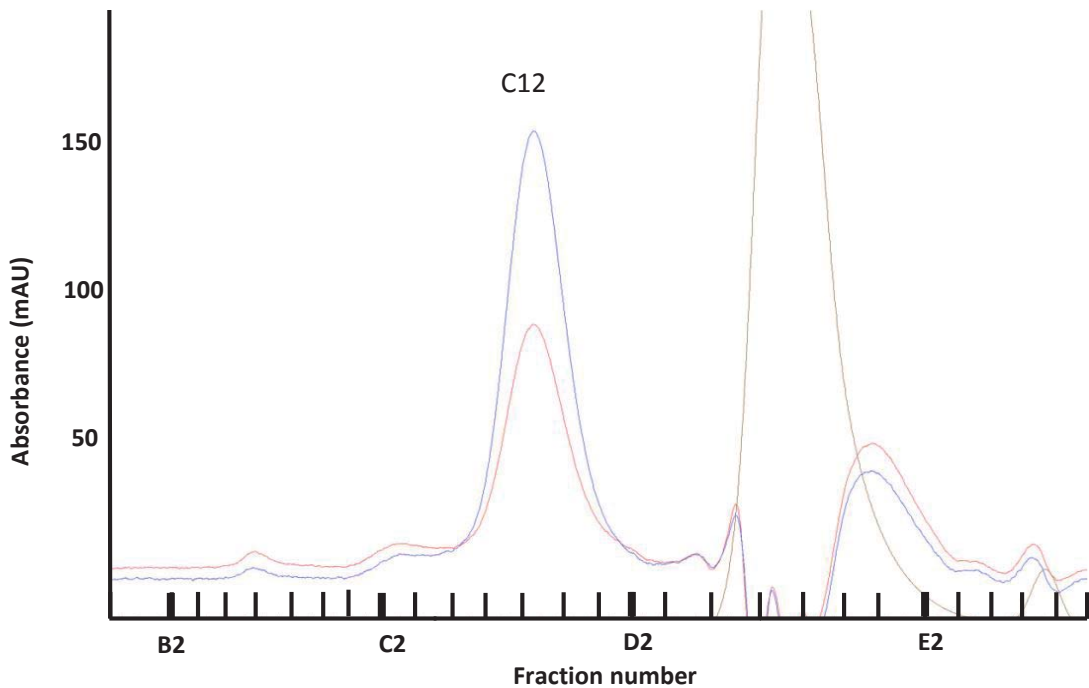


Figure 3.3.8: The elution profile of fraction F13, fractionated by superdex 200 column (GE Healthcare 10/30); buffer A (10 mM HEPES pH7.0 and 10% glycerol). Dark Blue line: absorbance at 260 nm. Red line: absorbance at 280 nm. Brown line: Conductivity. X axis: each partition represents 2 fractions.

## Results and Discussion

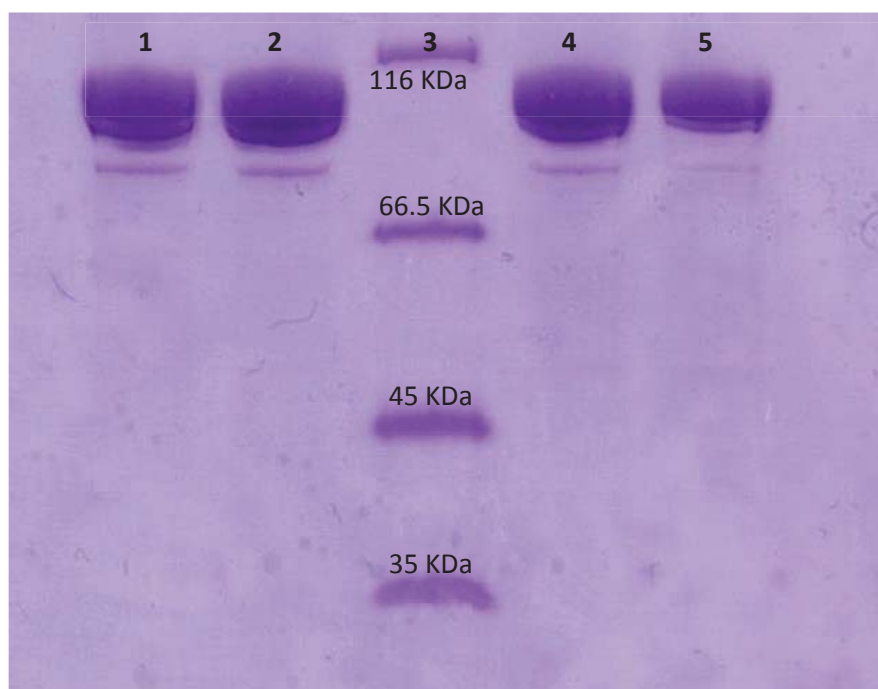


Figure 3.3.9: 7.5% acrylamide gel of fractions separated by SEC stained with colloidal Coomassie G-250 Lane 1: fraction C8, Lane 2: fraction C10, Lane 3: standard marker, Lane 4: fraction C11, Lane 5: fraction C13.

The SEC chromatography elution profile contained three peaks (Figure 3.3.8). The ratio of Abs at 260 over Abs at 280 ( $A_{260}/A_{280}$ ) can be used to assess the possible DNA content of fraction *i.e.* ratio  $> 1.06$  indicates at least 95% protein present. The ratio of  $A_{260}/A_{280}$  of the first peak was 1.7 which indicated that the peak is likely to be protein, and is most likely the glycosidase as suggested from the presence of a single major band in fraction F13 from AEX (Figure 3.3.6). Analysis of the peak fractions by SDS-PAGE showed three distinct bands; two with very similar molecular masses 91 KDa and 88 KDa, and a third band of a lower molecular mass around 78 KDa (Figure 3.3.9). The presence of two dominant bands at about 90KDa is observed in glycosidase active fractions obtained from both SEC (Figure 3.3.9) and IEX (Figure 3.3.6), suggesting that the glycosidase could be either one or both of these bands.

### 3.3.5 Final purification method using chromatography

Some minor adjustments were made to the final purification protocol. Dialysis was used to desalt and lower the conductivity of the secretome instead of ultrafiltration to save time, and to prevent loss of material through non-specific binding to the ultrafiltration device. The secretome was still initially filtered through glass wool before being dialysed using pre DDH<sub>2</sub>O soaked 16mm dialysis tubing (Serva) against 2 litres of 50mM HEPES pH 7.0 with 10% glycerol (Buffer A). The secretome was dialysed at 4°C overnight with stirring to equilibrate. The buffer was changed once during this time. The dialysed secretome was then filtered through a 0.2 µ filter before being diluted to the appropriate conductivity with cold DDH<sub>2</sub>O. The solution was then loaded on to the AEX column using a sample pump, and separated as before. The final protocol was then reassessed to ensure all conditions had been optimised.

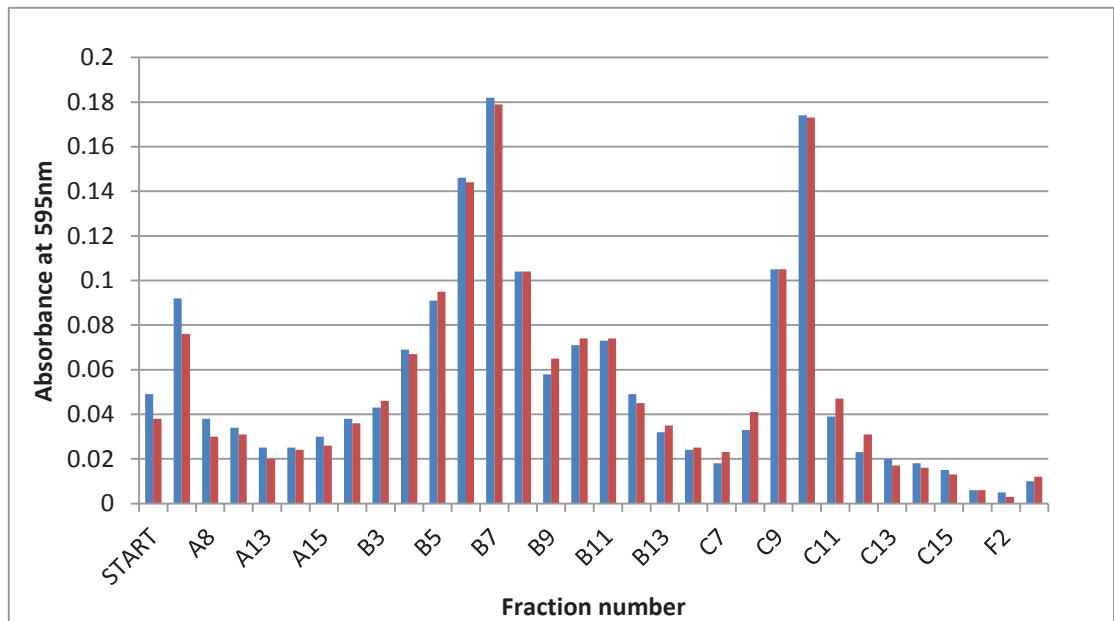


Figure 3.3.10: Bradford assays across fractions obtained from AEX. Each assay was done in duplicate (red and blue lines).

## Results and Discussion

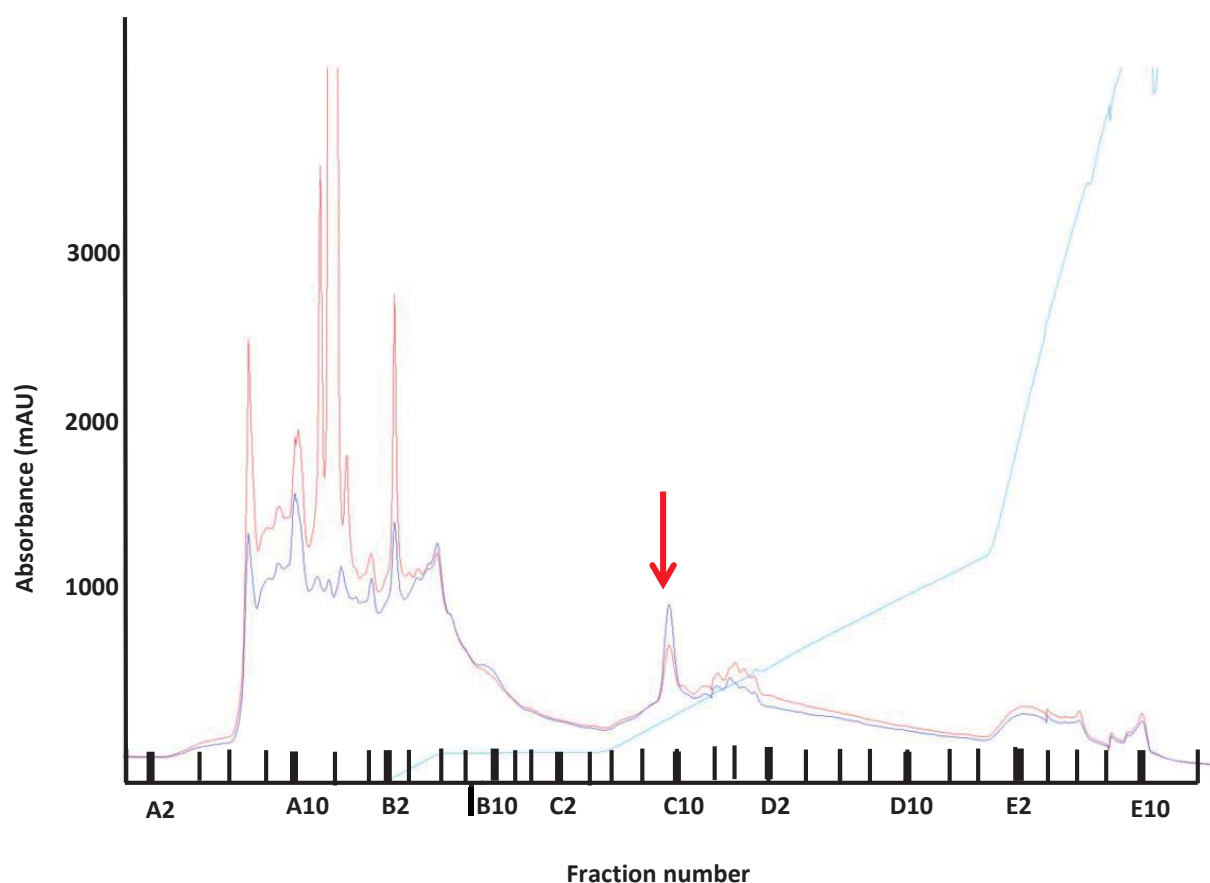


Figure 3.3.11: The elution profile of the secretome of *Wallemia ichthyophaga* with 10% glycerol from Q sephadex resin (GE Healthcare 10/80) buffer A (10 mM HEPES with 10% glycerol pH7.0) and buffer B (10mM HEPES pH7.0 with 2 M NaCl and 10% glycerol). Dark Blue line: absorbance at 280 nm. Red line: absorbance at 260 nm. Light blue line: Conductivity. X axis: each partition represents 2 fractions. Arrow represents the active peak.

The final elution profile from the AEX chromatography (Figure 3.3.11) clearly showed that the glycosidase has been eluted in a single peak. This was confirmed by SDS-PAGE and activity assays.

The elution profiles obtained from the A280 absorbance measurements (Figure 3.3.11) and Bradford assays (Figure 3.3.10) when compared, indicated that even after subsequent dialysis, the secretome still contained a high percentage of non-protein molecules. Again the A280 reading showed peaks between fractions A5 to B3 which had much lower absorbances in the Bradford assay.

## Results and Discussion

Each peak fraction was then assayed for glycosidase activity (Figure 3.3.13). Before the activity was assayed, the protein concentrations of the fractions of interest were normalised to 1.0 mg/mL. This allowed for direct comparison of activities between fractions. Fractions that had no activity at this protein concentration were deemed inactive. Each peak was concentrated using ultrafiltration, with the concentration factor calculated from the original protein concentration (Figure 3.3.10). The concentrated fractions were then re-assayed, diluting the fraction until the absorbance read within the linear range of the Bradford standard curve. This was required as even though, in theory, the ultrafiltration devices retain all proteins larger than 10 kDa, protein losses do occur due to non-specific binding of proteins to both the membrane and plastic.

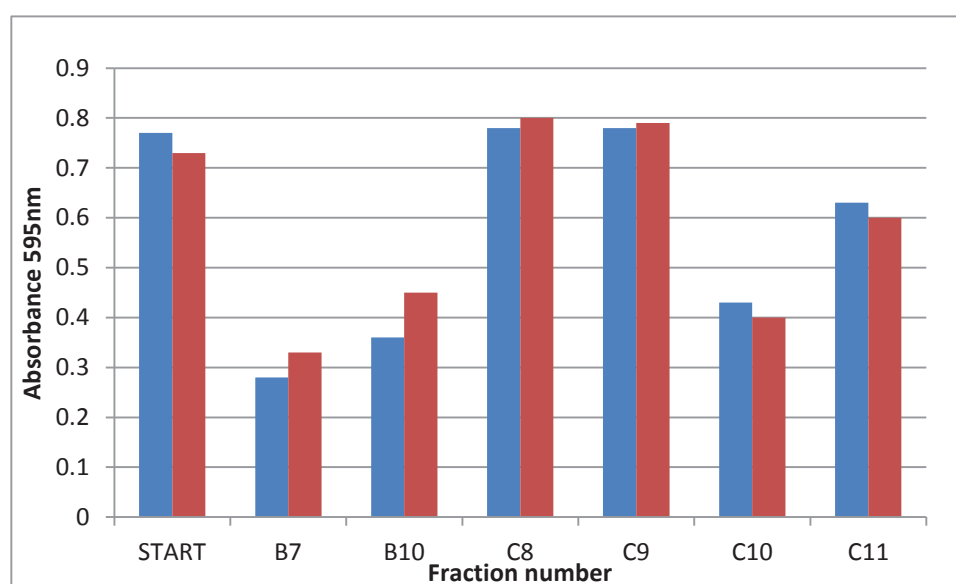


Figure 3.3.12: Bradford assays of concentrated fractions obtained from AEX. Each assay was done in duplicate (red and blue lines).

With the final and initial concentration known, the true concentration factor could be calculated, and the glycosidase activities were adjusted accordingly. Figure 3.3.12 is a graph of the final concentration of each fraction and clearly shows that protein has been lost during concentration as all fractions should have an absorbance of 1.0 AU at 595 nm; this is approximately the same as 0.1 mg/mL of

## Results and Discussion

protein. As all flow throughs tested negative for protein content, losses are unlikely due to faulty devices. It was evident that after each consecutive fraction was concentrated, the Bradford assays of the concentrate, were consecutively lower than what they should have been based on the concentration of the original fraction. This suggests that protein was binding to the membranes and/or devices to a greater extent than expected, even though all devices were pre-treated with Thesit detergent (0.2% wash-dry) or had been pre-used with secretome and stored at 4°C in DDH<sub>2</sub>O.

As expected from previous experiments, peak C10 contained the glycosidase activity while peaks B7 and B10 had no glycosidase activity (Figure 3.3.13). Activity assays of fractions over the whole peak confirmed that the activity is present in fractions C8 to C11. These fractions were concentrated to 0.1 mg/mL, using ultrafiltration to allow direct comparison between fractions. SDS-PAGE analysis of these fractions showed a dominant band at approximately 90kDa, and some lower molecular weight proteins were also present but at much lower concentrations.

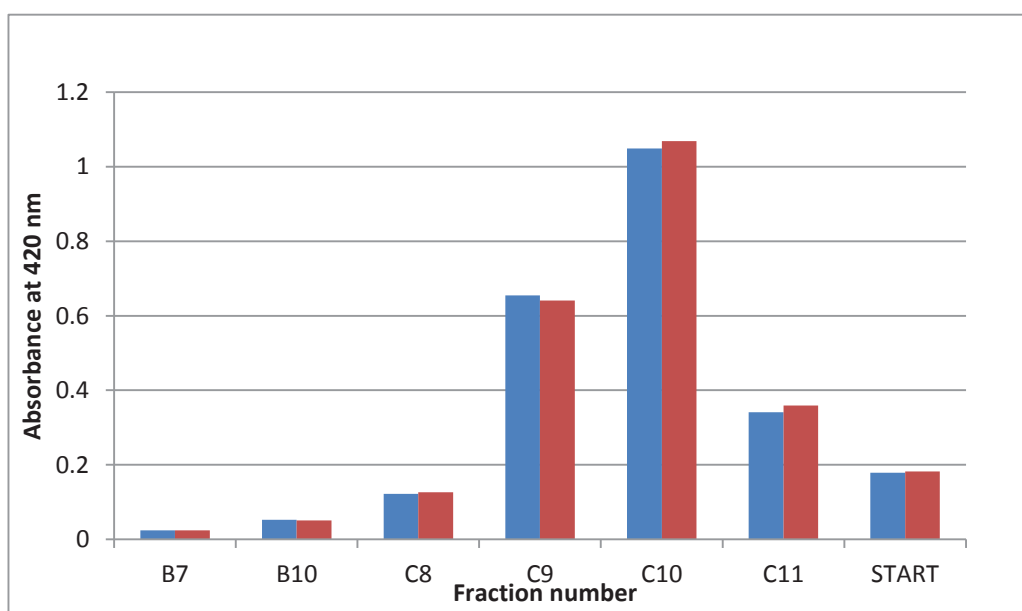


Figure 3.3.13: Glycosidase activity across fractions obtained from AEX using *o*-nitrophenyl-glucopyranoside as a substrate. Each assay was done in duplicate (red and blue lines).

## Results and Discussion

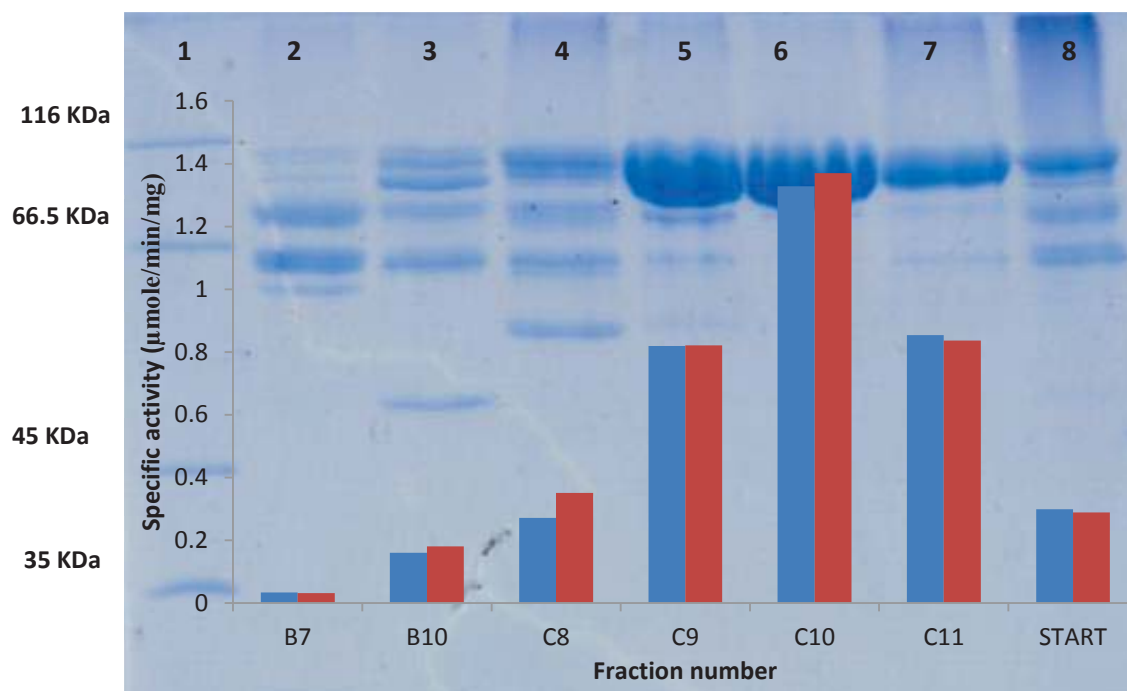


Figure 3.3.14: 7.5% acrylamide gel of fractions obtained from AEX, stained with colloidal Coomassie G-250, and corresponding specific activity. Lane 1: standard marker, Lane 2: fraction B7, Lane 3: fraction B10, Lane 4: fraction C8, Lane 5: fraction C9, Lane 6: fraction C10, Lane 7: fraction C11, Lane 8: original secretome before AEX.

Overlay: Specific activity of the fractions obtained from AEX. Protein concentrations were measured using the Bradford assay, and the glycosidase activity was measured using *o*-nitrophenyl-glucopyranoside as a substrate. Each assay was done in duplicate (red and blue lines).

The specific activity of each fraction was assessed and compared with the SDS-PAGE results to predict which band was responsible for the activity observed (Figure 3.3.14). The specific activity peaked at fraction C10 which coincided with the fraction showing a large band at approximately 90 kDa, with very few other proteins. This fraction was deemed to be pure enough for subsequent characterisation assays. Fractions C9 and C11 had lower specific activities and were pooled for further purification.

## Results and Discussion

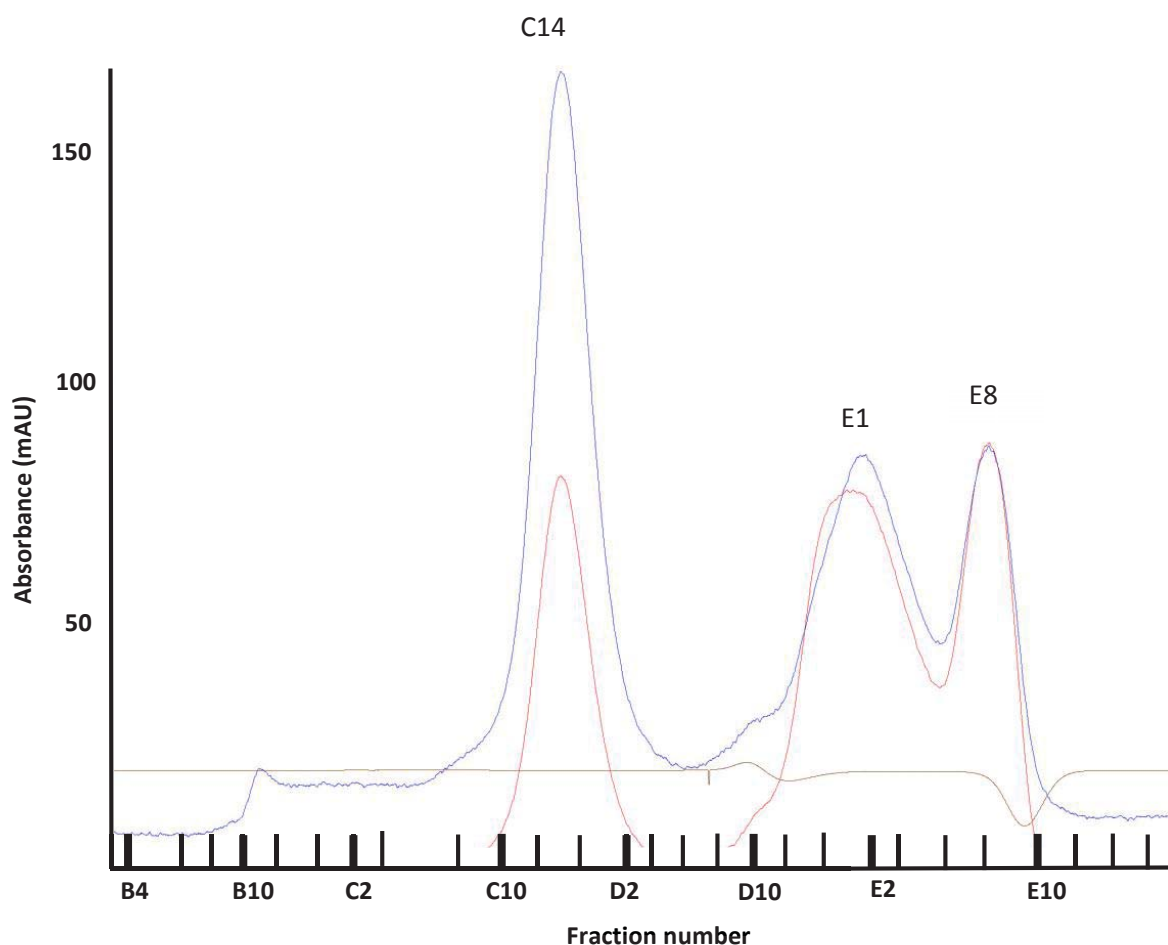


Figure 3.3.15: SEC of the fractions C9 and C11 from AEX. Sephadex 200 column (10/300 GL- GE Healthcare); buffer A (10 mM HEPES with 10% glycerol pH7.0). Dark Blue line: absorbance at 280 nm. Red line: absorbance at 260 nm. Brown line: Conductivity. X axis: each partition represents 2 fractions.

The elution profile in Figure 3.3.15 showed 3 well resolved peaks and the Bradford assay confirmed that peak C14 contained protein, while peaks E1 and E8 did not and are most likely buffer components (Figure 3.3.16). Fractions C10 to D3 were then concentrated to 0.1mg/mL by ultrafiltration, and the protein concentration re-measured. Despite trying many times, duplicate results within a 10% error could not be obtained.

## Results and Discussion

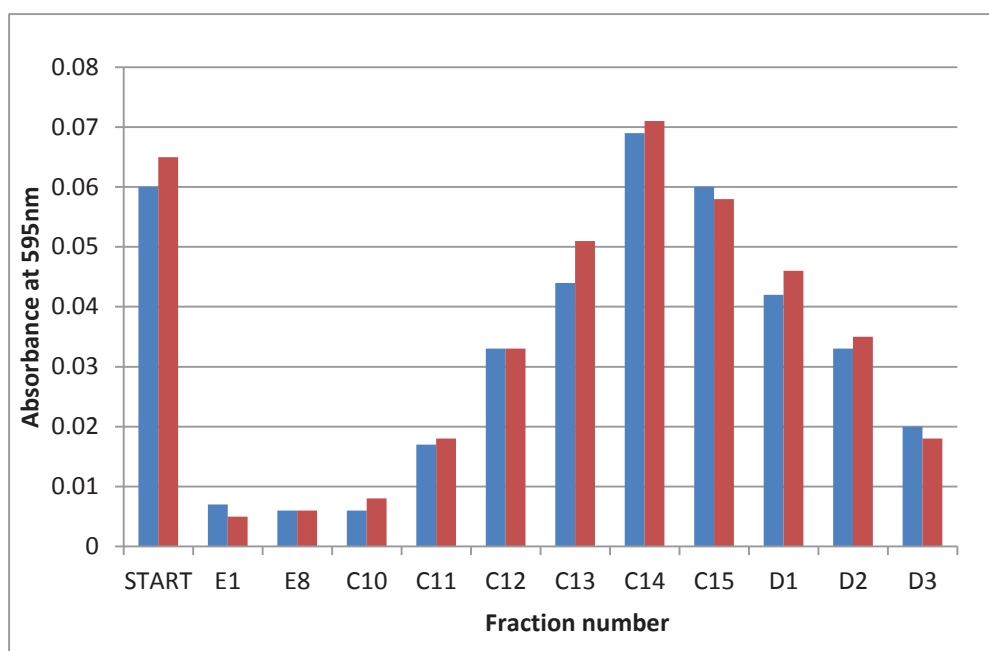


Figure 3.3.16: Bradford assays of fractions obtained from SEC. Each assay was done in duplicate (red and blue lines).

In order to determine the cause of these variable results, each step in the assay was repeated. Firstly, a standard curve of different BSA concentrations was used to check the integrity of the Bradford reagent, as over several months the dye can precipitate causing variable results. The resultant standard curve was straight and duplicate assays were within 10%. The Bradford reagent was also centrifuged, and no pellet was formed, confirming that the reagent had not precipitated. The standard curve was also repeated using sample buffer, rather than deionised water, to check if the sample buffer had an effect on the assay. Again, the resultant standard curve could be fitted to a straight line. The calibration of the pipettes used was also checked for accuracy by weighing set volumes of water. The assay was repeated using P<sub>10</sub> (Eppendorf) rather than the P<sub>2.5</sub> pipette, but the variation in results was no different and were too high to be confident of the results. The sample itself therefore appears to be the source of the variability, though how this can occur is difficult to explain.

## Results and Discussion

One possible cause is that as the protein is purified, the protein may denature and/or aggregate causing the solution to become non-heterogeneous. This would affect the repeatability of the Bradford assay. To test this hypothesis, buffer (50mM HEPES with 10% glycerol) instead of water was used to dilute the enzyme and the Bradford reagent had 10% glycerol added, the rationale being that the presence of glycerol would prevent or slow down degradation and/or aggregation of the glycosidase. Unfortunately, the addition of glycerol did not improve the accuracy or reproducibility of the assay. Sonication of the sample to disrupt any aggregates or to remove any protein non-specifically bound to the Eppendorf plastic, did not improve the accuracy either. The sample itself is thus the most likely cause of the inaccuracy, although the underlying reason could not be determined.

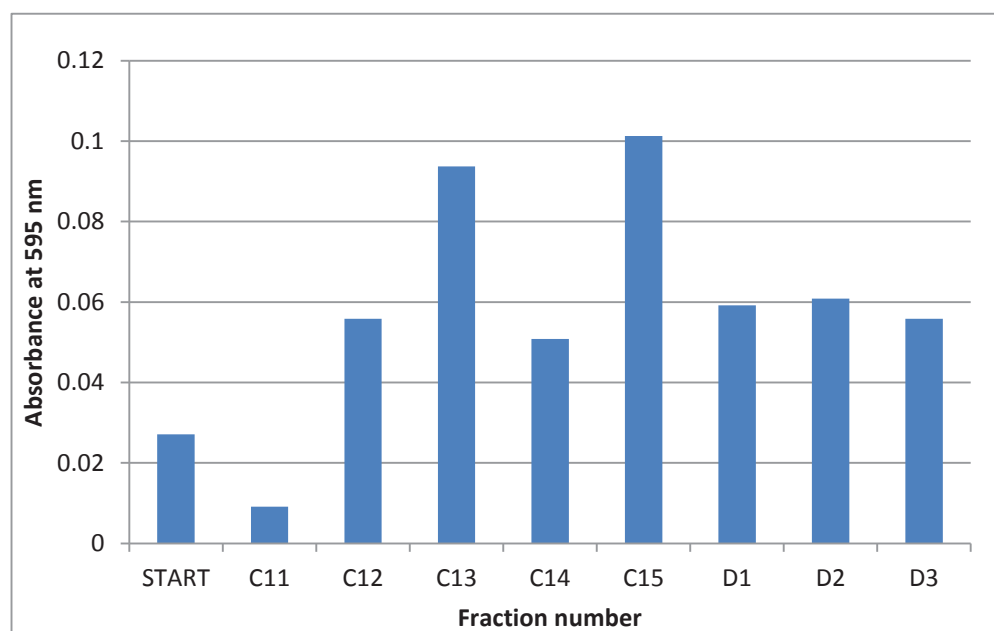


Figure 3.3.17: The average protein concentration, measured by Bradford assays, on fractions obtained from SEC (from combined fractions C8 and C11 from AEX) after being concentrated to 0.1 mg/mL using ultrafiltration.

## Results and Discussion

As accurate protein concentrations are required to measure specific activity accurately, it was decided to average all 12 assays to find the final concentration of each fraction (Figure 3.3.18). The glycosidase activity was then measured (Figure 3.3.19) and both values were then used to calculate specific activities.

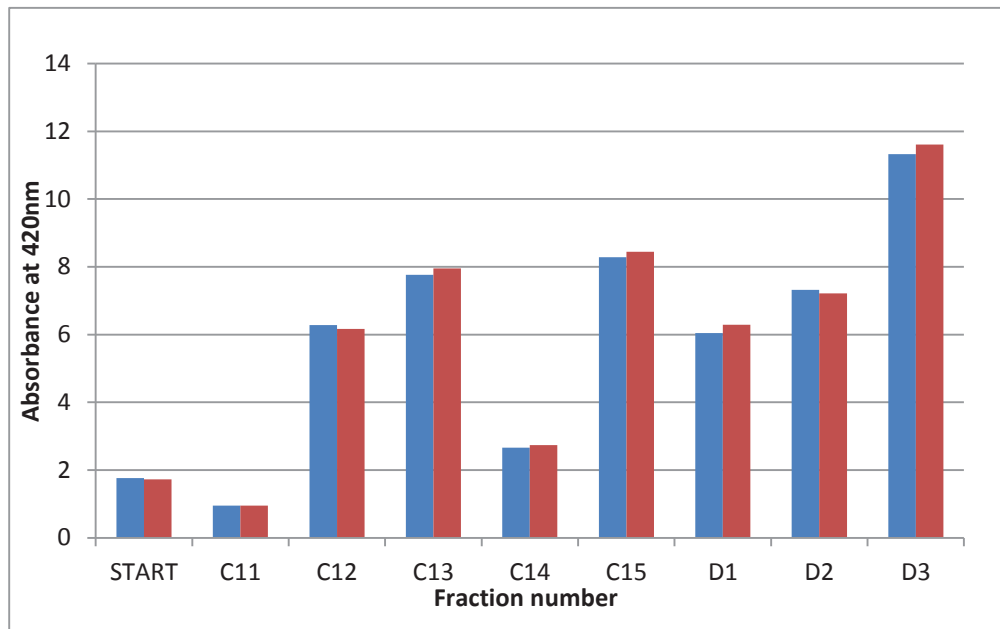


Figure 3.3.18: Glycosidase activity of fractions obtained from SEC from combined fractions C8 and C11 from AEX. Each assay was done in duplicate (red and blue lines).

Unfortunately, fractions D4 onwards were not analysed as the fractions did not contain enough protein for the Bradford assays, glycosidase assays, and SDS-PAGE. In general, the activity along with the specific activity increased across the peak (Figure 3.3.19). This would suggest that there is another protein present of very similar molecular weight or associated with the glycosidase, which is eluting off at the start of the peak but is not present in the later fractions. This was confirmed by SDS-PAGE which showed the presence of a band approximately 65KDa in the earlier fractions only. Again, there is a band doublet present between 80 to 100 KDa. Finally, the bimodal distribution of the specific activity across the fractions could be further evidence of the bifunctional activity of the glycosidase for both  $\alpha$ - and  $\beta$ -linked sugars.

## Results and Discussion

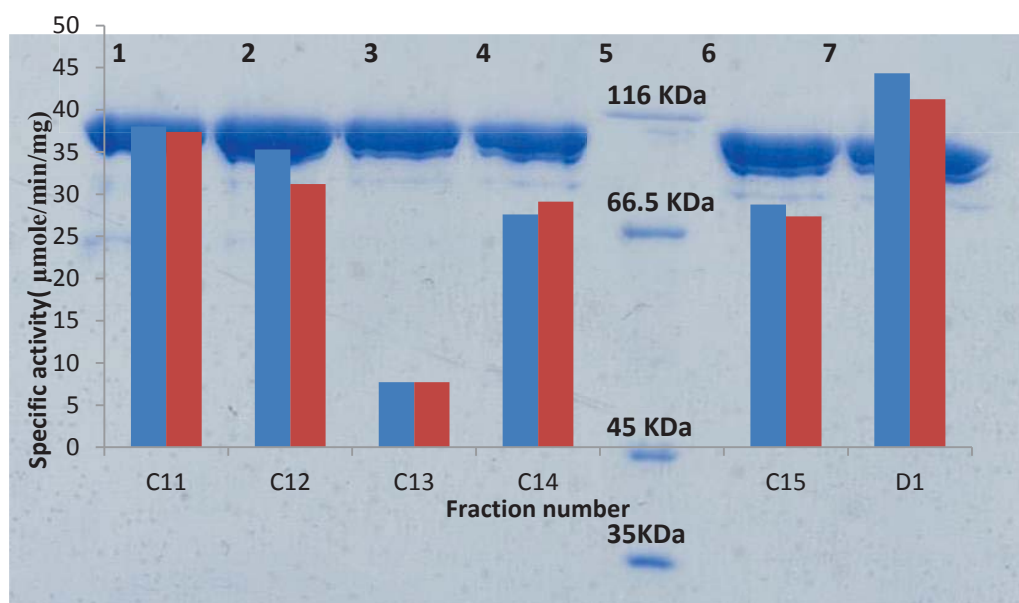


Figure 3.3.19: 7.5% SDS-PAGE analysing the concentrated fractions obtained from SEC and corresponding specific activity. Lane 1: fraction C11, Lane 2: fraction C12, Lane 3: fraction C13, Lane 4: fraction C14, Lane 5: standard marker, Lane 6: fraction C15, Lane 7: fraction D1.

Overlay: The specific activity across fractions obtained from SEC. Protein concentration were measured using the Bradford assay, and glycosidase activity was measured using *o*-nitrophenyl-glucopyranoside as a substrate. Each assay was done in duplicate (red and blue lines).

Table 3.3.5: Glycosidase purification summary

Sample	Volume (mL)	Protein concentration (mg/mL)		Total protein (mg)	Glycosidase activity (Abs at 420 nm)		Average glycosidase activity (μmole/min)	Total activity (μmole/min)	Specific activity (μmole/min/mg)	Fold purification	Percentage yield (%)
		Assay 1#	Assay 2#		Assay 1#	Assay 2#					
filtered secretome	50.00										
Dialysis	50.00	0.05	0.04	2.18	0.18	0.18	0.02	1.19	0.55	1.00	100.0
IEX fractions											
B7	3.00	0.18	0.18	0.54	0.02	0.02	0.00	0.01	0.01	0.03	0.7
B10	3.00	0.07	0.07	0.22	0.05	0.05	0.01	0.02	0.09	0.16	1.7
C8	3.00	0.03	0.04	0.11	0.12	0.13	0.02	0.05	0.45	0.82	4.2
C9	3.00	0.11	0.11	0.32	0.65	0.64	0.09	0.26	0.80	1.45	21.5
C10	3.00	0.17	0.17	0.52	1.05	1.07	0.14	0.42	0.81	1.47	35.3
C11	3.00	0.04	0.05	0.13	0.34	0.36	0.05	0.14	1.07	1.94	11.7
SEC fractions (C9 and C11)											
START	6.00	0.06	0.07	0.38	0.81	0.80	0.11	0.64	1.68	3.06	53.7
C11	0.30	0.02	0.02	0.01	0.36	0.36	0.05	0.01	1.43	2.60	1.2
C12	0.30	0.03	0.03	0.01	0.74	0.73	0.10	0.03	2.92	5.30	2.5
C13	0.30	0.04	0.05	0.01	0.79	0.81	0.11	0.03	3.17	5.77	2.7
C14	0.30	0.07	0.07	0.02	0.73	0.75	0.10	0.03	1.47	2.67	2.5
C15	0.30	0.06	0.06	0.02	0.97	0.98	0.13	0.04	1.93	3.52	3.3
D1	0.30	0.04	0.05	0.01	0.90	0.94	0.12	0.04	3.65	6.64	3.1
D2	0.30	0.03	0.04	0.01	0.82	0.81	0.11	0.03	3.23	5.88	2.7
D3	0.30	0.02	0.02	0.01	0.77	0.79	0.10	0.03	3.10	5.63	2.6

Results and Discussion

Table 3.3.6: The overall percentage yield and purification fold for the purification of the glycosidase from *W.ichthyophaga*

<b>Summary of AEX (fractions C9, C10, and C11)</b>	
Specific Activity ( $\mu\text{moles}/\text{min}/\text{mg}$ )	0.85
Fold purification	1.5
Percentage yield (%)	69

<b>Summary of SEC (fractions C12, C13, D1, D2, and D3)</b>	
Specific Activity ( $\mu\text{moles}/\text{min}/\text{mg}$ )	2.67
Fold purification	4.9
Percentage yield (%)	13

The overall purification of the glycosidase from the secretome of *W.ichthyophaga* resulted in a 13% yield, and the enzyme was purified 4.9-fold. Percentage yields from other purified fungal enzymes range from 5% to 80%, with the majority within 5% to 25%, and yields within 70% to 80% commonly achieved using affinity chromatography. The purification method used on the secretome of *W.ichthyophaga*, therefore achieved a percentage yield within the expected range, given that affinity chromatography was not used. The fold purification achieved by most purification methods range between 2- to 100-fold (Anindyawati, Ann, Ito, Iizuka, & Minamiura, 1998; Farag & Hassan, 2004; Han *et al.*, 2012; Liu *et al.*, 2012; Sharma & Gupta, 2001), therefore the fold purification achieved for this glycosidase is in the lower end of this range.

When the two chromatography steps are compared separately: there is a larger amount of glycosidase purified from the IEX (69%), but at a lower purity (0.85  $\mu\text{moles}/\text{min}/\text{mg}$ ), then SEC (13% and 2.67  $\mu\text{moles}/\text{min}/\text{mg}$  respectively). The IEX fractions are therefore more suitable for characterisation assays, while SEC fractions are more suitable for crystallography studies.

## Results and Discussion

From the overall purification method 0.06 mg of protein was purified from 50 mL, or 1.2 mg per litre, which contributes to 2.8% of the secretome. When proteins are expressed in fungal hosts, protein concentrations range from 500 mg/L to 2 g/L, with expression levels for extremophile proteins in the 100 mg/L range (Nevalainen, Te'o, & Bergquist, 2005). The purification method developed for the glycosidase is therefore considered very reasonable for an extremophile.

## Results and Discussion

### **3.4 Characterisation of a secreted glycosidase from *W.ichthyophaga*.**

A novel glycosidase was successfully isolated from the secretome of *Wallemia ichthyophaga* using liquid chromatography. The purified fractions from both AEX and SEC, when analysed using SDS-PAGE, showed two distinct and proportionally abundant bands of approximately 80-100 kDa. Possible explanations for the formation of the doublet included heterodimerisation, different glycosylation states, or co-purification with another protein. It was important to identify both bands before characterisation of the glycosidase to insure the results were due to a single enzyme.

#### **3.4.1 Quaternary structure of the glycosidase**

SDS-PAGE is a reducing gel which results in proteins separated based on their molecular weight alone. Multimeric proteins are therefore denatured and may be observed as multiple bands, only when the subunits are of different sizes. It was therefore possible that the band doublet may represent subunits of a heterodimer.

For size exclusion chromatography a linear relationship exists between the log of the molecular weight of a protein and the corresponding elution time or volume; under a specific set of parameters. Proteins of known molecular weights can therefore be eluted from a column and their elution times or volumes can be used to produce a calibration curve. This in turn can be used to estimate the molecular weight of an unknown protein separated by the same conditions. The advantage of this technique is that an unknown protein can be measured in its native conformation, and can then be compared to the SDS-PAGE measurement to deduce the quaternary structure of the protein. A calibration curve was constructed for the sephadex 200 column (GE Healthcare, 10/300 GL) used to purify the glycosidase.

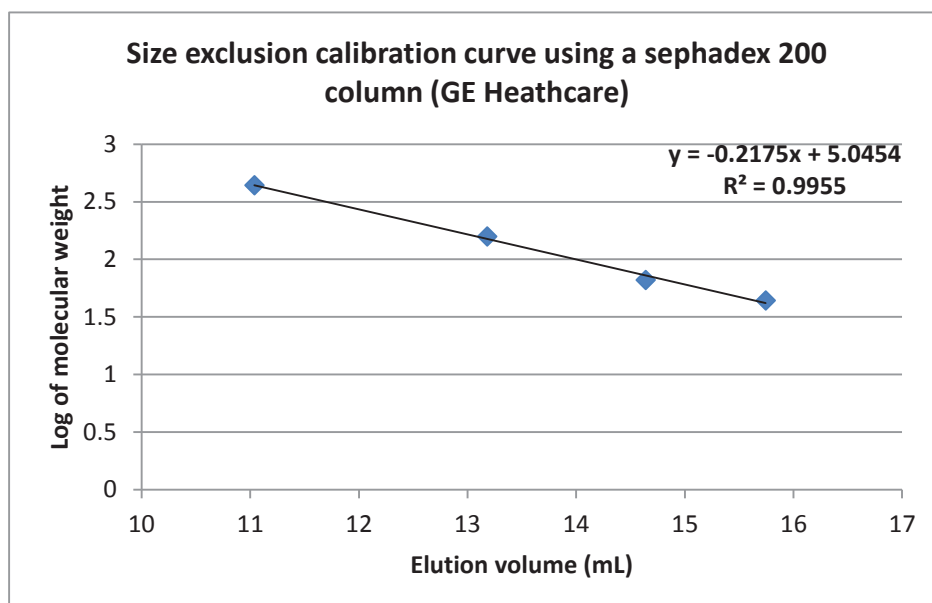


Figure 3.4.1: Size exclusion calibration curve using a sephadex 200 column (GE Heathcare, 10/300 GL) using the following markers: Ferritin (440 kDa), Catalase (250 kDa), Aldolase (158 kDa), Ovalbumin (44 kDa).

From the graph (Figure 3.4.1) the glycosidase has an elution volume which corresponds to a molecular weight of approximately 100 kDa. This is similar to the molecular weight estimated from the SDS-PAGE gel of the purified glycosidase (Table 3.3.1), and confirms that the glycosidase is indeed a monomer. Furthermore, the proteomic identification of the band identifies the protein as a glycosidase of a molecular weight of 88 kDa.

### **3.4.2 Deglycosylation of the glycosidase using PNGase F and Endo H**

On an SDS-PAGE gel, the glycosylation state of a protein may affect its migration rate. This is because both the protein and attached glycans contribute to its mass, resulting in an observed molecular weight that is greater than expected. Glycoproteins can also run anomalously on SDS-PAGE because SDS does not bind to the carbohydrate moieties. It is known that fungi often glycosylate secreted proteins and therefore the band doublet could be due to different glycosylation states of the same glycosidase.

In order to investigate whether the glycosidase was itself glycosylated, the protein was treated with the following endoglycosidases; PNGase F which removes intact N-linked glycans by cleaving the amide bond between the GlcNAc and the Asn side chain of the protein, or Endo H which cleaves only high mannose N-linked glycans between the two GlcNAc directly proximal to the asparagine (Figure 3.4.2) (Leonard *et al.*, 1990).

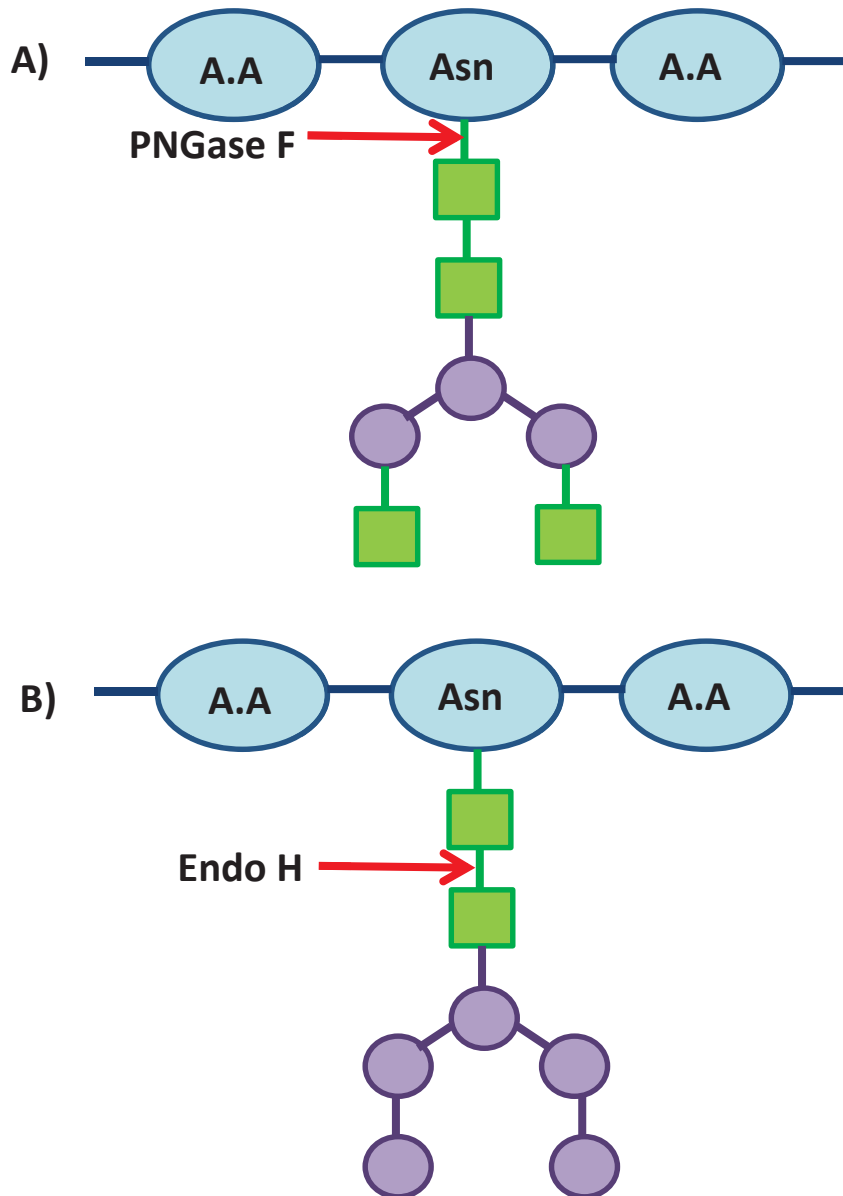


Figure 3.4.2: Cleavage sites of endoglycosidases PNGase F (A) and Endo H (B). Blue Circles= amino acids. Green Squares= GlcNAc. Purple Circles= mannose. Red Arrow= cleavage site.

## Results and Discussion

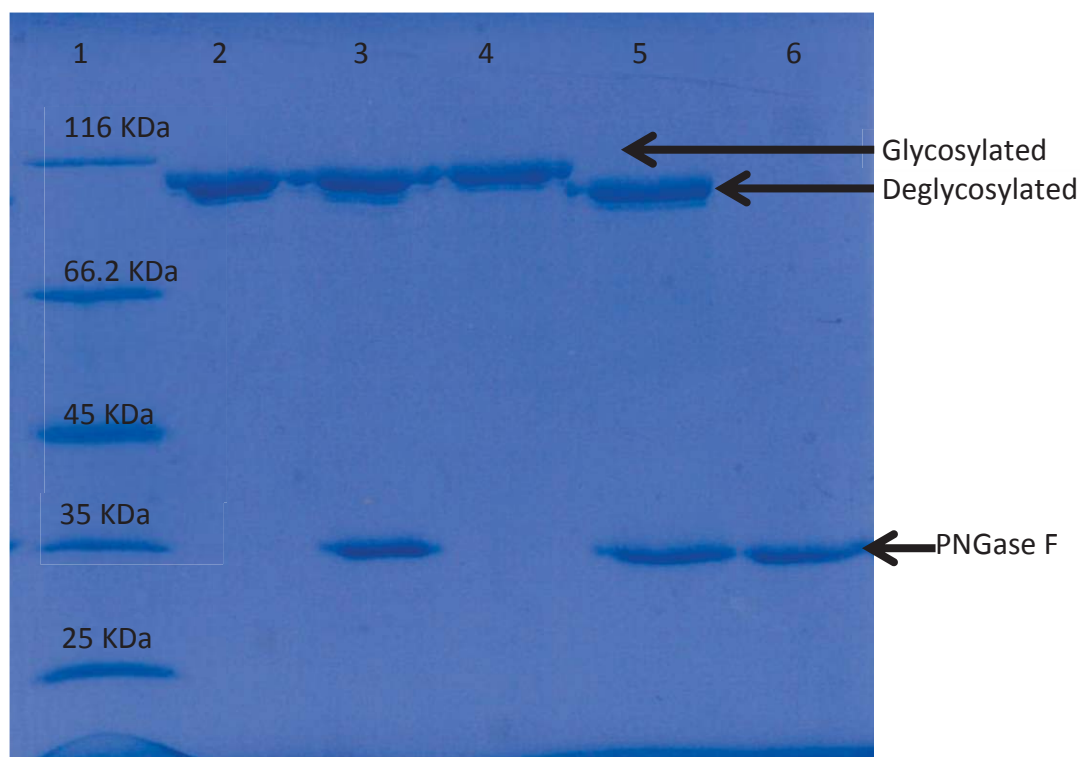


Figure 3.4.3: 7.5% SDS-PAGE of a PNGase digest of the glycosidase from *Wallemia ichthyophaga*. The glycosidase was incubated over night at 25°C with and without PNGase before being analysed on SDS-PAGE. The glycosidase was denatured with 0.1% Tween 20 and 1% SDS followed by boiling for 5min. Lane 1: Standard marker, Lane 2: native glycosidase, Lane 3: native glycosidase + PNGase F, Lane 4: Denatured glycosidase, Lane 5: Denatured glycosidase + PNGase F, Lane 6: PNGase F.

Figure 3.4.3 contains the results from the PNGase F digest, with all controls showing the expected bands. The comparison of lane 5 (denatured glycosidase plus PNGase F) to lane 4 (denatured glycosidase only) indicates that the glycosidase is N-glycosylated, and that the protein was fully deglycosylated. All reactions had protease inhibitor added to prevent any degradation of the glycosidase. As both bands moved proportionally downwards, the doublet cannot be caused by the same protein containing different N-linked glycans.

## Results and Discussion

Interestingly, PNGase F is unable to deglycosylate the native glycosidase (Lane 3), indicating that the proximal sugars are buried. Only when the protein is denatured, are the cleavage sites accessible to PNGase F (Lane 5).

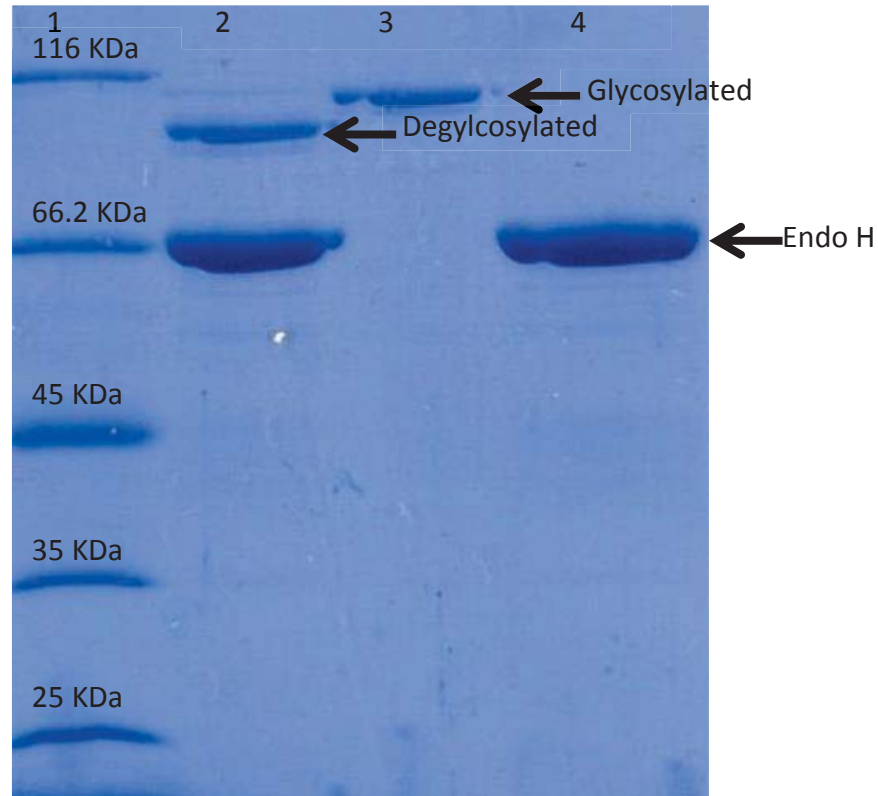


Figure 3.4.4: 7.5% SDS-PAGE of a Endo H digest of the glycosidase from *Wallemia ichthyophaga*. The glycosidase was incubated over night at 25°C before being analysed on SDS-PAGE. The glycosidase was denatured with 0.1% Tween 20 and 1% SDS followed by boiling for 5min. Lane 1: Standard marker, Lane 2: native glycosidase and Endo H, Lane 3: native glycosidase, Lane 4: Endo H.

Figure 3.4.4 contains the results from the Endo H digest. When lane 2 (native glycosidase and Endo H) is compared to lane 3 (native glycosidase only) again both bands shifted proportionally downwards, supporting the PNGase F results. Interestingly, the native enzyme was deglycosylated. As the cleavage site for Endo H is between the two proximal GlcNAcs, rather than between the asparagine side chain and the GlcNAc as for PNGase F, this further provides evidence that the PNGase F cleavage site is buried (Figure 3.4.2). Furthermore the chain must be high mannose as complex glycans are not cleaved by Endo H (Leonard, *et al.*, 1990).

### 3.4.3 Mass spectrometry of the final purified glycosidase fraction

The bands obtained from both SEC (Figure 3.3.21) and Endo H digestion (Figure 3.4.4) gels, were identified by in-gel tryptic digestion followed by mass spectrometry (Table 3.4.1), using the same parameters for the database search as described in the material and method section 2.2.18.

Table 3.4.1: Protein identification of bands obtained from SEC and Endo H digestion gels using in-gel tryptic digestion and mass spectrometry.

<b>Band</b>	<b>Molecular weight (kDa)</b>	<b>Gel</b>	<b>Protein</b>	<b>Identification number</b>
1	103	SEC	Putative $\beta$ -glycosidase L	EOQ98916.1
2	98	SEC	Putative $\beta$ -glycosidase L	EOQ98916.1
3	83	SEC	No significant matches	
1	103	Endo H glycosylated	Not enough protein	
2	98	Endo H glycosylated	Putative $\beta$ -glycosidase L	EOQ98916.1
1	103	Endo H deglycosylated	Putative $\beta$ -glycosidase L	EOQ98916.1
1	98	Endo H deglycosylated	Putative $\beta$ -glycosidase L	EOQ98916.1

All bands contained only the putative  $\beta$ -glycosidase L confirming the isolation of this glycosidase from the secretome. Both bands, formed when the purified glycosidase is run on SDS-PAGE, are therefore the same protein. An explanation for this phenomenon is unknown, but it does not occur due to heterodimerisation, different glycosylation states of the same protein, or co-purification. The molecular weight difference of the two bands is approximately 5,000 Da which equates to approximately 45 a.a residues, given that the average molecular weight of an a.a is 110 Da (Table 3.4.1) (Nei, 1971). When the genomic/protein sequence of the glycosidase was analysed using BLAST, a 20 a.a or 2200 Da intron was seen to be present at the N-terminal end (Figure 3.4.5). Unfortunately, the intron is not large

## Results and Discussion

enough to account for the molecular weight difference between the two bands. A signal sequence of 27 a.a or 2970 Da, was predicted by the Signal p database tool on ExPASy. The difference in a.a between the whole unmodified protein (823 a.a.), and the protein with the signal sequence and intron removed (776 a.a) is 47 a.a, therefore approximately the molecular weight difference of the band doublet. But the scenario where the signal sequence, with or without the intron, is not removed from the majority of the secreted protein is very unlikely.

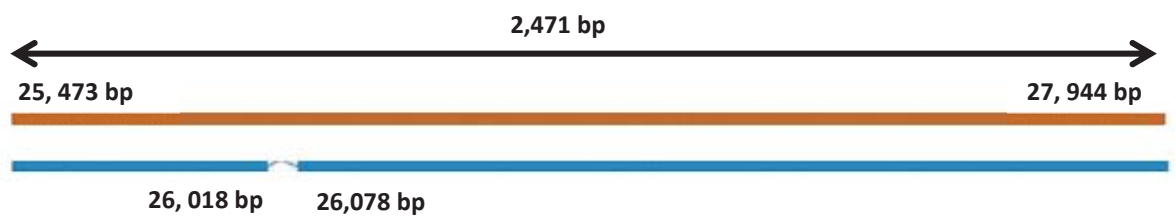


Figure 3.4.5: Graphical representation of the gene encoding the glycosidase purified from the secretome of *W.ichthyophaga* that was identified by mass spectrometry (from BLAST) Brown line: DNA. Blue line: mRNA

Another possible explanation for the formation of the band doublet is alternative start codons. The next potential start codon is M165 which produces a 638 a.a protein or 618 a.a protein with the intron removed. Even with the intron removed from the original start codon protein, and the intron present for the alternative protein, there is still a 118 a.a difference: given that the signal sequence has been removed from both proteins. This difference is much larger than what was measured by SDS-PAGE, therefore an alternative start codon is unlikely to be the cause of the doublet.

Finally, there are 6 cysteines present in the protein sequence of the purified glycosidase, which may form disulfide bonds upon protein folding. When subjected to DTT, SDS, and heat, any putative bonds may resist denaturation differently. This could result in the formation of two different protein groups that differ in both structure and the amount of bound SDS. This would result in a band doublet when analysed by SDS-PAGE. Unfortunately, investigation into the possibility of

incomplete reduction has yet to be done, and therefore this is still a possible explanation for the formation of the band doublet (Hong, 2007).

So far no explanation has been found for the formation of the band doublet, but the mass spectrometry results do indicate that only one protein is present in the SEC fractions, therefore the next step will be to characterise this purified glycosidase.

#### 3.4.4 Characterisation of the glycosidase

The protein sequence of the purified glycosidase, identified by mass spectrometry, was analysed by BLAST to investigate the possible protein domains present (Table 3.4.2 and Figure 3.4.6). All domains identified were from  $\beta$ -glycosidases, each with varying substrate specificities, except for the Fn3-like domain which function is unknown. From the e-values alone, the purified glycosidase from *W.ichthyophaga* is most likely a GH3 glycosidase. This family contains glycosidases which catalyse a variety of substrates, though all are retaining glycosidases that catalyse by the double nucleophilic displacement mechanism. GH3 glycosyl hydrolases are made up of two domains: the N-terminal domain which adopts a TIM barrel fold, while the C-terminal domain adopts a 6 stranded  $\beta$ -barrel made up from 5 parallel and 1 anti-parallel strands with 3  $\alpha$ -helices at either end. The substrate is thought to bind at the domain interface, with both N- and C- terminal residues contributing to the catalytic activity. With this glycohydrolase family in mind, the optimum pH, effect of NaCl, the requirement for metal cofactors, and substrate specificity, of the glycosidase were investigated.

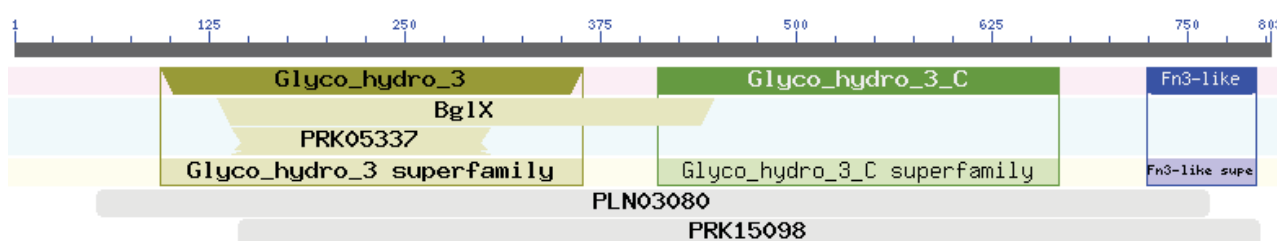


Figure 3.4.6: Graphical representation of the possible protein domains present in the glycosidase purified from the secretome of *W.ichthyophaga* (from BLAST).

Table 3.4.2: Domains predicted to be present in the isolated glycosidase protein

Domain	Description	E-value
Glyco_hydro_3	glycosyl hydrolase family 3 N terminal domain	8.98e-98
Glyco_hydro_3_C	glycosyl hydrolase family 3 C terminal domain	7.71e-61
BglX	beta-glucosidase-related glycosidases	2.67e-53
Prk05337	beta-hexosaminidase	5.53e-05
PLN03080	Probable beta-xylosidase	1.46e-45
PRK15098	beta-D-glucoside glucohydrolase	4.04e-56
Fn3-like	fibronectin type III-like domain, unknown function	5.79e-15

### 3.4.5 Optimum pH

First the optimum pH for the glycosidase was determined. A three component buffer, MIB (Sodium Malonate, Imidazole, and Boric acid), was initially trialled as it covers the pH range from 4.0 to 8.0. Unfortunately, during the process of preparing the different buffer solutions, it was noted that the pH did not remain stable, and so this buffer system was rejected.

Next, the buffer originally used in the purification procedure, acetate:acetic acid, was trialled. Assays over the recommended buffer range of pH 4.4 to pH 5.4, showed that the optimum pH lay towards the basic end of this range (first half of Figure 3.4.7). A pH range of 5.8 to 8.0 was therefore tested next using sodium phosphate buffer, the second half of the pH range in figure 3.4.7, and showed that the pH optimum is pH 6.0. There was, however, a large difference in the activity at the changeover pH point between the two buffer systems, most likely due to the different buffer salts present. Activities between pH 5.0 and pH 7.0 were thus re-measured using a single buffer.

## Results and Discussion

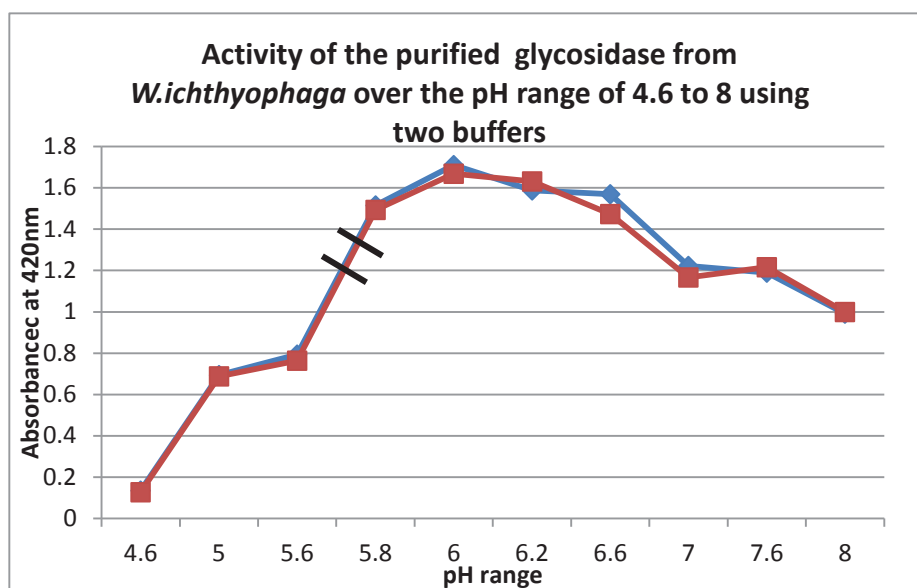


Figure 3.4.7: Activity of the glycosidase from *Wallemia ichthyophaga* at different pH. The break indicates the boundary between the two different buffering systems pH 4.6-5.6 100mM acetate:acetic acid buffer and pH 5.8-8 100mM sodium phosphate buffer. The red and blue lines are duplicates.

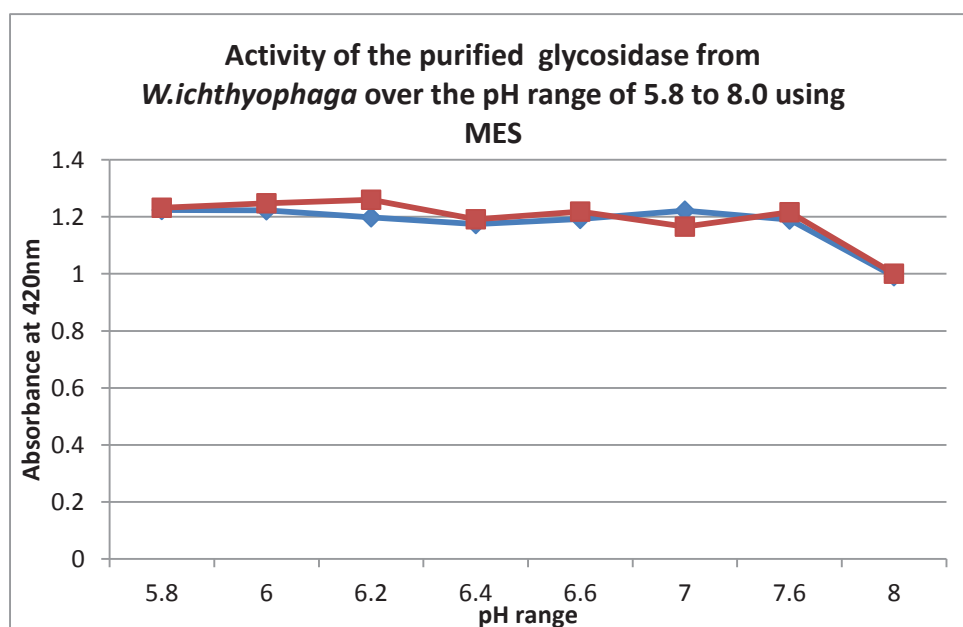


Figure 3.4.8: Activity of the glycosidase from *Wallemia ichthyophaga* using 100mM MES.

## Results and Discussion

MES was chosen as an appropriate buffer for the pH range of 5.8 to 8.0 (Figure 3.4.8). Interestingly, when this buffer was used, the glycosidase was active but was apparently unaffected by changes across the pH range tested. Furthermore, the activity measured was close to the optimum rate previously observed.

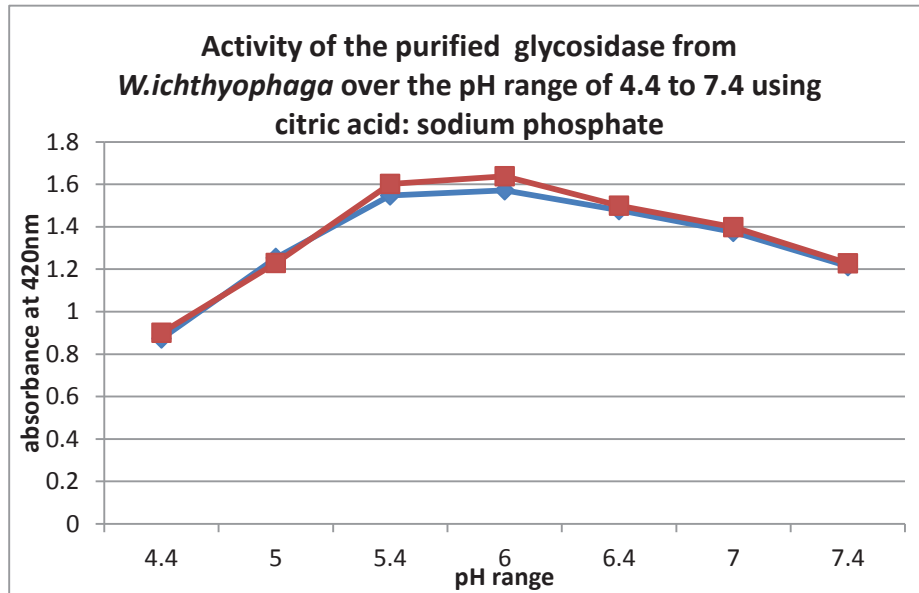


Figure 3.4.9: Activity of the glycosidase from *Walleimia ichthyophaga* over different pH ranges using 100mM citric acid:sodium phosphate.

The next buffer trialled was citric acid: sodium phosphate, which covers the pH range of 4.4 to 8.0. Figure 3.4.9 clearly shows that the optimum pH for the purified glycosidase from *Walleimia ichthyophaga* is pH 6.0. This buffer was thus chosen for all subsequent experiments.

### **3.4.6 The effect of NaCl on the activity of the glycosidase**

When *Walleimia ichthyophaga* is grown at 25°C in the presence of NaCl a minimum concentration of 10% NaCl is required for growth, and concentrations up to the saturation point of 30% NaCl can be tolerated. Previous experiments have shown that with increasing NaCl concentrations, the growth rate observed on agar plates decreases. NaCl concentrations between 5% and 30% were therefore tested, with 0% salt as a control.

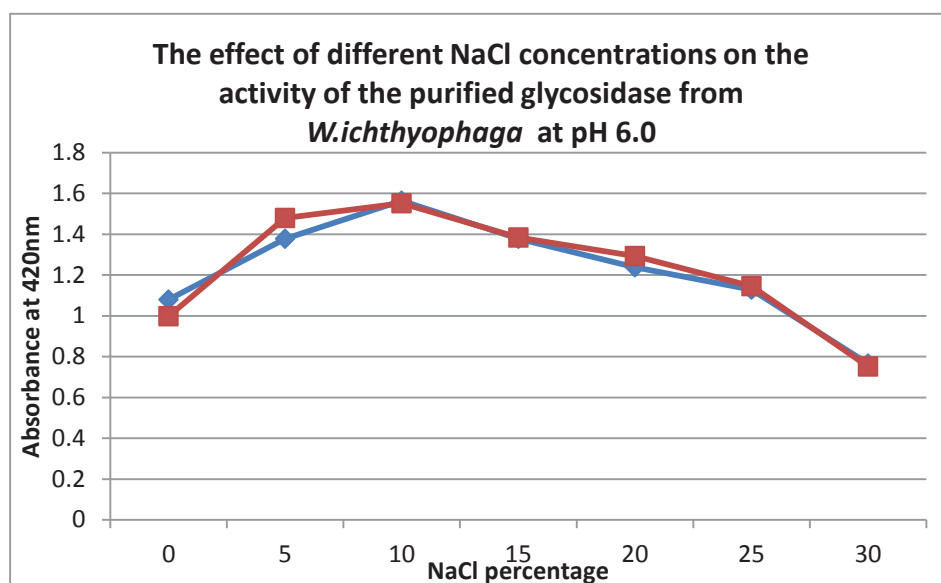


Figure 3.4.10: Activity of the glycosidase from *Wallemia ichthyophaga* at different NaCl concentrations in 100mM citric acid: sodium phosphate at pH 6.0.

Figure 3.4.10 shows the effect that NaCl has on the activity of the purified glycosidase, with the optimum salt concentration being at 10% NaCl. Over the NaCl concentration range of 10% to 30% there is a drop in activity of 50%, implying that at high salt concentrations, the activity of the glycosidase is retarded. This could be due to the high ionic strength interfering with substrate recognition and binding or it could be affecting the catalytic mechanism. In contrast, there is a 60% increase in activity with the addition of 10% NaCl, when compared to 0% NaCl, suggesting that the higher ionic strength is enhancing activity. It is possible that binding involves hydrophobic interactions which are enhanced by low NaCl concentrations. Above this 10% threshold, NaCl inhibits activity most likely through denaturation of the glycosidase.

### **3.4.7 The effect of metal ions on the activity of the glycosidase**

Enzymatic activity can be enhanced by metal cofactors which bind near the active site of an enzyme. EDTA (Ethylenediaminetetraacetic acid), a metal chelating agent, was used to test if the glycosidase was a metalloprotein. If a metal cofactor is

essential for activity, the addition of EDTA will result in either a loss or reduction of activity.

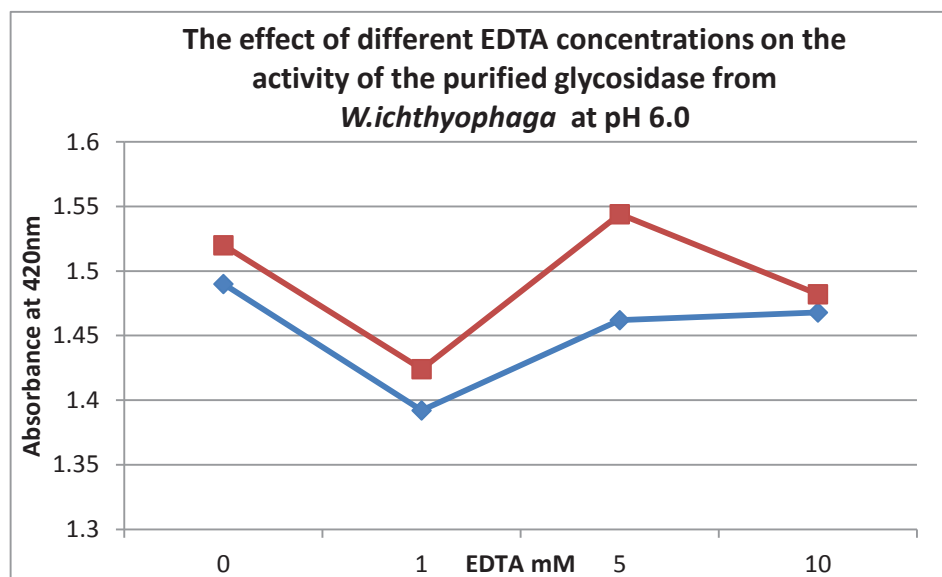


Figure 3.4.11: Activity of the secreted glycosidase from *Wallemia ichthyophaga* at different concentrations of EDTA in 100mM citric acid: sodium phosphate.

The addition of both low and high concentrations of EDTA had no significant effect on the activity of the glycosidase, implying that a metal ion is not required for activity (Figure 3.4.11). This is not surprising as only a few glycosidases, from the glycosidase family 4, are known to have a requirement for metal cofactors (Cantarel, *et al.*, 2009), and the mass spectrometry results, of the purified glycosidase, indicate that this glycosidase belongs to the glycosidase family 3.

#### 3.4.8 Stability at 25°C

In order to investigate the substrate specificity of the purified glycosidase, the stability of the glycosidase over time at 25°C was investigated. This will allow for slow reacting substrates to be left until sufficient product is produced, without the risk of activity being lost due to inactivation. When the glycosidase was left at 25°C for 24 hours the activity decreased only by 0.2 AU. The glycosidase is therefore stable at this temperature for at least 24 hours, and so this was the maximum incubation time tested for each substrate (Figure 3.4.12).

## Results and Discussion

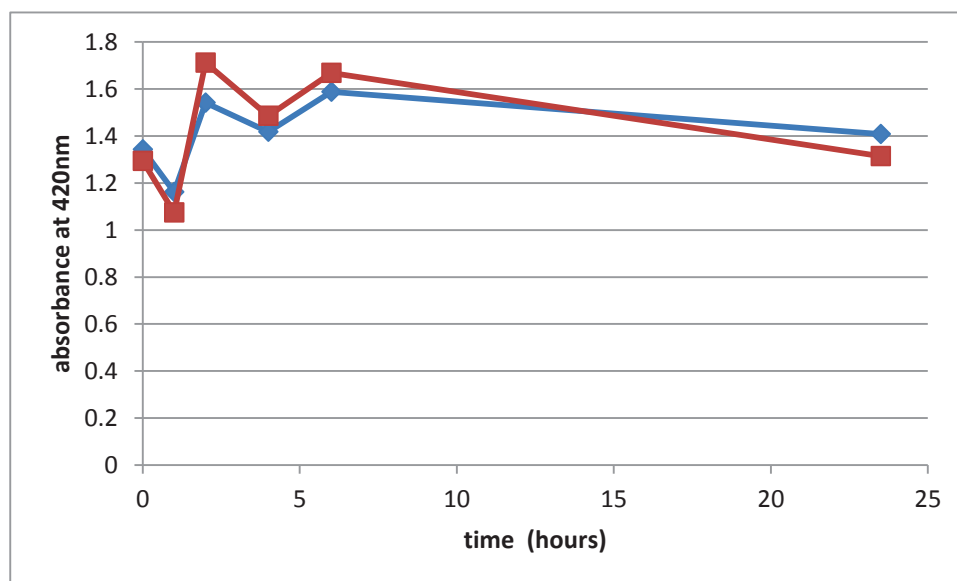


Figure 3.4.12: The stability of glycosidase from *Wallemia ichthyophaga* at 25°C.

### 3.4.9 Inactivation of the glycosidase

Glycosidases cleave the bond between monosaccharide sugars within the disaccharide or polysaccharide and so a glucose assay kit was used to assess the substrate specificity of the purified glycosidase. This assay uses glucose oxidase to oxidise  $\beta$ -D-Glucose, hydrolysed from the di/polysaccharide by the glycosidase in question, to  $\beta$ -D-Glucose-1,5-Lactone +  $H_2O_2$ . The  $H_2O_2$  is then utilised by the peroxidase to convert the colour reagent *o*-Dianisidine from the colourless reduced form to the brown oxidised form. The addition of sulfuric acid lowers the pH changing the brown *o*-Dianisidine to pink, allowing the absorbance of the colour reagent to be read at 520 nm (Figure 3.4.13).

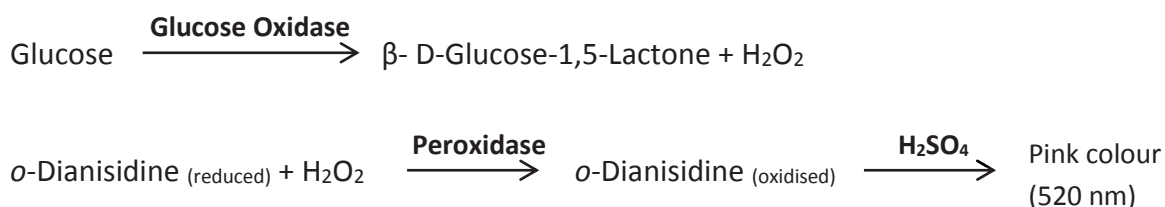


Figure 3.4.13: Glucose assay kit reaction involving glucose oxidase and peroxidase for the conversion of *O*-dianisidine (GE Healthcare, glucose GO kit).

Discontinuous assays require an efficient method to inactivate the enzyme before the end product can be measured. Changing the pH cannot be used as the glucose assay kit uses glucose oxidase and peroxidase enzymes which require a pH around 6.0 to be active. An alternative method is to use heat. Tests showed that heating the glycosidase at 70°C for 5 mins was sufficient to fully denature the enzyme. In order to account for any colour change due to heating, a negative control was used for each sugar as a blank.

#### **3.4.10 Mini scale glucose test**

The glucose assay kit contained enough reagents for 20X 5 mL reactions. In order to increase the number of reactions that could be performed, the reaction volume was reduced to 1 mL. The standard curve produced using a 1 mL reaction showed that the linear relationship between the absorbance at 520nm and glucose concentrations was maintained, validating the method (Figure 3.4.14).

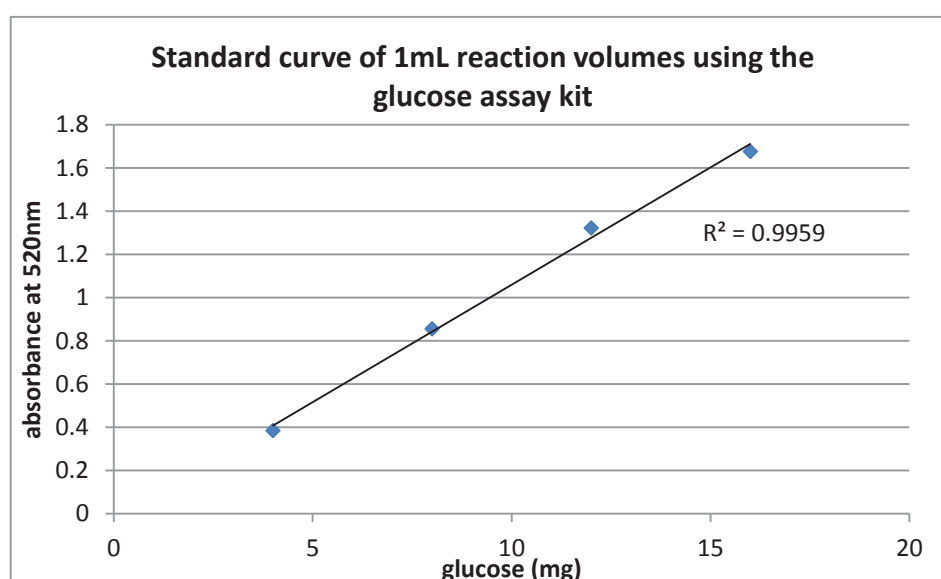


Figure 3.4.14: Standard curve of different glucose concentrations using 1mL reactions from Glucose (GOD) assay kit (Sigma).

#### **3.4.11 Substrate specificity**

Glycosidases cleave the linkage between monosaccharides, with the stereochemistry of the linkage and sugar composition both contributing to the

## Results and Discussion

substrate specificity of the enzyme. A range of different disaccharides and polysaccharides were incubated with the purified glycosidase to test the substrate specificity of the enzyme. Activity was detected either by the release of a nitrophenol group, attached to the monosaccharide, or the levels of glucose released from the disaccharide or polysaccharide, using a glucose (GOD) assay kit (GE Healthcare, glucose GO kit).

Table 3.4.3: Substrate specificity of the glycosidase secreted from *Wallemia ichthyophaga*.

Substrate	Composition	4 hour incubation	24 hour incubation
<i>o</i> -nitrophenol-glucopyranocidase	<i>o</i> -nitrophenol- $\beta$ -(1,4)-glucose	✓	-
<i>o</i> -nitrophenol-galactopyranocidase	<i>o</i> -nitrophenol- $\beta$ -(1,4)-galactose	✗	✗
Cellobiose	Glucose- $\beta$ -(1,4)-Glucose	✓	-
Lactose	Glucose- $\beta$ -(1,4)-Galactose	✗	✗
Sucrose	Glucose- $\beta$ -(1,4)-Fructose	✓	-
Mannose	Glucose- $\alpha$ -(1,4)-Glucose	✓	-
Starch	Glucose- $\alpha$ -(1,4)-Glucose (branched)	✗	✓

✓ Activity detectable by either nitrophenol release or glucose levels.

✗ No activity detected

- Not tested

The resultant assays showed that the glycosidase isolated from the secretome of *W.ichthyophaga* can cleave both  $\beta$ -(1,4) linkages and  $\alpha$ -(1,4) linkages (Table 3.4.3). It is highly unlikely that this is due to the presence of a co-purified  $\alpha$ / $\beta$ -glycosidase, as the mass spectrometry results of the purified glycosidase, confirmed that only a single protein was present (Table 3.4.1). This particular bifunctional catalytic activity is not usually observed in GH3 glycosidases, as most cleave different types of  $\beta$ -linkages (Bao *et al.*, 2012; Ferrara *et al.*, 2014). But a few GH3 glycosidases have

been found that can cleave  $\beta$ -glucose and/or  $\beta$ -xylose along with  $\alpha$ -arabinose from disaccharides. Such lack of specificity is thought to occur because the hydroxyl-groups and glycosidic bonds of the  $\alpha$ -linked substrate are in similar steric locations to the  $\beta$ -linked substrate, except for the OH group on carbon 4. Also, when the substrate binds to the active site, most of it sticks out from the cleft, therefore allowing greater variability in the type of substrate that can bind, as only a small portion of the substrate interacts with the enzyme (Gruninger, Gong, Forster, & McAllister, 2013; J. Lee, *et al.*, 2011; R. C. Lee, Hrmova, Burton, Lahnstein, & Fincher, 2003). The isolated glycosidase is therefore unique in the types of carbohydrates cleaved, but not in the ability to cleave both  $\alpha$ - and  $\beta$ - linkages.

When the glycosidase was incubated with either *o*-nitrophenol- $\beta$ -(1,4)-galactose or lactose (Glucose- $\beta$ -(1,4)-Galactose), no activity was detected. The purified glycosidase therefore does not cleave carbohydrates containing galactose monosaccharides. This is in contradiction to what is seen for other GH3  $\alpha/\beta$  bifunctional enzymes, in which the only variability between substrates occurs at carbon 4, while for the purified glycosidase variability at carbon 4, which is the only difference in stereochemistry between glucose and galactose, prevents activity.

Finally, alternative splicing is one mechanism used to transcribe and translate enzymes from the same gene, with different activities or enzymes directed to different cellular locations (Iwashita *et al.*, 1999). The bifunctional activity of the purified glycosidase, if it is real, could therefore be a result of alternative splicing of the intron as the intron is located in the N-terminal GH3 domain, which is involved in catalysis and substrate binding. While many GH3 genes contain introns, alternative splicing is not a common occurrence for GH3 glycosidases (Bierfreund, Tintelnot, Reski, & Decker, 2004; Okrent & Wildermuth, 2011; Terol, Domingo, & Talón, 2006). The mechanism responsible for the bifunctional activity observed for the purified glycosidase, or even the existence of the bifunctional activity, still remains unknown.



### 4.0 Conclusion and Future work

#### 4.1 Conclusion

Two bacterial species, one budding yeast, and a range of filamentous fungi, were isolated from the contaminated salted ovine pelts from LASRA. *W.ichthyophaga*, one of the filamentous fungi, did show depilation activity early on, but this activity was lost for unknown reasons. Even the addition of dried ground ovine skin directly into the media used to culture *W.ichthyophaga*, to induce production of the depilation enzyme, did not restore the depilation activity. Possible explanations for the loss/lack of depilation activity are: i) that the microorganism/s responsible for the observed depilation activity were not isolated because of inadequate culture conditions, ii) that depilation was not achieved as the correct combination of organisms required to attain depilation was not tested, iii) that changes in gene expression over time altered the composition of the secretome resulting in the loss of depilation activity. The secretome of *W.ichthyophaga* was then chosen to be further analysed as this microorganism was consistently isolated from the pelts, and is a unique extreme xerophile in the fungal kingdom.

The composition of the secretome of *W.ichthyophaga* was analysed using proteomic methods. This involved in-gel tryptic digestion of each protein band, obtained from 1D SDS-PAGE of the secretome, followed by mass spectrometry. Ultrafiltration was found to be the best method for concentrating and desalting the secretome before SDS-PAGE and purification, rather than precipitation. When dried ground ovine skin was added as a supplement to the media used to culture *W.ichthyophaga*, to try and induce the production of the depilation enzyme/s, depilation activity was not restored. Instead the skin was converted to a gelatinous substrate which made future analysis of the secretome impossible.

Overall, mass spectrometry identified many different types of  $\beta$ -glycosidases, one  $\alpha$ -glycosidase, and a range of intracellular proteins. Interestingly, no proteases, lipases, or esterases were identified, and only one protein was possibly misidentified. The lack of proteases in the secretome may explain why the

## Conclusion and Future work

secretome of *W.ichthyophaga* failed to depilate ovine skin. It is possible that the loss of depilation activity may have been due to the down regulation of protease expression as a result of the carbon rich media used to culture the fungus. Overall, the composition of the secretome of *W.ichthyophaga* was simpler than expected. This could be due to substantial loss of protein from the sample during processing and preparation for mass spectrometry and/or that a large majority of enzymes secreted remain attached to the outer-membrane of the fungi through a polysaccharide chain (REF).

Generalised enzymatic activity assays were carried out on the secretome for glycosidase, protease, and lipase/esterase activities. As predicted by the mass spectrometry results,  $\beta$ -glycosidase activity was detected in the secretome. Lipase/esterase activity was also detected, and this could be due to the phytase, which cleaves a phosphate ester bond, or some of the hypothetical proteins which have unknown activities. As expected, no protease activity was detected. Initial anion exchange chromatography on the secretome, linked the glycosidase activity to a single fraction, and this activity was thus chosen for further purification.

The use of AEX followed by SEC chromatography successfully purified a glycosidase from the secretome of *W.ichthyophaga*. The addition of glycerol during purification increased the stability of the glycosidase: the enzyme remained active at 4°C after 1 month with glycerol present, rather than only 3 days without glycerol present. Once frozen at -80°C, the glycosidase (in 10% glycerol) remained active, even after being stored for 6 months, but 30% of activity was lost upon thawing.

At each stage of the purification process the protein concentration, using the Bradford assay, and the glycosidase activity, using a generalised glycosidase assay, was measured. In addition the protein content of each fraction was also analysed by SDS-PAGE. The specific activity was then calculated, and thus the purity of each fraction. Overall, these readings gave enough information to select fractions for either further purification or enzymatic characterisation. Quite surprisingly, the generalised  $\beta$ -glycosidase assay accurately tracked a single glycosidase enzyme,

## Conclusion and Future work

even though the mass spectrometry results indicated that the secretome contained multiple  $\beta$ -glycosidases. This could have occurred due to the 'general'  $\beta$ -glycosidase substrate being specific to only one of the secreted glycosidases or that the other glycosidases were either denatured or lost during purification. The resultant purified fractions contained a band doublet between 90 kDa and 100 kDa.

The final purification procedure of the secreted glycosidase from *W.ichthyophaga* had a 13% yield, and the enzyme was purified 4.9-fold. The glycosidase made up 2.4% of the total secreted protein or 1.2 mg per litre. The yield achieved for the overall procedure was within the expected range, while the purification fold for the overall procedure was below the norm. Finally, IEX produced a fraction of average purity useful for characterisation assays, while SEC produced fractions of high purity useful for crystallography.

Mass spectrometry identified the purified glycosidase as a putative  $\beta$ -glycosidase L (EOQ98916.1) from *W.ichthyophaga*, and also confirmed that both bands, on the SDS-PAGE gel of the purified fraction, were the same protein. The band doublet is therefore not due to co-purification of another protein. The glycosidase is a monomer, as indicated by the SEC calibration curve, therefore the band doublet is not due to heterodimerisation. PNGase F and Endo H digests of the glycosidase, showed that the band doublet was not due to different glycoforms of the same protein. This experiment also showed that the glycans were high mannose, and that the link to the asparagine side chain was buried.

Analysis of both the DNA and protein sequence of the glycosidase using BLAST, showed that it was made up of both the N- and C- terminal domains from the GH3 family, and contained a 20 a.a intron in the N-terminal domain as well as a 27 a.a signal sequence. This intron is too small to account for the estimated difference in the masses of the two bands in the doublet, a possibility that could occur through alternative splicing. An alternative start codon is also not responsible for the formation of the band doublet, as the next ATG is too far along the gene to account for the molecular weight difference. Finally, there are 6 cysteines present in the

## Conclusion and Future work

glycosidase sequence. It is therefore possible that the band doublet may have formed because of incomplete reduction of these hypothetical disulfide bonds, resulting in the production of two populations of the same protein, which differ only in structure and amount of SDS bound. This would produce a band doublet when analysed by SDS-PAGE (Hong, 2007). An experiment to test this theory has yet to be done.

The optimum pH of the purified glycosidase was at pH 6.0. The optimum NaCl concentration was at 10%, which was unexpected as 10% NaCl is the minimum concentration of NaCl required for *W.ichthyophaga* to grow. The glycosidase is not a metalloprotein, like most of the other glycosyl hydrolases. When the substrate specificity of the purified glycosidase was tested, both  $\alpha$ - and  $\beta$ - linked sugars were cleaved. Interestingly, branching resulted in a reduced catalytic rate, and the presence of galactose prevented cleavage. The ability of this glycosidase to cleave both  $\alpha$ - and  $\beta$ - glycoside bonds has been documented in other GH3 glycosidases but not for these particular substrates. Also the glycosidases inability to cleave galactose, most likely due to the difference in the stereochemistry of the OH group at carbon 4, contradicts the mechanism proposed by other GH3  $\alpha/\beta$  bifunctional enzymes.

### **4.2 Future work**

For complete characterisation of the purified glycosidase from the secretome of *W.ichthyophaga*, the ability of the glycosidase to cleave both  $\alpha$ - and  $\beta$ - glycoside bonds first needs to be confirmed. This would be achieved through additional assays involving a range of substrates, such as other  $\alpha$ -linked disaccharides. Also, an explanation for the formation of the band doublet needs to be investigated, such as reducing and alkylating the cysteines. It would also be interesting to investigate the effect of skin on both the expression and activity of the glycosidase. The structure of the glycosidase could be analysed using crystallography, and the subdomains/domains could be analysed by NMR. Finally kinetics of the glycosidase with and without NaCl could be investigated. Complete characterisation will most likely require recombinant glycosidase, to attain high quantities of protein, and therefore the gene will need to be successfully cloned and expressed.

The structural and kinetic characteristics of the purified glycosidase could then be used to confirm the classification of this enzyme into the GH3 family. Also, the glycosidase could be compared to other characterised glycosidases, to analyse whether the effect of high NaCl/low water activity has led to any significant evolutionary changes.

## Conclusion and Future work

## 5.0 Reference list

- Aebersold, R., & Mann, M. (2003). Mass spectrometry-based proteomics. *Nature*, 422(6928), 198-207.
- Ahn, M. (2012). [LASRA dewooling enzymes].
- Altayar, M., & Sutherland, A. (2006). *Bacillus cereus* is common in the environment but emetic toxin producing isolates are rare. *Journal of applied microbiology*, 100(1), 7-14.
- Andersen, R. B., Karring, H., Møller-Pedersen, T., Valnickova, Z., Thøgersen, I. B., Hedegaard, C. J., Enghild, J. J. (2004). Purification and structural characterization of transforming growth factor beta induced protein (TGFBIp) from porcine and human corneas. *Biochemistry*, 43(51), 16374-16384.
- Anindyawati, T., Ann, Y. G., Ito, K., Iizuka, M., & Minamiura, N. (1998). Two kinds of novel alpha-glucosidases from *Aspergillus awamori* KT-11: Their purifications, properties and specificities. *Journal of Fermentation and Bioengineering*, 85(5), 465-469. doi: 10.1016/s0922-338x(98)80063-9
- Arahal, D. R., & Ventosa, A. (2002). Moderately halophilic and halotolerant species of *Bacillus* and related genera. *Applications and Systematics of Bacillus and Relatives*, 83-99.
- Aranda, C., Robledo, A., Loera, O., Contreras-Esquivel, J. C., Rodríguez, R., & Aguilar, C. N. (2006). Fungal Invertase Expression in Solid-State Fermentation. *Food Technology & Biotechnology*, 44(2).
- Aravindhan, R., Madhan, B., Thanikaivelan, P., Kanth, S. V., Rao, J. R., Gnanasekaran, C., & Nair, B. U. (2008). Upgradation of leathers: Masking defects using pigments in pre-finishing processes. *Journal of Scientific and Industrial Research*, 67(3), 233.
- Aravindhan, R., Saravanabhavan, S., Thanikaivelan, P., Rao, J. R., & Nair, B. U. (2007). A chemo-enzymatic pathway leads towards zero discharge tanning. *Journal of Cleaner Production*, 15(13-14), 1217-1227. doi: 10.1016/j.jclepro.2006.07.010
- Asgher, M., Bhatti, H. N., Ashraf, M., & Legge, R. L. (2008). Recent developments in biodegradation of industrial pollutants by white rot fungi and their enzyme system. *Biodegradation*, 19(6), 771-783.
- Bao, L., Huang, Q., Chang, L., Sun, Q., Zhou, J., & Lu, H. (2012). Cloning and characterization of two  $\beta$ -glucosidase/xylosidase enzymes from yak rumen metagenome. *Applied biochemistry and biotechnology*, 166(1), 72-86.
- Berka, R. M., Rey, M. W., Brown, K. M., Byun, T., & Klotz, A. V. (1998). Molecular characterization and expression of a phytase gene from the thermophilic fungus *Thermomyces lanuginosus*. *Applied and environmental microbiology*, 64(11), 4423-4427.
- Bernstein, E. F., Underhill, C. B., Hahn, P. J., Brown, D. B., & Uitto, J. (1996). Chronic sun exposure alters both the content and distribution of dermal glycosaminoglycans. *British Journal of Dermatology*, 135(2), 255-262. doi: 10.1111/j.1365-2133.1996.tb01156.x
- Bierfreund, N. M., Tintelnot, S., Reski, R., & Decker, E. L. (2004). Loss of GH3 function does not affect phytochrome-mediated development in a moss, *Physcomitrella patens*. *Journal of plant physiology*, 161(7), 823-835.

- Bourne, Y., & Henrissat, B. (2001). Glycoside hydrolases and glycosyltransferases: families and functional modules. *Current opinion in structural biology*, 11(5), 593-600.
- Bouws, H., Wattenberg, A., & Zorn, H. (2008). Fungal secretomes—nature's toolbox for white biotechnology. *Applied microbiology and biotechnology*, 80(3), 381-388.
- Breuer, U., & Harms, H. (2006). *Debaryomyces hansenii*—an extremophilic yeast with biotechnological potential. *Yeast*, 23(6), 415-437.
- Brown, K. J., Formolo, C. A., Seol, H., Marathi, R. L., Duguez, S., An, E., Hathout, Y. (2012). Advances in the proteomic investigation of the cell secretome.
- Cantarel, B. L., Coutinho, P. M., Rancurel, C., Bernard, T., Lombard, V., & Henrissat, B. (2009). The Carbohydrate-Active EnZymes database (CAZy): an expert resource for glycomics. *Nucleic acids research*, 37(suppl 1), D233-D238.
- Caspers, P. J., Lucassen, G. W., Wolthuis, R., Bruining, H. A., & Puppels, G. J. (1998). In vitro and in vivo Raman spectroscopy of human skin. *Biospectroscopy*, 4(5), S31-S39. doi: 10.1002/(sici)1520-6343(1998)4:5+<s31::aid-bsp4>3.0.co;2-m
- Chiba, S. (2011). A historical perspective for the catalytic reaction mechanism of glycosidase; so as to bring about breakthrough in confusing situation. *Bioscience, biotechnology, and biochemistry*, 76(2), 215-231.
- Chitlaru, T., Gat, O., Grosfeld, H., Inbar, I., Gozan, Y., & Shafferman, A. (2007). Identification of in vivo-expressed immunogenic proteins by serological proteome analysis of the Bacillus anthracis secretome. *Infection and Immunity*, 75(6), 2841-2852. doi: 10.1128/iai.02029-06
- Cottrell, J., & London, U. (1999). Probability-based protein identification by searching sequence databases using mass spectrometry data. *Electrophoresis*, 20(18), 3551-3567.
- Davies, G. J., Planas, A., & Rovira, C. (2011). Conformational analyses of the reaction coordinate of glycosidases. *Accounts of chemical research*, 45(2), 308-316.
- Dayanandan, A., Kanagaraj, J., Sounderraj, L., Govindaraju, R., & Rajkumar, G. S. (2003). Application of an alkaline protease in leather processing: an ecofriendly approach. *Journal of Cleaner Production*, 11(5), 533-536. doi: 10.1016/s0959-6526(02)00056-2
- Deb Choudhury, S., Allsop, T., Passman, A., & Norris, G. (2006). Use of a proteomics approach to identify favourable conditions for production of good quality lambskin leather. *Analytical and bioanalytical chemistry*, 384(3), 723-735.
- Derler, S., & Gerhardt, L.-C. (2012). Tribology of skin: review and analysis of experimental results for the friction coefficient of human skin. *Tribology Letters*, 45(1), 1-27.
- Desmet, T., & Soetaert, W. (2011). Enzymatic glycosyl transfer: mechanisms and applications. *Biocatalysis and Biotransformation*, 29(1), 1-18.
- Deuschle, K., Funck, D., Hellmann, H., Däschner, K., Binder, S., & Frommer, W. B. (2001). A nuclear gene encoding mitochondrial  $\Delta^1$ -pyrroline-5-carboxylate dehydrogenase and its potential role in protection from proline toxicity. *The Plant Journal*, 27(4), 345-356.
- Dial, J. R., & Moore, C. O. (1997). Method for making liquid-centered jelly candies: Google Patents.

- Drobniewski, F. (1994). The safety of *Bacillus* species as insect vector control agents. *Journal of applied bacteriology*, 76(2), 101-109.
- Edmonds, R. (2008). *Proteolytic depilation of lamnskin*. Masters in Biochemistry, Massey University, Palmerston North
- Edmonds, R. L., Deb Choudhury, S., Haverkamp, R. G., Birtles, M., Allsop, T. F., & Norris, G. E. (2008). Using proteomics, immunohistology, and atomic force microscopy to characterize surface damage to lambskins observed after enzymatic dewooling. *Journal of agricultural and food chemistry*, 56(17), 7934-7941.
- Eidhammer, I., Flikka, K., Martens, L., & Mikalsen, S.-O. (2007). *Computational methods for mass spectrometry proteomics*. Chichester, England: John Wiley and Sons, Ltd.
- Ellis, J. G., Rafiqi, M., Gan, P., Chakrabarti, A., & Dodds, P. N. (2009). Recent progress in discovery and functional analysis of effector proteins of fungal and oomycete plant pathogens. *Current opinion in plant biology*, 12(4), 399-405.
- Elthon, T. E., & Stewart, C. R. (1981). Submitochondrial location and electron transport characteristics of enzymes involved in proline oxidation. *Plant physiology*, 67(4), 780-784.
- Farag, A. M., & Hassan, M. A. (2004). Purification, characterization and immobilization of a keratinase from *Aspergillus oryzae*. *Enzyme and Microbial Technology*, 34(2), 85-93.
- Ferrara, M. C., Cobucci-Ponzano, B., Carpentieri, A., Henrissat, B., Rossi, M., Amoresano, A., & Moracci, M. (2014). The identification and molecular characterization of the first archaeal bifunctional exo- $\beta$ -glucosidase/N-acetyl- $\beta$ -glucosaminidase demonstrate that family GH116 is made of three functionally distinct subfamilies. *Biochimica et Biophysica Acta (BBA)-General Subjects*, 1840(1), 367-377.
- Filitcheva, J., Ahn, M., & Norris, G. (2011). *Progress Report*. Research. IMBS Massey University, Palmerston North. Palmerston North.
- Flint, S., Palmer, J., Bloemen, K., Brooks, J., & Crawford, R. (2001). The growth of *Bacillus stearothermophilus* on stainless steel. *Journal of applied microbiology*, 90(2), 151-157.
- Gadda, G., & McAllister-Wilkins, E. E. (2003). Cloning, expression, and purification of choline dehydrogenase from the moderate halophile *Halomonas elongata*. *Applied and environmental microbiology*, 69(4), 2126-2132.
- George, S., Raju, V., Krishnan, M., Subramanian, T., & Jayaraman, K. (1995). Production of protease by *Bacillus amyloliquefaciens* in solid-state fermentation and its application in the unhairing of hides and skins. *Process Biochemistry*, 30(5), 457-462.
- Ghorai, S., Banik, S. P., Verma, D., Chowdhury, S., Mukherjee, S., & Khowala, S. (2009). Fungal biotechnology in food and feed processing. *Food research international*, 42(5), 577-587.
- Girard, V., Dieryckx, C., Job, C., & Job, D. (2013). Secretomes: the fungal strike force. *Proteomics*, 13(3-4), 597-608.

- Gruninger, R., Gong, X., Forster, R., & McAllister, T. (2013). Biochemical and kinetic characterization of the multifunctional  $\beta$ -glucosidase/ $\beta$ -xylosidase/ $\alpha$ -arabinosidase, Bgxa1. *Applied microbiology and biotechnology*, 1-10.
- Gunde-Cimerman, N., Ramos, J., & Plemenitaš, A. (2009). Halotolerant and halophilic fungi. *Mycological research*, 113(11), 1231-1241.
- Han, Z.-h., Liu, J.-n., Dang, A. I., Zhang, P.-q., Dai, X.-d., & Zhang, J.-c. (2012). Purification and Characterization of Laccase from *Auricularia auricula*. *Journal of Fungal Research*, 10(4), 234-239.
- Harvey, A. J., Hrmova, M., De Gori, R., Varghese, J. N., & Fincher, G. B. (2000). Comparative modeling of the three-dimensional structures of family 3 glycoside hydrolases. *Proteins: Structure, Function, and Bioinformatics*, 41(2), 257-269.
- Henrissat, B. (1991). A classification of glycosyl hydrolases based on amino acid sequence similarities. *Biochem. J*, 280, 309-316.
- Henrissat, B., Coutinho, P. M., & Davies, G. J. (2001). A census of carbohydrate-active enzymes in the genome of *Arabidopsis thaliana* Plant Cell Walls. *Springer*, 55-72
- Hewitson, J. R., Harcus, Y. M., Curwenb, R. S., Dowle, A. A., Atmadja, A. K., Ashton, P. D., Maizels, R. M. (2008). The secretome of the filarial parasite, *Brugia malayi*: Proteomic profile of adult excretory-secretory products. *Molecular and Biochemical Parasitology*, 160(1), 8-21.
- Hibbett, D. S. (2006). A phylogenetic overview of the Agaricomycotina. *Mycologia*, 98(6), 917-925.
- Hong, K. (2007). *Heterologous production and characterisation of a yeast peptide: N-glycanase*. Master of Science in Biochemistry, Massey University, Palmerston North.
- Hua, S.-S. T., Lichens, G. M., Guirao, A., & Tsai, V. Y. (1986). Biochemical properties of glutamate synthase of salt-tolerant *Bradyrhizobium* sp. strain WR1001. *FEMS microbiology letters*, 37(2), 209-213.
- Huelsken, J., Vogel, R., Erdmann, B., Cotsarelis, G., & Birchmeier, W. (2001).  $\beta$ -Catenin controls hair follicle morphogenesis and stem cell differentiation in the skin. *Cell*, 105(4), 533-545.
- Iwashita, K., Nagahara, T., Kimura, H., Takano, M., Shimoi, H., & Ito, K. (1999). The bglA gene of *Aspergillus kawachii* encodes both extracellular and cell wall-bound  $\beta$ -glucosidases. *Applied and environmental microbiology*, 65(12), 5546-5553.
- Johnson, L., & Tate, M. (1969). Structure of "phytic acids". *Canadian Journal of Chemistry*, 47(1), 63-73.
- Joshua-Tor, L., Xu, H. E., Johnston, S. A., & Rees, D. C. (1995). Crystal structure of a conserved protease that binds DNA: the bleomycin hydrolase, Gal6. *Science*, 269(5226), 945-950.
- Kadowaki, M. K., de Cassia Garcia, R., da Conceicao Silva, S. L., & Aoki, C. (2013). Biotechnological Advances in Fungal Invertases. *Fungal Enzymes*, 1.
- Knisely, R. F. (1966). Selective medium for *Bacillus anthracis*. *Journal of Bacteriology*, 92(3), 784.
- Kruger, N. J. (2009). The Bradford method for protein quantitation *The protein protocols handbook* (pp. 17-24): Springer.

- Kumar, S., Karan, R., Kapoor, S., Singh, S., & Khare, S. (2012). Screening and isolation of halophilic bacteria producing industrially important enzymes. *Brazilian Journal of Microbiology*, *43*(4), 1595-1603.
- Kuncic, M. K., Kogej, T., Drobne, D., & Gunde-Cimerman, N. (2010). Morphological Response of the Halophilic Fungal Genus *Wallemia* to High Salinity. *Applied and Environmental Microbiology*, *76*(1), 329-337. doi: Doi 10.1128/Aem.02318-09
- Kuncic, M. K., Zajc, J., Drobne, D., Pipan Tkalec, Ž., & Gunde-Cimerman, N. (2013). Morphological responses to high sugar concentrations differ from adaptation to high salt concentrations in the xerophilic fungi *Wallemia* spp. *Fungal biology*, *117*(7), 466-478.
- Lassen, S. F., Breinholt, J., Østergaard, P. R., Brugger, R., Bischoff, A., Wyss, M., & Fuglsang, C. C. (2001). Expression, gene cloning, and characterization of five novel phytases from four basidiomycete fungi: *Peniophora lycii*, *Agrocybe pediades*, a *Ceriporia* sp., and *Trametes pubescens*. *Applied and Environmental Microbiology*, *67*(10), 4701-4707.
- Lee, J., Hyun, Y. J., & Kim, D. H. (2011). Cloning and characterization of  $\alpha$ -L-arabinofuranosidase and bifunctional  $\alpha$ -L-arabinopyranosidase/ $\beta$ -D-galactopyranosidase from *Bifidobacterium longum* H-1. *Journal of applied microbiology*, *111*(5), 1097-1107.
- Lee, R. C., Hrmova, M., Burton, R. A., Lahnstein, J., & Fincher, G. B. (2003). Bifunctional Family 3 Glycoside Hydrolases from Barley with  $\alpha$ -L-Arabinofuranosidase and  $\beta$ -d-Xylosidase Activity characterization, primary structures, and cooh-terminal processing. *Journal of Biological Chemistry*, *278*(7), 5377-5387.
- Lenassi, M., Zajc, J., Gostincar, C., Gorjan, A., Gunde-Cimerman, N., & Plemenitas, A. (2011). Adaptation of the glycerol-3-phosphate dehydrogenase Gpd1 to high salinities in the extremely halotolerant *Hortaea werneckii* and halophilic *Wallemia ichthyophaga*. *Fungal Biology*, *115*(10), 959-970. doi: 10.1016/j.funbio.2011.04.001
- Leonard, C. K., Spellman, M. W., Riddle, L., Harris, R. J., Thomas, J. N., & Gregory, T. (1990). Assignment of intrachain disulfide bonds and characterization of potential glycosylation sites of the type 1 recombinant human immunodeficiency virus envelope glycoprotein (gp120) expressed in Chinese hamster ovary cells. *Journal of Biological Chemistry*, *265*(18), 10373-10382.
- Lilius, G., Holmberg, N., & Bülow, L. (1996). Enhanced NaCl stress tolerance in transgenic tobacco expressing bacterial choline dehydrogenase. *Nature Biotechnology*, *14*(2), 177-180.
- Lim, R., Zaheer, A., Yorek, M. A., Darby, C. J., & Oberley, L. W. (2000). Activation of Nuclear Factor- $\kappa$ B in C6 Rat Glioma Cells After Transfection with Glia Maturation Factor. *Journal of Neurochemistry*, *74*(2), 596-602.
- Liu, J.-l., Lou, Y.-k., Hu, Z.-y., Zheng, Z.-h., Huang, Y.-j., & Xu, Q.-y. (2012). Purifications and Structure Elucidations of Cyclophenol and Cyclophenin. *Xiamen Daxue Xuebao (Ziran Kexue Ban)*, *51*(3), 386-390.
- Lyne, A. (1961). The postnatal development of wool follicles, shedding, and skin thickness in inbred Merino and Southdown-Merino crossbred sheep. *Australian Journal of Biological Sciences*, *14*(1), 141-156.

- Marra, R., Ambrosino, P., Carbone, V., Vinale, F., Woo, S. L., Ruocco, M., Soriente, I. (2006). Study of the three-way interaction between *Trichoderma atroviride*, plant and fungal pathogens by using a proteomic approach. *Current genetics*, 50(5), 307-321.
- McIntosh, L. P., Hand, G., Johnson, P. E., Joshi, M. D., Korner, M., Plesniak, L. A., Withers, S. G. (1996). The pK(a) of the general acid/base carboxyl group of a glycosidase cycles during catalysis: A C-13-NMR study of *Bacillus circulans* xylanase. *Biochemistry*, 35(31), 9958-9966.
- Meng, F.-G., Hong, Y.-K., He, H.-W., Lyubarev, A. E., Kurganov, B. I., Yan, Y.-B., & Zhou, H.-M. (2004). Osmophobic effect of glycerol on irreversible thermal denaturation of rabbit creatine kinase. *Biophysical journal*, 87(4), 2247-2254.
- Nazer, D. W., Al-Sa'ed, R. M., & Siebel, M. A. (2006). Reducing the environmental impact of the unhairing–liming process in the leather tanning industry. *Journal of Cleaner Production*, 14(1), 65-74.
- Nei, M. (1971). Interspecific gene differences and evolutionary time estimated from electrophoretic data on protein identity. *American Naturalist*, 385-398.
- Nelson, E. K., Piehler, B., Eckels, J., Rauch, A., Belew, M., Hussey, P., Ramsay, S., Nathe, C., Lum, K., Krouse, K., Stearns, D., Connolly, B., Skillman, T., & Igra, M. (2011). LabKey server: An open source platform for science data intergration, analysis and collaboration. *BMC Bioinformatics*, 12 (71),
- Nevalainen, K., Te'o, V. S., & Bergquist, P. L. (2005). Heterologous protein expression in filamentous fungi. *TRENDS in Biotechnology*, 23(9), 468-474.
- Nickel, W., & Rabouille, C. (2009). Mechanisms of regulated unconventional protein secretion. *Nature Reviews Molecular Cell Biology*, 10(2), 148-155.
- Nombela, C., Gil, C., & Chaffin, W. L. (2006). Non-conventional protein secretion in yeast. *Trends in microbiology*, 14(1), 15-21.
- Oikarinen, A. (1994). Aging of the skin connective-tissue - how to measure the biochemical and mechanical-properties of aging dermis. *Photodermatology Photoimmunology & Photomedicine*, 10(2), 47-52.
- Okrent, R. A., & Wildermuth, M. C. (2011). Evolutionary history of the GH3 family of acyl adenylases in rosids. *Plant molecular biology*, 76(6), 489-505.
- Oliver, R. F., & Jahoda, C. A. B. (1988). Dermal-epidermal interactions. *Clinics in dermatology*, 6(4), 74-82.
- Oren, A. (2002). Diversity of halophilic microorganisms: environments, phylogeny, physiology, and applications. *Journal of Industrial Microbiology and Biotechnology*, 28(1), 56-63.
- Orwin, D. (1970). A Polysaccharide-Containing Cell Coat on Keratinizing Cells of the Romney Wool Follicle. *Australian Journal of Biological Sciences*, 23(3), 623-636.
- Paulsrud, P., & Lindblad, P. (2002). Fasciclin domain proteins are present in *Nostoc* symbionts of lichens. *Applied and environmental microbiology*, 68(4), 2036-2039.
- Phalip, V., Delalande, F., Carapito, C., Goubet, F., Hatsch, D., Leize-Wagner, E., Jeltsch, J.-M. (2005). Diversity of the exoproteome of *Fusarium graminearum* grown on plant cell wall. *Current genetics*, 48(6), 366-379.

- Prakash, B., Vidyasagar, M., Madhukumar, M., Muralikrishna, G., & Sreeramulu, K. (2009). Production, purification, and characterization of two extremely halotolerant, thermostable, and alkali-stable  $\alpha$ -amylases from *Chromohalobacter* sp. TVSP 101. *Process Biochemistry*, 44(2), 210-215.
- Queiroz, J., Tomaz, C., & Cabral, J. (2001). Hydrophobic interaction chromatography of proteins. *Journal of Biotechnology*, 87(2), 143-159.
- Ravindran, C., Varatharajan, G. R., Rajasabapathy, R., Vijayakanth, S., Kumar, A. H., & Meena, R. M. (2012). A role for antioxidants in acclimation of marine derived pathogenic fungus (NIOCC 1) to salt stress. *Microbial Pathogenesis*.
- Ritz-Timme, S., Laumeier, I., & Collins, M. J. (2003). Aspartic acid racemization: evidence for marked longevity of elastin in human skin. *British Journal of Dermatology*, 149(5), 951-959.
- Roeßler, M., & Müller, V. (2001). Osmoadaptation in bacteria and archaea: common principles and differences. *Environmental microbiology*, 3(12), 743-754.
- Rye, C. S., & Withers, S. G. (2000). Glycosidase mechanisms. *Current opinion in chemical biology*, 4(5), 573-580.
- Sajidan, A., Farouk, A., Greiner, R., Jungblut, P., Müller, E.-C., & Borriss, R. (2004). Molecular and physiological characterisation of a 3-phytase from soil bacterium *Klebsiella* sp. ASR1. *Applied microbiology and biotechnology*, 65(1), 110-118.
- Sánchez-Porro, C., Tokunaga, H., Tokunaga, M., & Ventosa, A. (2007). *Chromohalobacter japonicus* sp. nov., a moderately halophilic bacterium isolated from a Japanese salty food. *International journal of systematic and evolutionary microbiology*, 57(10), 2262-2266.
- Saravanabhavan, S., Aravindhan, R., Thanikaivelan, P., Rao, J. R., & Nair, B. U. (2003). Green solution for tannery pollution: effect of enzyme based lime-free unhairing and fibre opening in combination with pickle-free chrome tanning. *Green Chemistry*, 5(6), 707-714.
- Saravanabhavan, S., Thanikaivelan, P., Rao, J. R., Nair, B. U., & Ramasami, T. (2006). Reversing the conventional leather processing sequence for cleaner leather production. *Environ Sci Technol*, 40(3), 1069-1075.
- Saulo, A. A. (2002). Common Food Additives in Candy.
- Scopes, R. K. (1994). *Protein purification: principles and practice*: Springer.
- Senthilvelan, T., Kanagaraj, J., & Mandal, A. (2011). Application of enzymes for dehairing of skins: cleaner leather processing. *Clean Technologies and Environmental Policy*, 1-9.
- Shah, P., Atwood, J. A., Orlando, R., El Mubarek, H., Podila, G. K., & Davis, M. R. (2009). Comparative Proteomic Analysis of *Botrytis cinerea* Secretome. *Journal of Proteome Research*, 8(3), 1123-1130.
- Sharma, A., & Gupta, M. N. (2001). Purification of pectinases by three-phase partitioning. *Biotechnology Letters*, 23(19), 1625-1627.
- Sigler, L., Hanselman, B., Ruotsalo, K., Kar Tsui, G., & Richardson, S. (2013). Cytological, microbiological and therapeutic aspects of systemic infection in a dog caused by the fungus *Phialosimplex caninus*. *Medical mycology case reports*, 2, 32-36.
- Sigler, L., Sutton, D. A., Gibas, C. F. C., Summerbell, R. C., Noel, R. K., & Iwen, P. C. (2010). *Phialosimplex*, a new anamorphic genus associated with infections in

- dogs and having phylogenetic affinity to the Trichocomaceae. *Medical Mycology*, 48(2), 335-345.
- Sivasubramanian, S., Manohar, B. M., & Puvanakrishnan, R. (2008 ). Mechanism of enzymatic dehairing of skins using a bacterial alkaline protease. *Chemosphere*, 70(6), 1025-1034.
- Sivasubramanian, S., Manohar, B. M., Rajaram, A., & Puvanakrishnan, R. (2008 ). Ecofriendly lime and sulfide free enzymatic dehairing of skins and hides using a bacterial alkaline protease. *Chemosphere*, 70(6), 1015-1024.
- Sophos, N. A., & Vasiliou, V. (2003). Aldehyde dehydrogenase gene superfamily: the 2002 update. *Chemico-biological interactions*, 143, 5-22.
- Stackebrandt, E., & Goebel, B. (1994). Taxonomic note: a place for DNA-DNA reassociation and 16S rRNA sequence analysis in the present species definition in bacteriology. *International Journal of Systematic Bacteriology*, 44(4), 846-849.
- Sudha, T. B., Thanikaivelan, P., Aaron, K. P., Krishnaraj, K., & Chandrasekaran, B. (2009). Comfort, Chemical, Mechanical, and Structural Properties of Natural and Synthetic Leathers Used for Apparel. *Journal of Applied Polymer Science*, 114(3), 1761-1767.
- Terol, J., Domingo, C., & Talón, M. (2006). The GH3 family in plants: genome wide analysis in rice and evolutionary history based on EST analysis. *Gene*, 371(2), 279-290.
- Thanikaivelan, P., Bharath, C. K., Saravanabhavan, S., Rao, J. R., Chandrasekaran, B., Chandrababu, N. K., & Nair, B. U. (2007). Integrated hair removal and fiber opening process using mixed enzymes. *Clean Technologies and Environmental Policy*, 9(1), 61-68.
- Thanikaivelan, P., Rao, J. R., Nair, B. U., & Ramasami, T. (2003). Approach towards zero discharge tanning: role of concentration on the development of eco-friendly liming-reliming processes. *Journal of Cleaner Production*, 11(1), 79-90.
- Thiede, B., Höhenwarter, W., Krah, A., Mattow, J., Schmid, M., Schmidt, F., & Jungblut, P. R. (2005). Peptide mass fingerprinting. *Methods*, 35(3), 237-247.
- Tjalsma, H., Bolhuis, A., Jongbloed, J. D., Bron, S., & van Dijk, J. M. (2000). Signal peptide-dependent protein transport in *Bacillus subtilis*: a genome-based survey of the secretome. *Microbiology and Molecular Biology Reviews*, 64(3), 515-547.
- Varghese, J. N., Hrmova, M., & Fincher, G. B. (1999). Three-dimensional structure of a barley beta-D-glucan exohydrolase, a family 3 glycosyl hydrolase. *Structure with Folding & Design*, 7(2), 179-190.
- Vidyasagar, M., Prakash, S., Jayalakshmi, S., & Sreeramulu, K. (2007). Optimization of culture conditions for the production of halothermophilic protease from halophilic bacterium *Chromohalobacter* sp. TVSP101. *World Journal of Microbiology and Biotechnology*, 23(5), 655-662.
- Walther, T. C., & Mann, M. (2010). Mass spectrometry-based proteomics in cell biology. *The Journal of cell biology*, 190(4), 491-500.
- Wang, H. Y., Liu, D. M., Liu, Y., Cheng, C. F., Ma, Q. Y., Huang, Q., & Zhang, Y. Z. (2007). Screening and mutagenesis of a novel *Bacillus pumilus* strain

- producing alkaline protease for dehairing. *Letters in Applied Microbiology*, 44(1), 1-6.
- Wilson, K., Padhye, A., & Carmichael, J. (1969). Antifungal activity of *Wallemia ichthyophaga* (= *Hemispora stellata* Vuill.= *Torula epizoa* Corda). *Antonie van Leeuwenhoek*, 35(1), 529-532.
- Yates, J. R., Ruse, C. I., & Nakorchevsky, A. (2009). Proteomics by mass spectrometry: approaches, advances, and applications. *Annual review of biomedical engineering*, 11, 49-79.
- Zajc, J., Liu, Y., Dai, W., Yang, Z., Hu, J., Gostinčar, C., & Gunde-Cimerman, N. (2013). Genome and transcriptome sequencing of the halophilic fungus *Wallemia ichthyophaga*: haloadaptations present and absent. *BMC genomics*, 14(1), 1-21.
- Zalar, P., de Hoog, G. S., Schroers, H. J., Frank, J. M., & Gunde-Cimerman, N. (2005). Taxonomy and phylogeny of the xerophilic genus *Wallemia* (Wallemiomycetes and Wallemiales, cl. et ord. nov.). *Antonie Van Leeuwenhoek International Journal of General and Molecular Microbiology*, 87(4), 311-328. doi: 10.1007/s10482-004-6783-x
- Zámocký, M., Hallberg, M., Ludwig, R., Divne, C., & Haltrich, D. (2004). Ancestral gene fusion in cellobiose dehydrogenases reflects a specific evolution of GMC oxidoreductases in fungi. *Gene*, 338(1), 1-14.